

MOLECULAR DEVELOPMENTAL ANALYSIS OF ARTIFICIAL
SELECTION OF ARTIFICIAL SELECTION RESPONSE IN THE MALE
SEX COMBS OF DROSOPHILA MELANOGASTER

MOLECULAR DEVELOPMENTAL ANALYSIS OF ARTIFICIAL
SELECTION OF ARTIFICIAL SELECTION RESPONSE IN THE MALE
SEX COMBS OF DROSOPHILA MELANOGASTER

By

SHENG CHENG B.Sc (Hons)

A Thesis
Submitted to the School of Graduate Studies
in Partial Fulfillment of the Requirements
for the Degree
Master of Science

McMaster University
Copyright by Sheng Cheng, January 2014

McMaster University MASTER OF SCIENCE (2014) Hamilton, Ontario (Biology)

TITLE: Molecular developmental analysis of artificial selection response in the male sex combs of *Drosophila melanogaster*

AUTHOR: Sheng Cheng, B. Sc (Hons) (University of Toronto)

SUPERVISOR: Professor Rama Singh

NUMBER OF
PAGES: x, 125

ABSTRACT

Evolutionary innovations, at the molecular level, represent the novel establishment of regulation networks among previously unconnected genes. Understanding the cellular and molecular mechanisms that underlies the development of such innovations is of central importance in evolutionary-developmental research (evo-devo). The sex comb of *Drosophila* is an excellent model to study the molecular basis of evolutionary innovations. Highline and Lowline are two artificial selected *D. melanogaster* lines differing in the number of sex comb bristles. It was expected that the “cross-regulation loop” between two transcription factors, *Doublesex* male isoform (DSX^M) and *Sexcombs reduced* (SCR), evolves rapidly and promotes the morphological evolution of sex combs. We used immunofluorescent technique (antibody staining) to compare the expression of DSX^M and SCR in the forelegs of three different lines (Highline, Wildtype and Lowline). We hypothesized that artificial selection will increase expression of DSX^M and SCR in the Highline and reduce expression in the Lowline. The fluorescent pictures of antibody staining experiments indicate that the expression region of DSX^M in the Highline is significantly higher than the expression region in the Lowline, and the expression levels of SCR has minor difference among the three lines. DSX^M expression is altered by the artificial selection, but SCR expression is not. The influence of artificial selection appears to have been constrained by development. Our investigation provides an approach to test the validity of the models of cross-regulation s between SCR and DSX^M during development.

ACKNOWLEDGEMENT

It would have been impossible for me to finish this thesis without the help and support provided by the kind and generous people around me.

Above all, I would like to express my special appreciation and thanks to my advisor and supervisor Dr. Rama Singh for his continuous support. His motivation, patience, erudition and enthusiasm guided and encouraged me throughout my entire Masters study, especially when I was frustrated. He provided me the opportunity to learn and study the topic that I was very interested in. His advice on both my research and my academia was priceless. I will remember and be grateful for him for the rest of my life.

I would like to thank Dr. Richard Morton for his sense of humor and challenging critiques. He showed me the correct and positive attitude towards the scientific research and how to be a real scientific researcher. I deeply appreciated his strictness when he was reviewing my thesis.

I would also like to thank the other two committee members of mine, Dr. Bhagwati Gupta and Dr. Ana Campos for their insightful and encouraging comments. They helped to make my committee meetings to be enjoyable moments of my life.

I am grateful for every member (both present and former) in Dr. Singh's Lab. To Sogol Eizadshenass, thanks for being a great colleague and lab-mate. Thanks for the personal talks from you. The support from you gave me a lot of strength when I was frustrated. You will always be my friend. To Abha Ahuja, thanks for artificial selected lines you created. These lines were the foundation of my project. I deeply appreciate the Abha and Sogol's contributions to my project. To Santosh Jagadeeshan, thanks for being

a kind mentor and priceless thesis editor. I could not imagine how my thesis would be without your help. To Jacqueline Thompson, thanks for being an unbiased data analyst for my project. The objective view from you made my conclusion convincible.

My appreciation also goes to Dr. Michelle Arberitman and Dr. Brian Oliver. The DSX antibodies used in my project were provided by them. Words cannot express how grateful I am for their generosity.

I would like to express my gratitude to Dr. Ellen Larsen. Three years ago she introduced me into the research area of sex comb. Her research enthusiasm was always inspiration for me. I am grateful to Nicolas Malagon. He never said “no” when I asked for his help, even when he was preparing for his own PhD defense. His dedication to the scientific research always motivated me to overcome any challenges.

I would also like to thank Joel Atallah and Olga Barmina from Dr. Artyom Kopp’s lab. They taught me every detail steps of the antibody staining procedures. Without their guidance and the protocol they provided, this thesis would not have been possible.

A special thank goes to my family, especially my parents, Huaming Cheng and Hongfei Lu, for their love and support. I know, no matter what happens you will be there with me. You gave me the strength and help me overcome every difficulty in my life. I love you. At last, I dedicate my thesis to my late grandpa, Lanhua Lu. I am honored to be your grandson, and you make me proud every day.

Table of Contents

CHAPTER 1. INTRODUCTION	1
1. 1 Sex comb, a good model to study evolutionary innovations	1
1.1.1 <i>Evolutionary innovations and sex comb</i>	1
1.1.2 <i>Mechanisms that control/alter sex comb development</i>	6
<i>First Process: Leg development</i>	6
<i>Second Process: Bristle morphogenesis</i>	10
<i>Third Process: Sex determination</i>	15
<i>Fourth Process: Cross-regulation between “Sex comb reduced” and “doublesex”</i> ...	19
1.1.3 <i>Development process variation</i>	26
1.1.4 <i>Summary</i>	31
1.2. Artificially selected traits are good targets to study the development of evolutionary innovations	31
2.1 <i>Artificial selection and development</i>	31
1.3. Project Objective	32
CHAPTER 2. MATERIALS AND METHODS.....	35
2.1 Artificial selection.....	35
2.2 Fly maintenance	40
2.3 Antibody staining of DSX and SCR	40
2.4 Fluorescent pictures modifications and analysis.....	42
Chapter 3. RESULTS	46
3.1 Artificial selection	47

3.2 Differential expression of DSX ^M and SCR.....	48
3.2.1 SCR Expression at AP5.....	48
3.2.2 DSX ^M Expression at AP5.....	50
3.2.3 DSX ^M expression on tarsus 1.....	53
3.2.4 DSX ^M expression on tarsus 2-4	65
3.2.5 Expression patterns of SCR and DSX ^M	76
Chapter 4. DISCUSSION.....	77
4.1 Experimental investigation of innovation	78
4.1.1 Significance of artificial selected lines in studying the developmental genetics of evolutionary innovations	78
4.1.2 Role of macro-vs micro-mutations in innovation.....	79
4.2 Main findings of this investigation and its significance	80
4.2.1 Predominant expression divergence in DSX ^M underlying divergent sex comb morphologies.....	80
4.2.2 Role of DSX and SCR in an interactive model	80
4.2.3 Significance of the experiment	83
Chapter 5. CONCLUSIONS AND FUTURE DIRECTIONS.....	85
REFERENCES.....	87
SUPPLEMENTARY FIGURES AND TABLES	92-125

List of Figures

Figure 1. SEM pictures of <i>D.melanogaster</i> tarsus 1 and sex comb.....	3
Figure 2a. Sex comb morphology of <i>D. pseudoobscura</i>	4
Figure 2b. Sex comb morphology of <i>Lordiphosa magnipectinata</i>	5
Figure 3. Leg disc development	9
Figure 4. <i>Bab</i> expression gradient and the phenotype of overexpression <i>Dac</i>	13
Figure 5. Structure of the mechanosensory bristle	14
Figure 6. Model of <i>Drosophila</i> sexual determination mechanism.....	18
Figure 7. <i>D. melanogaster</i> sex comb expression pattern of SCR and DSX ^M in tarsus 1 at AP16	23
Figure 8. The pathway of regulation between <i>Scr</i> and <i>Dsx</i> in <i>D. melanogaster</i>	24
Figure 9. Model of <i>Scr</i> regulation mechanism	25
Figure 10. <i>D. melanogaster</i> sex comb rotation process	28
Figure 11. Morphology of sex comb in the <i>obscura</i> and <i>melanogaster</i> species groups	30
Figure 12. Sex comb morphology of Highline, Lowline and Control	34
Figure 13. Selection experiment of sex comb bristle number	38-39
Figure 14. Example of expression level (EL) calculation	44
Figure 15. Example of width of expression pattern measurement	45
Figure 16. Comparison of the expression pattern of SCR on the forelegs	49
Figure 17. Comparison of the expression pattern of the DSX ^M and SCR on the forelegs	51-52
Figure 18. DSX ^M expression level on the tarsus 1	55

Figure 19. Distribution of the average width of the DSX ^M expression pattern on tarsus1	63- 64
Figure 20. DSX ^M expression in Lowline	67
Figure 21. DSX ^M expression level on the tarsus 2-4	68
Figure 22. Distribution of the area of DSX ^M expression pattern on tarsus 2-4	74-75

Supplementary Figures

Figure S1-S15 DSX ^M expression on Highline foreleg	92-106
Figure S16-S24 DSX ^M expression on Wildtype foreleg.....	107-115
Figure S25-S33 DSX ^M expression on Lowline foreleg	116-124

List of Tables

Table 1. Mean value and standard deviation of the average width of DSX ^M expression pattern in tarsus 1 for three lines: Highline, Wildtype and Lowline.....	56
Table 2. Shapiro-Wilk's Normality Test for the data from Table 1	57
Table 3. One-Way ANOVA for the average width of DSX ^M expression pattern in tarsus 1 of Highline, Lowline and Wildtype	60
Table 4. Tukey's HSD test for the average width of DSX ^M expression pattern in tarsus 1 (Highline, Lowline and Wildtype).....	61
Table 5. LSD comparison test for the average width of DSX ^M expression pattern in tarsus 1 (Highline, Lowline and Wildtype).....	62

Table 6. Mean value and standard deviation of the area of DSX ^M expression pattern in tarsus 2-4 for three lines: Highline, Wildtype and Lowline	69
Table 7. Shapiro-Wilk's Normality Test for the data from Table 6	70
Table 8. Result of One-Way ANOVA test for the area of DSX ^M expression pattern in tarsus 2-4 of Highline, Lowline and Wildtype	71
Table 9. Tukey's HSD comparison test for the area of DSX ^M expression pattern in tarsus 2-4 (Highline, Lowline and Wildtype).....	72
Table 10. LSD comparison test for the area of DSX ^M expression pattern in tarsus 2-4 (Highline, Lowline and Wildtype).....	73

Supplementary Tables

Table S1. Raw data of the DSX ^M expression pattern width at 5 different places in tarsus 1 and the area of DSX ^M expression in tarsus 2-4.....	125
--	-----

Chapter 1. INTRODUCTION

1.1 Sex comb, a good model to study evolutionary innovations

1.1.1 Evolutionary innovations and sex comb

Evolutionary innovations, at the molecular level, represent the novel establishment of regulation networks among previously unconnected genes (Carroll, 2005, 2008; Kopp, 2011; Wagner, 2011). Understanding the cellular and molecular mechanism that underlies the development of such innovations is of central importance in evolutionary-developmental research (evo-devo). The sex comb of *Drosophila* is one such remarkable evolutionary innovation and is a good model to study the molecular basis of evolutionary innovations. The sex comb is a row of “male-specific mechanosensory bristles” (Tanaka et al., 2009) located at the distal region of the tarsus 1 of the forelegs (the front pair legs) of *Drosophila* (Figure 1) (Tanaka et al., 2009). However, not all *Drosophila* species have sex combs (Kopp, 2011; Tanaka et al., 2009). The sex comb appears to be a newly evolved structure that is restricted to the species in subgenus *Sophophora: melanogaster* (e.g. *D. melanogaster*) (Figure 1), *obscura* (e.g. *D. pseudoobscura*) (Figure 2a), *fima*, and *dentissima*, and some specific species in the genus *Lordiphosa* (e.g. *Lo. magnipectinata*) (Figure 2b) (Atallah et al., 2012; Hu and Toda, 2001; Kopp, 2011; Tanaka et al., 2009). Sex comb morphologies vary dramatically in different species, and sex comb teeth are derived from different kinds of bristles on the forelegs in different species (Atallah et al., 2009a). For instance, for *D. melanogaster*, sex comb teeth are derived from transverse row bristles, and for *D. nikananu*, sex comb teeth are derived from longitudinal row bristles (Atallah et al., 2009a). Among the species

without sex combs, the patterns of the mechanosensory bristles on the first tarsal segments are identical (Kopp, 2011). The female bristle patterns are conserved throughout *Drosophilidae* (Kopp, 2011). These data suggest considerable variation in the evo-devo of sex combs across species and sexes of *Drosophila*. Sex combs are involved in stereotypical mating behavior, but the specific function of sex comb is speculated to vary among different species during evolution (Coyne, 1985; Kopp, 2011). For example, in *D. melanogaster*; sex comb is believed to be used by the male to hold the female genitalia transitorily; in contrast, in other species, the sex comb is used to grasp the abdomen or to spread the wings of female (Cook, 1977; Coyne, 1985). It is highly possible that the functional variability is due to the sexual selection (Ahuja and Singh, 2008; Atallah et al., 2009a; Kopp, 2011). The pressure from sexual selection drives the divergence of cellular and genetic mechanisms that control morphogenesis of sex comb.

There are two major reasons that make sex comb structure a good model in the study of evolutionary innovations:

- (1) There are multiple mutations involving four different pathways (described in detail below) that are known to perturb the presence or morphogenesis of sex comb.
- (2) The development process of sex comb structure varies significantly among different *Drosophila* species (e.g. the rotation process, described in detail below) and at the same time, the development process evolves rapidly during evolutionary history. The underlying mechanisms of such a dynamic evo-devo system are of considerable interest to developmental and evolutionary biologists.

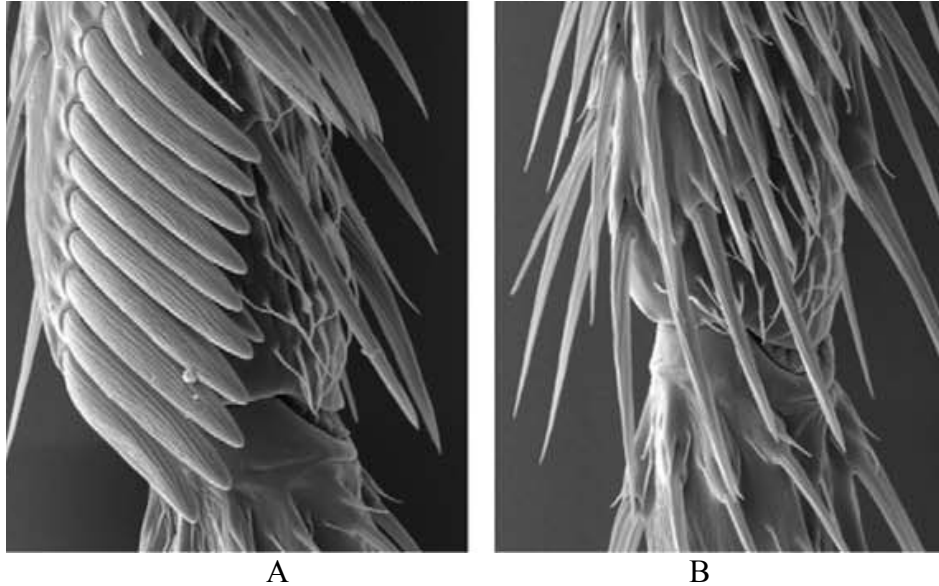


Figure 1. Scanning Electron Microscope (SEM) pictures of *D. melanogaster* tarsus 1 and sex combs

A: SEM picture of tarsus 1 of *D. melanogaster* male. The sex comb teeth are the blunt, longitudinal row of bristles in A. The average size of the *D. melanogaster* sex comb tooth is about 50 μm and the number of teeth varies between 9 to 12. B: SEM picture of tarsus 1 of *D. melanogaster* female. The sex comb structure does not exist in female tarsus 1. This figure was taken without modification from Tanaka et al., 2011. This figure was reproduced with permission.



Figure 2a. Sex comb morphology of *D. pseudoobscura*

Males of this species have two transverse sex combs in tarsus 1 and tarsus 2. “ta1” stands for tarsus 1 and “ta2” stands for tarsus 2. The sex comb in tarsus 1 has more teeth than in tarsus 2. This figure was taken without modification from Tanaka et al., 2011. This figure was reproduced with permission.



Figure 2b. Sex comb morphology of *Lordiphosa magnipectinata*

Males of this species have two longitudinal sex combs and are indicated by the arrows. The scale bar is 20 μm . The sex comb in tarsus 1 has more bristles than in tarsus 2. This figure was adapted from Atallah et al., 2012. This figure was reproduced with permission.

1.1.2 Mechanisms that control/alter sex comb development

Four different hierarchical processes are involved in *D.melanogaster* sex comb development: (1) leg development, (2) bristle morphogenesis, (3) sex-determination pathway and (4) cross-regulation between *Sex comb reduced* and *doublesex*.

First Process: Leg development

Imaginal discs

The structures of many adult appendages come from imaginal discs (Fristrom, 1988). The majority of adult tissues develop from imaginal disc cells during embryogenesis (Condic et al., 1991; Fristrom, 1988; Kojima, 2004). *D. melanogaster* has 10 different types of imaginal discs, which include halteres, wings and legs (Bate and Martinez Arias, 1991; Condic et al., 1991; Fristrom, 1988). Despite the morphological diversity of different types of imaginal discs, there are certain developmental commonalities. In *D. melanogaster*, the primordial imaginal discs are formed during embryonic development (Condic et al., 1991; Fristrom, 1988). Each imaginal disc is composed of 10 to 40 epithelial cells that show a specific cell shape (Bate and Martinez Arias, 1991). In the larval stage, the epithelial sheet of imaginal discs develops through cell proliferation and at the final stage of the third instar an imaginal disc can reach up to 60,000 cells (Bate and Martinez Arias, 1991; Fristrom, 1988).

Leg discs development and adult leg proximal-distal orientation determination

The leg imaginal disc has been used as a good example to study tissue elongation and regeneration (von Kalm et al., 1995). The leg disc originally contains only 10-30 cells (Condic et al., 1991; Kojima, 2004). The leg disc cells proliferate to over 10,000 cells in the 2nd and 3rd instar larval period (Kojima, 2004). The leg disc remains “flat” during the 1st and 2nd instar larval stage (Kojima, 2004). The sheet starts to fold concentrically at the beginning of 3rd instar stage. By late 3rd instar stage, the leg disc is still a monolayer sheet but not “flat” anymore (Figure 3A, 3B, 3C and 3D) (Condic et al., 1991; Kojima, 2004). The leg segments are specified as “concentric domains” (Kojima, 2004).

During the pupal period, the adult leg structure is formed through the elongation of the leg disc and sensory bristles and joints are formed at the same time (Kojima, 2004; Mirth and Akam, 2002; Soler et al., 2004). The morphological process to achieve leg elongation is called “evagination” (Kojima, 2004). During the elongation process, the outer membrane (PE layer) is unfolded, and the concentric epithelium evaginates outward (Figure 3E, 3F) (Kojima, 2004; Soler et al., 2004). Dramatic cell morphological changes happen in the first six hours of the pupal period (AP6) (Condic et al., 1991).

The leg narrowing and elongation are caused by the remarkable cell shape and size changes after pupation (Condic et al., 1991). Besides the changes of cell morphologies, cell divisions also take place in the early pupal stage. However, these cell divisions are not all oriented in the axis of elongation (Taylor and Adler, 2008). In the mid-pupal stage, three main processes of leg development take place: leg elongation (continues), joints formation and the emergence of bristles (Atallah et al., 2009a; Atallah

et al., 2009b; Taylor and Adler, 2008). The leg structure is fully developed by the time of AP50 (50 hours post pupation) (Mirth and Akam, 2002).

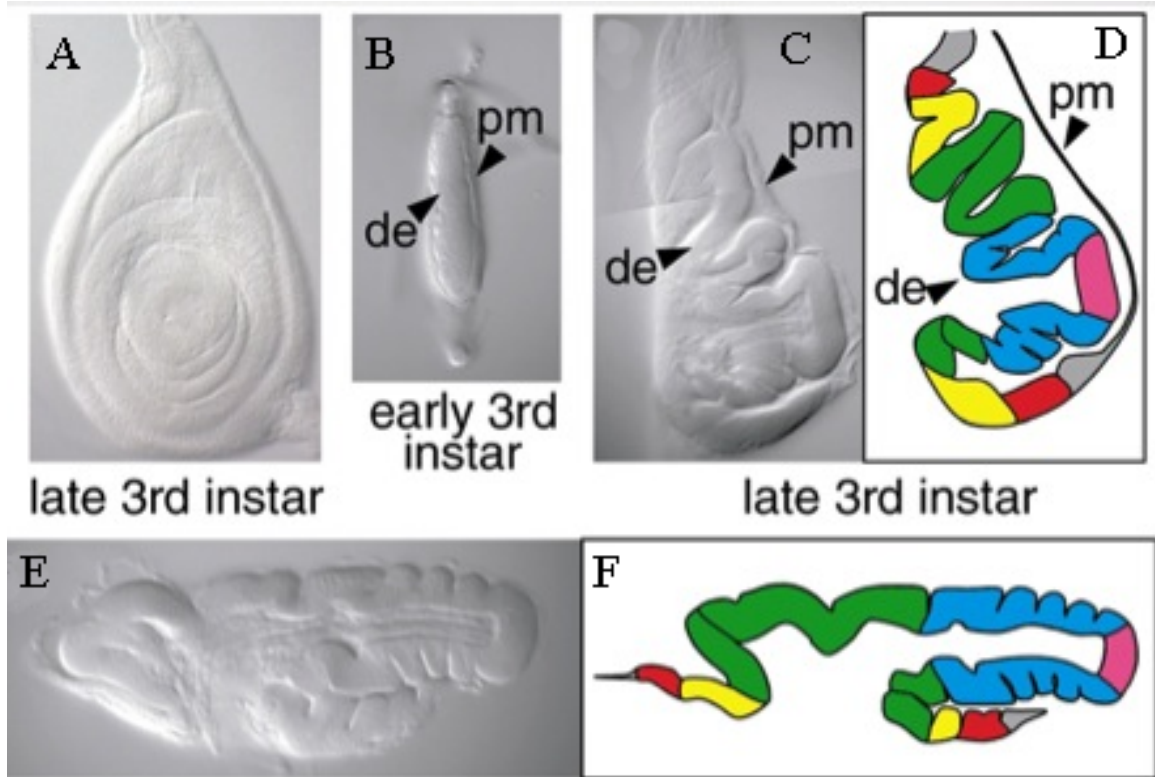


Figure 3. Leg disc development

The SEM pictures of the leg disc evagination at different stages of development process. **pm**: peripodial membrane; **de**: disc epithelium. A: Ventral view of the imaginal disc at late 3rd instar. At this moment, the cells start to fold concentrically. The cell sheet is not flat anymore. B: A cross section of imaginal disc at early 3rd instar. The cell sheet remains “flat” in B. C and D: Cross section of A. E and F: leg development at early pupal stage. PE membrane breaks, and the imaginal disc evaginates outward to form the leg structure. The development timeline from early to later: (B) → (A, C) → (E), B is the earliest and E is the latest. This figure was adapted from Kojima, 2004. This figure was reproduced with permission.

Drosophila adult legs are segmented (Kojima, 2004). For *D. melanogaster*, the leg disc morphogenesis along the proximal-distal direction of the forelegs is determined by the expression pattern of four kinds of gene that are expressed in the leg disc: *homothorax* (*hth*), *Distalless* (*Dll*), *dachshund* (*dac*) and *bric a` brac* (*bab*) (Lecuit and Cohen, 1997; Randsholt and Santamaria, 2008). The HTH protein is expressed in the proximal region, the DLL protein defines the distal region and DAC is expressed in the middle (tibia and tarsus 1) (Atallah et al., 2009a; Lecuit and Cohen, 1997; Randsholt and Santamaria, 2008). No distal leg structure develops in *Dll* knockout lines, and no median portion develops in *dac* knockouts (Lecuit and Cohen, 1997; Randsholt and Santamaria, 2008). Segmentation of the intermediary portion of the foreleg requires BAB proteins (includes BAB1 and BAB2), which are expressed from the *bab* gene (Randsholt and Santamaria, 2008). *Bab* gene is activated by DLL protein in the third larva instar in the domain between tarsus 1 (tarsal segment 1, ts1) and tarsus 4 (ts4) (Randsholt and Santamaria, 2008), and repressed by DAC proximally (Randsholt and Santamaria, 2008). Deletion or knocking down expression of BAB proteins causes the fly to lose the structure from ts2 to ts4 (Randsholt and Santamaria, 2008). The expression level of BAB proteins increases along the ts1 to ts4 axis (Figure 4), and using UAS-GAL4 system (BAB proteins binding element as the promoter) to overexpress DAC the foreleg region from ts2 to ts4 causes ectopic sex combs (Figure 4) (Randsholt and Santamaria, 2008). Ectopic SCR expression is detected on ts2 to ts4 when DAC is overexpressed (Randsholt and Santamaria, 2008).

Second Process: Bristle morphogenesis

While vertebrates have an internal skeleton, arthropods have an external skeleton that supports and protects the body tissue inside. On the other hand, the external skeleton constrains arthropod tactile sensation. In order to solve this problem, fruit flies have approximately 5,000 bristles covering the body (Held, 1991).

D. melanogaster bristles, based on their different functions, display huge variation in morphology (size and shape) and arrangement. Based on the stimulus sensed, *D. melanogaster* bristles can be divided into two different groups: mechanosensory bristles and chemosensory bristles (Held, 1991). In response to mechanical pressure or distortion, mechanosensory bristles send signals to the fly's brain (Held, 1991; Sturtevant, 1970). Chemosensory bristles detect chemical signals including smells and tastes in the environment (Held, 1991; Sturtevant, 1970). Mechanosensory bristles are made of four cells: the shaft cell, the socket cell, the sheath cell and the neuron cell (Figure 5) (Fabre et al., 2008). The shaft cell and socket cell are external cells, and the sheath cell and the neuron cell are internal cells (Fabre et al., 2008). These cells are all descended from a "sensory organ precursor" (SOP) (Gho et al., 1999). The SOP divides to form one cell (pIIa) that produces the external cells, and another cell (pIIb) that produces the internal cells (Gho et al., 1999). The socket cell provides the socket structure of the shaft cell, which makes the long bristle shaft body, at the base (Fabre et al., 2008). Underneath the epithelium, the sheath cell, wraps around the neuron cell and function like vertebrates glial cells, which provide support and protection for the neuron (Fabre et al., 2008). The chemosensory bristle contains four more neurons than the mechanosensory bristle. The

neurons project their dendrites to a pore at the shaft's tip where they can detect chemical signals (Fabre et al., 2008; Scott et al., 2001).

Sex comb bristles are macrochaetes and mechanosensory bristles. The development of sex comb teeth is controlled by the mechanism of bristle morphogenesis. Compromising the bristle morphogenesis systems will lead to severe defects of sex comb formation. For example, the locations of the SOPs are defined by the *achaete-scute complex*, and deletion of this complex removes most of the bristles, including sex comb teeth (García-Bellido and de Celis, 2009).

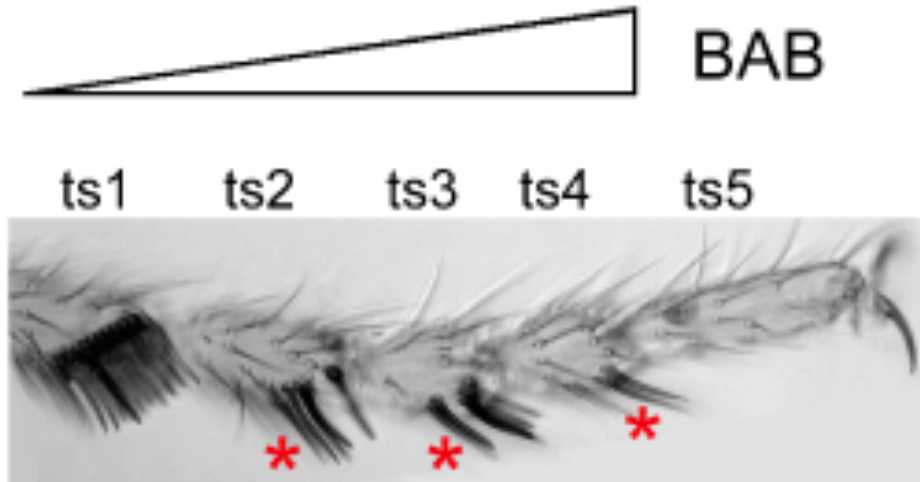


Figure 4. *Bab* expression gradient and the phenotype of overexpression *Dac*

The figure at the top is a demonstration of the BAB protein expression gradient along the foreleg in late pupal stage (Randsholt and Santamaria, 2008). The names of the segments of the leg from ts1 to ts5 are labeled. The triangle at the top indicates the expression level gradient of BAB proteins along the *D. melanogaster* foreleg. The expression level of BAB is increased along the foreleg from ts1 to ts4 (Randsholt and Santamaria, 2008). The picture at the bottom is the demonstration of the phenotype of ectopical expression of DAC protein. Using UAS-GAL4 system (BAB proteins binding element as the promoter), overexpression of DAC along the foreleg through the UAS-GAL4 system leads to the ectopic sex comb bristles formation along the foreleg. The red asterisks indicate the positions of ectopic sex comb bristles. This figure was taken without modification from Randsholt and Santamaria, 2008. This figure was reproduced with permission.

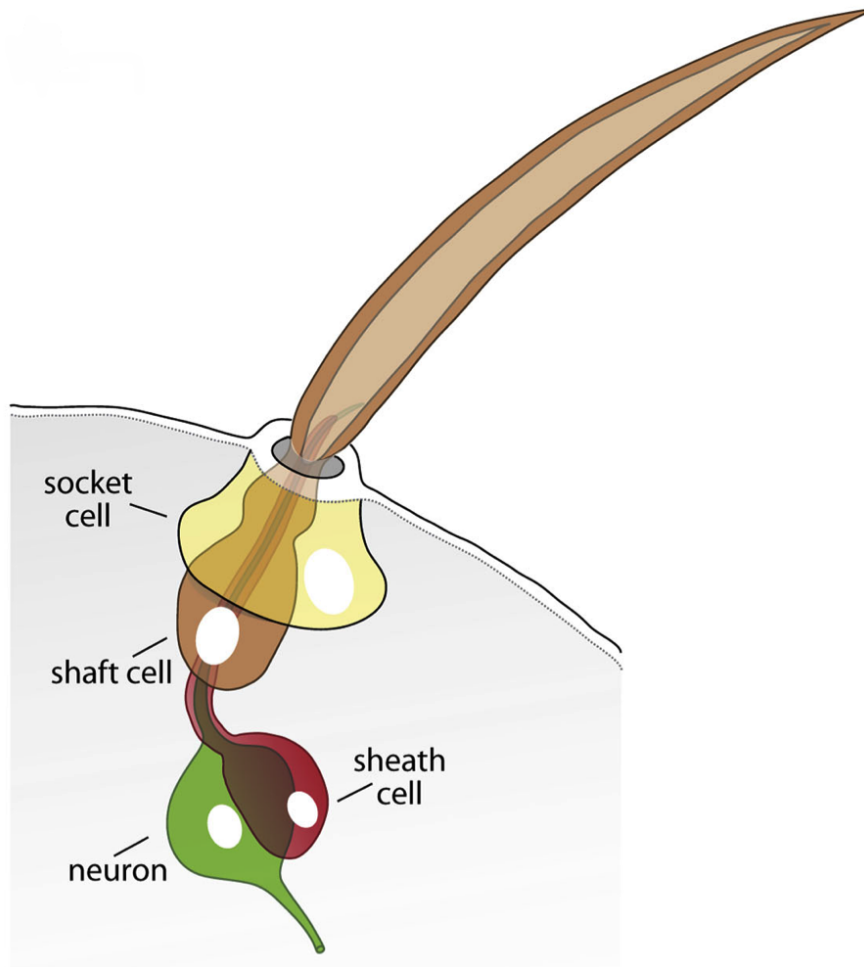


Figure 5. Structure of the mechanosensory bristle

The mechanosensory bristle contains four kinds of cells: shaft cell (brown), socket cell (yellow) sensory neuron (green) and sheath cell (red). The shaft cell and socket cell are external cells, and the sheath cell and the neuron cell are internal cells (Fabre et al., 2008). This figure was taken without modification from Fabre et al., 2008.

Third Process: Sex determination

The sex determination system of *D.melanogaster* is a multi-step cascade, which depends on the X chromosome of the individual (Baker et al., 2001; Robinett et al., 2010). If the individual contains only one copy of the X chromosome, it will develop as male; if the individual contains two copies of the X chromosome, it will become a female (Robinett et al., 2010). The function of this pathway is to determine the isoforms (male isoform or female isoform) of the gene, *doublesex (dsx)* (Kopp, 2011; Robinett et al., 2010; Tanaka et al., 2011). The specific isoforms of *dsx* will direct the development of somatic tissues of the fly including the secondary sexual characters that distinguish the male and the female (Kopp, 2011; Robinett et al., 2010; Tanaka et al., 2009). The formation and development of sex combs are strictly regulated by the “sex determination pathway” (Kopp, 2011; Robinett et al., 2010; Tanaka et al., 2011).

There are three very important pre-mRNA splicing factors in the *Drosophila* sexual determination pathway: *Sex-lethal (Sxl)*, *transformer (tra)*, and *transformer-2 (tra-2)* (Robinett et al., 2010). *Sxl* gene is a translational factor that controls mRNA splicing of *tra*; without SXL, *tra* pre-mRNA sequence will splice into nonsense message (Robinett et al., 2010; Tanaka et al., 2011). TRA and TRA-2 are both splicing regulator proteins, and they contact each other to form a protein complex that controls the splicing of the pre-mRNA transcript of two downstream sex-determination genes, *doublesex (dsx)* and *fruitless (fru)* (Meier et al., 2013; Robinett et al., 2010; Tanaka et al., 2011).

TRA-2 is constitutively expressed both in male and female flies (Robinett et al., 2010; Tanaka et al., 2011). However, TRA expression is sex dependent. In females (*X/X*),

the presence of two copies of X chromosomes turns on the expression of SXL protein (Figure 6) (Robinett et al., 2010). SXL directs *tra* pre-mRNA splicing and TRA protein is made (Figure 6) (Robinett et al., 2010). TRA-TRA-2 complex binds to the *dsx* pre-mRNA transcript and activate the splicing of the female isoform of *dsx* mRNA (*dsx^F*) (Burtis and Baker, 1989; Hedley and Maniatis, 1991). In males (*X/Y*), no SXL and TRA proteins are present and *dsx* and *fru* pre-mRNA transcripts are automatically self-spliced into the default male isoforms: *dsx^M* and *fru^M* (Figure 6) (Kopp, 2011; Robinett et al., 2010). *Fru^M* is almost exclusively expressed in central nervous system cells and is responsible for male courtship behavior (Baker et al., 2001; Meier et al., 2013). *Dsx^M* is responsible for the development of male somatic cells (Baker et al., 2001; Robinett et al., 2010; Tanaka et al., 2011). In males, the absence of *tra* is the prerequisite of the *Dsx^M* expression (Robinett et al., 2010). Any defects of this system will lead to the *Dsx^M* deficiency and tissue feminization (Ferveur et al., 1995; Ng and Kopp, 2008). Ectopic expressing *tra* in the male foreleg leads to the sex comb structure ablation and the feminization of the forelegs (Ferveur et al., 1995; Ng and Kopp, 2008).

DSX proteins (both isoforms) are transcription factors; they directly work on the target genes in somatic cells to regulate important steps in developmental processes, which result in sexually dimorphic adults (Burtis and Baker, 1989). DSX^M is 549-amino-acid long, and DSX^F is 427-amino-acid long (Burtis and Baker, 1989). Both isoforms share their first three exons but not the C-terminal domains (Burtis and Baker, 1989). DSX^M promotes the functions of male-specific genes and inhibits the transcription and functions of females-specific genes (Christiansen et al., 2002). Competitively, DSX^F

promotes female genes and inhibits the male-specific genes (Christiansen et al., 2002). It is highly possible that, both isoforms of DSX bind to the same set of genes but regulate the genes differently since the two forms of proteins share the same kind of DNA binding domain, a zinc-finger-related DNA-binding domain (Erdman et al., 1996).

The expression of DSX^M is crucial for sex comb development since the sex comb structure is compromised in the flies without DSX development (Robinett et al., 2010; Tanaka et al., 2011). In these flies there is neither a sex comb nor a transverse bristle row (Randsholt and Santamaria, 2008). Similarly, DSX^F overexpression in male flies also causes sex comb development to be compromised and the foreleg feminization (Tanaka et al., 2011).

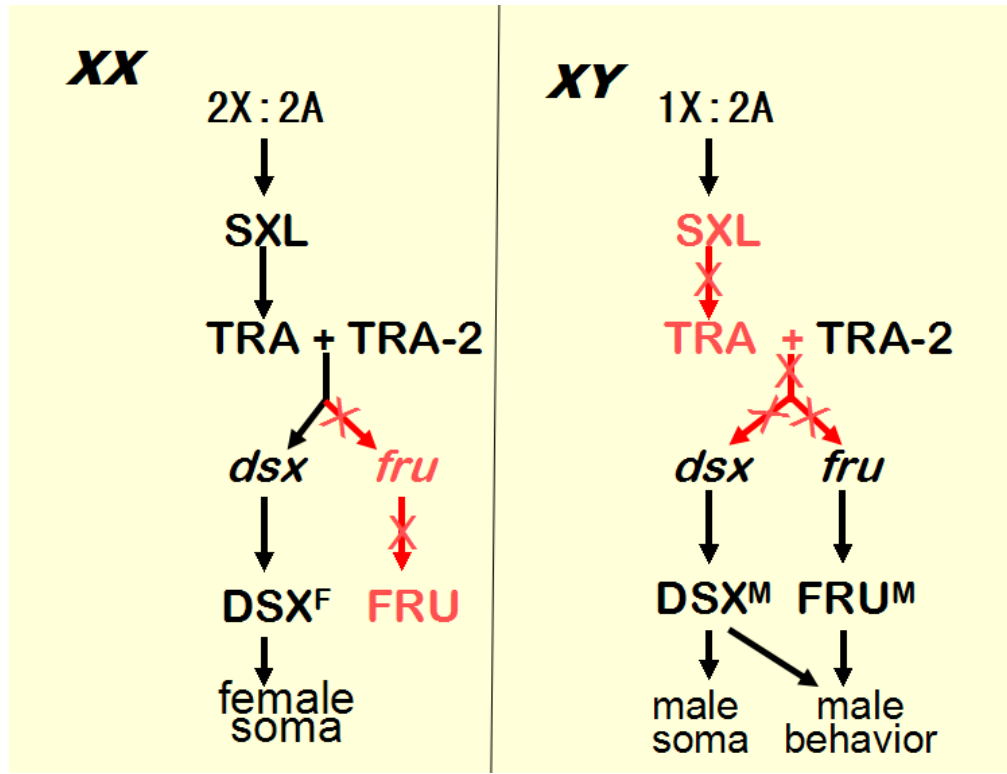


Figure 6. Model of *Drosophila* sex determination mechanism

The sex determination pathway is demonstrated above, the female version of the pathway on the left and male form on the right. The sex determination pathway of *Drosophila* is depending on the number of copies of the X chromosome of the individual. In females (*X/X*), SXL directs *tra* pre-mRNA splicing, and then the protein TRA is expressed. TRA-2 is constitutively expressed both in male and female flies. TRA and TRA-2 complex binds to the *dsx* pre-mRNA and *dsx^F* is made. In males (*X/Y*), no SXL and TRA proteins are present; the default male isoforms of *dsx* and *fru* mRNAs, *dsx^M* and *fru^M*, will be automatically formed.

Fourth Process: Cross-regulation between “Sex comb reduced” and “doublesex”

During the development process, the functions of DSX are strongly connected to a *HOX* gene called *sexcombs reduced* (*Scr*) (Kopp, 2011; Tanaka et al., 2011). SCR is a transcriptional factor that is expressed in the tibia and tarsus 1 (ts1) of the foreleg (Randsholt and Santamaria, 2008; Tanaka et al., 2011). SCR is important to sex comb formation as sex comb is completely absent in the individuals with *Scr-null* mutation (Randsholt and Santamaria, 2008; Struhl, 1982; Tanaka et al., 2011). Sex combs' locations on the foreleg are determined by SCR expression region (Barmina and Kopp, 2007). Furthermore, a male with a single copy of the *Scr* gene has fewer sex-comb teeth than wild type (Randsholt and Santamaria, 2008; Southworth and Kennison, 2002). On the other hand, the number of sex comb teeth increased as *Scr* is duplicated (Kopp, 2011). Ectopic sex comb structures are found if *Scr* overexpressed on tarsal segment 2 and tarsal segment 3 (Kopp, 2011). *Scr* RNA transcripts can be detected 3-4 hours after oviposition and SCR protein is expressed throughout larval and pupal stages (Pattatucci et al., 1991). Not only sex comb, SCR is also believed to be responsible for the formation of the pattern of transverse row bristles since the transverse row (TBR) pattern correlates with the expression of *Scr* in the tarsus 1 (Shroff et al., 2007; Tanaka et al., 2011). SCR expression is not different between male and female of the *Drosophila* species that primitively lacked sex comb structure (Barmina and Kopp, 2007). In contrast, *Scr* expression is regulated upwards in the putative sex comb region of the species whose sex combs orientation is longitudinal (Kopp, 2011). In *Drosophila* species that have sex combs on both tarsus 1 and tarsus 2 of the forelegs, SCR expression is increased in both tarsal

segments; but in *Drosophila* species that only have sex combs on tarsus 1, SCR expression is regulated upwards in tarsus 1 only (Kopp, 2011; Tanaka et al., 2011). The SCR expression differentiates the “sexual dimorphism” (Tanaka et al., 2011) in the species with longitudinal sex comb, which means that SCR expression is greater in male rather than in female (Barmina and Kopp, 2007; Kopp, 2011; Tanaka et al., 2011). SCR expression is monomorphic in the species with transverse sex combs, which means that SCR expression is the same in both genders (Kopp, 2011).

There is a strong correlation between the formation of sex comb and SCR and DSX expression (Kopp, 2011; Tanaka et al., 2011). At the time AP16 (16 hours post pupation) of development, DSX is expressed in their putative precursor cells on tarsus 1, but SCR expression is nonexistent in sex comb putative precursor cells (Tanaka et al., 2011). However, SCR expression is very high in epidermal cells that are located next to the sex comb precursor cells (Figure 7) (Tanaka et al., 2011). A “positive feedback loop” (Tanaka et al., 2011) between *dsx* and *Scr*, which is believed to be crucial in sex comb morphogenesis, was proposed by Tanaka et al. (2011) and Kopp (2011) (Figure 8). The model proposes that SCR and DSX are interacted with each other (Kopp, 2011; Tanaka et al., 2011). The expression of DSX is recruited and activated by SCR in tarsus 1 at larval stage and, at the same time, SCR is also up-regulated by the male isoform of DSX (DSX^M) from the default level (Kopp, 2011; Tanaka et al., 2011). Therefore SCR expression displays the sexual dimorphism (Tanaka et al., 2011). It is postulated that this positive regulation loop between *Scr* and *dsx* evolved rapidly and promoted the morphological evolution of sex comb (Kopp, 2011; Tanaka et al., 2011). Any

modifications of the expression of *Scr* and *dsx* will be amplified by this regulation loop to cause morphological changes of the species (Kopp, 2011). It is speculated that the positive regulation loop provides expression flexibility that allows species to respond selection pressures (Kopp, 2011).

Randsholt and Santamaria (2008) presented a model about how SCR was regulated in *Drosophila* (Figure 9). As mentioned before, BAB proteins are responsible for the segmentation of the intermediary portion of the foreleg and the expression level of BAB forms an increasing gradient from ts1 to ts4 (Figure 4). Since *bab* null mutants have ectopic sex combs formed along the foreleg tarsal segments and ectopic SCR expression can be detected on ts2, ts3 and ts4 (Atallah et al., 2009a; Randsholt and Santamaria, 2008), BAB proteins are repressors of SCR (Randsholt and Santamaria, 2008). Even though the suppression is not very strong (BAB expressed on ts1 too), BAB proteins delimit SCR expression at the joint between tarsus 1 and tarsus 2 (Randsholt and Santamaria, 2008). Similar results are found (ectopic sex combs and ectopic SCR expression formed) to the individuals with loss-function mutation of another gene called *sex combs distal (scd)* (Randsholt, 2008). SCD is also a repressor of SCR function, which may work in parallel or downstream of DAC (Randsholt and Santamaria, 2008). DAC, SCD and BAB are involved in the mechanism that controls sex comb morphology (Randsholt and Santamaria, 2008).

Combining the models shown above: Sex comb formation depends on *dac*, *bab*, *scd*, and *Scr* (Randsholt and Santamaria, 2008). DAC, BAB and SCD work together to determine the *Scr* expression region. The distal boundary of SCR expression region is the

joint located between tarsus 1 and tarsus 2 (Randsholt and Santamaria, 2008). Finally, the sex comb differentiation is initialized through the downstream regulators, which are controlled by DSX^M and SCR (Tanaka et al., 2011).

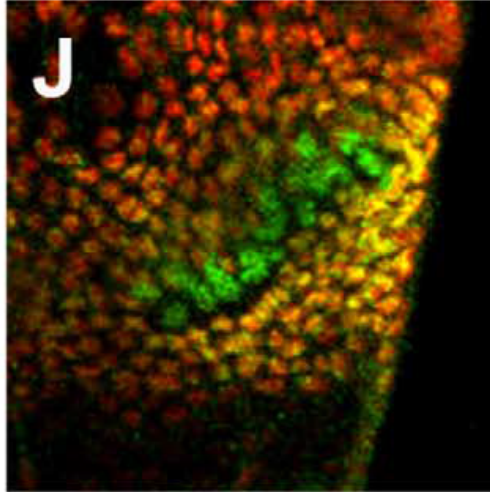


Figure 7. *D. melanogaster* sex comb expression pattern of *Scr* and *Dsx^M* in tarsus 1 at AP16
The expression pattern of SCR and DSX^M in tarsus 1 at AP16 (16 hours post pupation) is indicated. The red fluorescence represent the cells expressing *Scr*, green fluorescence represent the cells expressing *DSX^M* and yellow means that both genes are expressed within the specific cells. A cluster of green cells is surrounded with yellow cells. It is proposed that the green cluster is the collection of sex comb precursor cells at AP16. This figure was taken without modification from Tanaka et al., 2011. This figure was reproduced with permission.

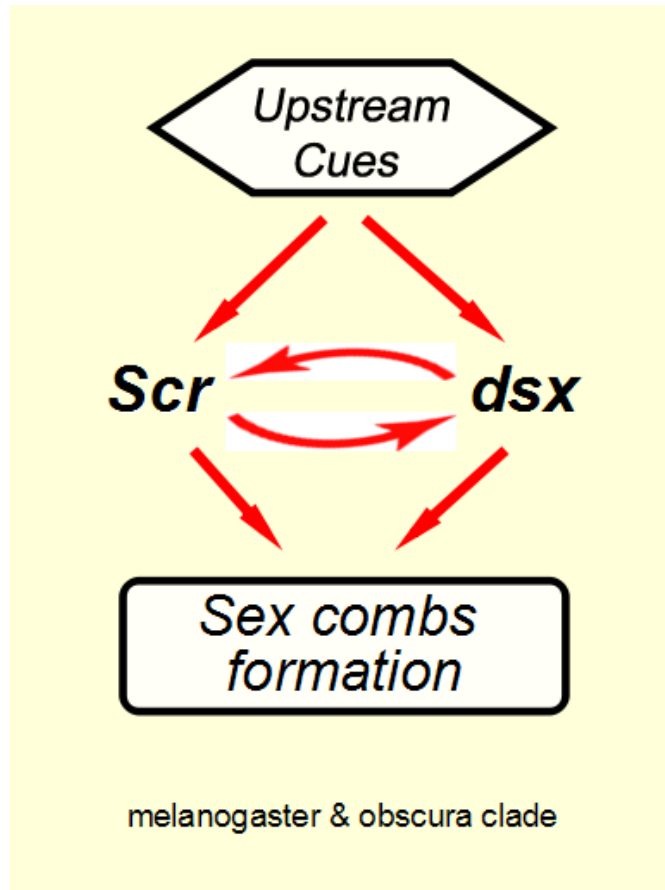


Figure 8. The pathway of regulation between *Scr* and *Dsx* in *D. melanogaster*

The cross regulation between *Scr* and *dsx* is positive regulation to each other in *melanogaster* and *obscura* clade. DSX is activated by SCR in tarsus 1 at larval stage and the male form of DSX (DSX^M) also up-regulates SCR expression. The positive regulation loop promotes the formation and development of the sex comb in *melanogaster* and *obscura* clade. The positive regulation loop between *Scr* and *dsx* evolves rapidly and promotes the morphological evolution of sex comb.

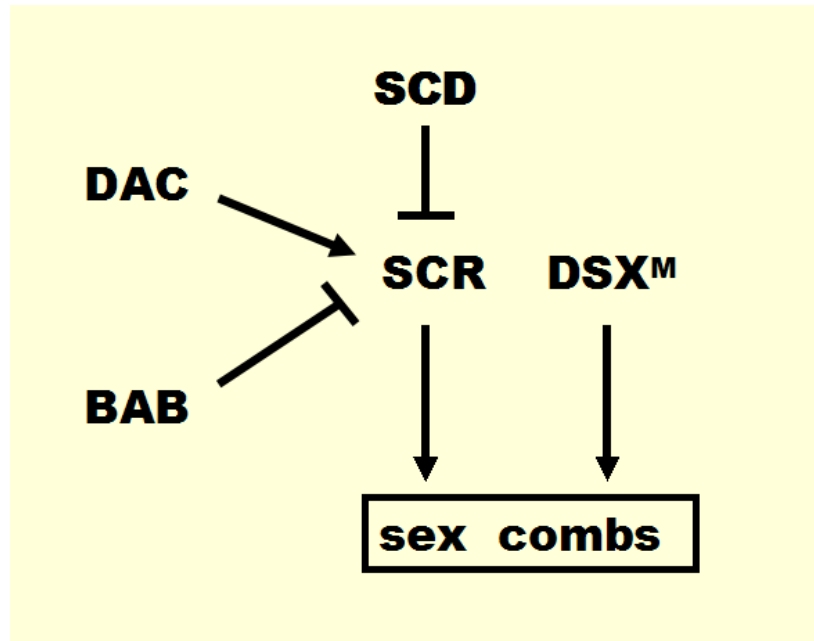


Figure 9. Model of *Scr* regulation mechanisms

Both BAB and SCD are repressors of SCR function. DAC is an activator of SCR. DAC, SCD and BAB are all involved in the mechanisms that control sex comb formation. DAC, BAB and SCD work together to determine the *Scr* expression region. SCR and DSX^M work together to control the downstream factors to initiate sex combs formation.

1.1.3 Development process variation

D. melanogaster sex comb and rotation

The *D. melanogaster* sex comb is on the tarsus 1 of the foreleg. The average size of the sex comb is around 50 μm and the teeth number varies from 9 to 12 (Hannah-Alava, 1958). Besides sex combs, the first tarsal segment is decorated with other types of bristles: longitudinal bristles and transverse row bristles (Hannah-Alava, 1958). In *D. melanogaster*, the sex comb teeth are derived from transverse row bristles, and the bristles rotate about 90° during the pupal stage (Figure 10) (Atallah et al., 2009a; Atallah et al., 2009b). The rotation starts around 10 hours post pupation (AP10), by that time the leg disc has completed its initial elongation (Atallah et al., 2009a). The sex comb bristles complete their localization at AP50 (50 hours post pupation) (Atallah, 2008).

The rotation process consists of two main stages. In the first stage (AP10-AP23), three morphological events happen in tarsus 1: (1) Cell proliferation, (2) Presumptive sex comb bristle appearance and (3) Bristle rows' formation (Atallah et al., 2009a; Atallah et al., 2009b; Tanaka et al., 2009). Between AP10-AP15, the SOPs that will turn into sex combs start appearing as individual bristles in a parallel position relative to the joint (Atallah et al., 2009b; Tanaka et al., 2009; Tanaka et al., 2011). By about AP16-17, the sex comb teeth form a continuous row of bristles, and the whole structure is ready to rotate (Atallah et al., 2009a; Tanaka et al., 2009; Tanaka et al., 2011). As cell division ends at approximately 17 hours of pupation, the rotation takes place without cell proliferation (Atallah et al., 2009a). Although the adult structure of sex comb row is tight and straight, a sex comb row is able to bend during rotation (Atallah et al., 2009b; Tanaka

et al., 2009; Tanaka et al., 2011). By 36 hours post pupation, the sex comb row becomes vertical and straight (Atallah et al., 2009b).

Sex comb rotation variation

Rotation process is important to the development of *D. melanogaster* sex comb, however not every species with sex comb structure rotate. There are two major kinds of sex combs: transverse sex comb and longitudinal sex combs (Tanaka et al., 2009). Some of the longitudinal sex combs are derived from longitudinal sensory bristles, and the others are derived from transverse row bristles (Atallah et al., 2009b). Among all kinds of sex combs, only the longitudinal ones that are derived from transverse row bristles have the rotation process (Tanaka et al., 2009). “Longitudinal” means that the sex combs are positioned along the proximal-distal leg axis (Tanaka et al., 2009). Among the longitudinal sex combs, some like *D. melanogaster* initiate as one or several transverse bristle rows, then form a single longitudinal row by rotation (Tanaka et al., 2009). In other *Drosophila* species, bristle cells that form the sex comb appear in longitudinal orientation by cell intercalation (Tanaka et al., 2009). This type of the sex comb formation is called “pre-specified” sex comb formation (Tanaka et al., 2009).

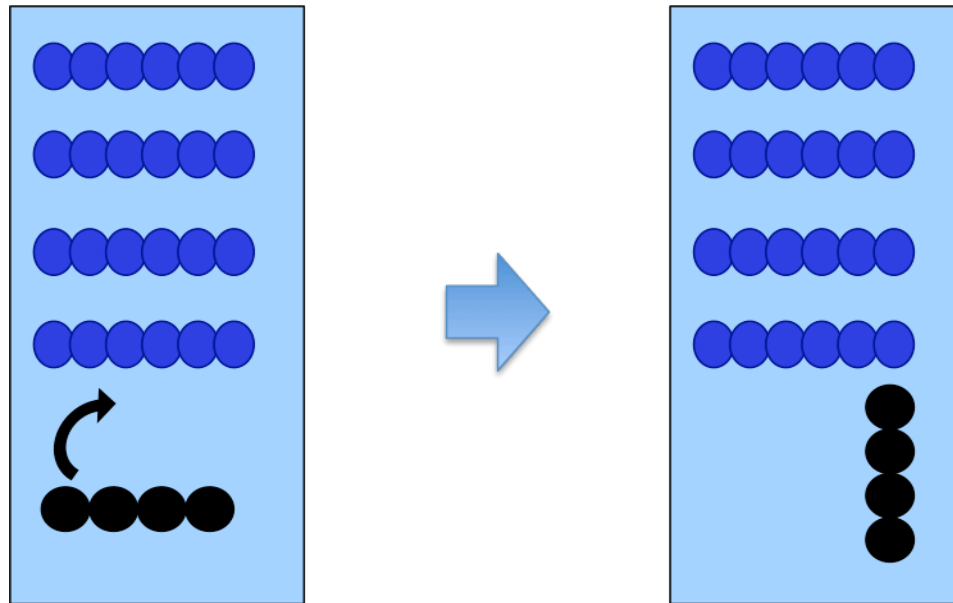


Figure 10. *D. melanogaster* sex comb rotation process

The sex combs of *D. melanogaster* are derived from transverse row bristles. The rectangular box represents the tarsus 1 in foreleg of *D. melanogaster*. Sex combs are represented by black particles and transverse bristles are represented by blue particles. During the development process, the sex comb rotates 90° to establish the longitudinal orientation.

Selection can recruit different mechanisms to establish similar function (Tanaka et al., 2009). Interestingly, species with and without sex comb rotation are distributed randomly on the phylogenetic tree (Figure 11) (Tanaka et al., 2009). This means the rotation process has been gained and lost by different species during evolution (Kopp, 2011; Tanaka et al., 2009). This implies a fairly rapid evolutionary change. We want to find explanations for rapid evolution of complex processes.

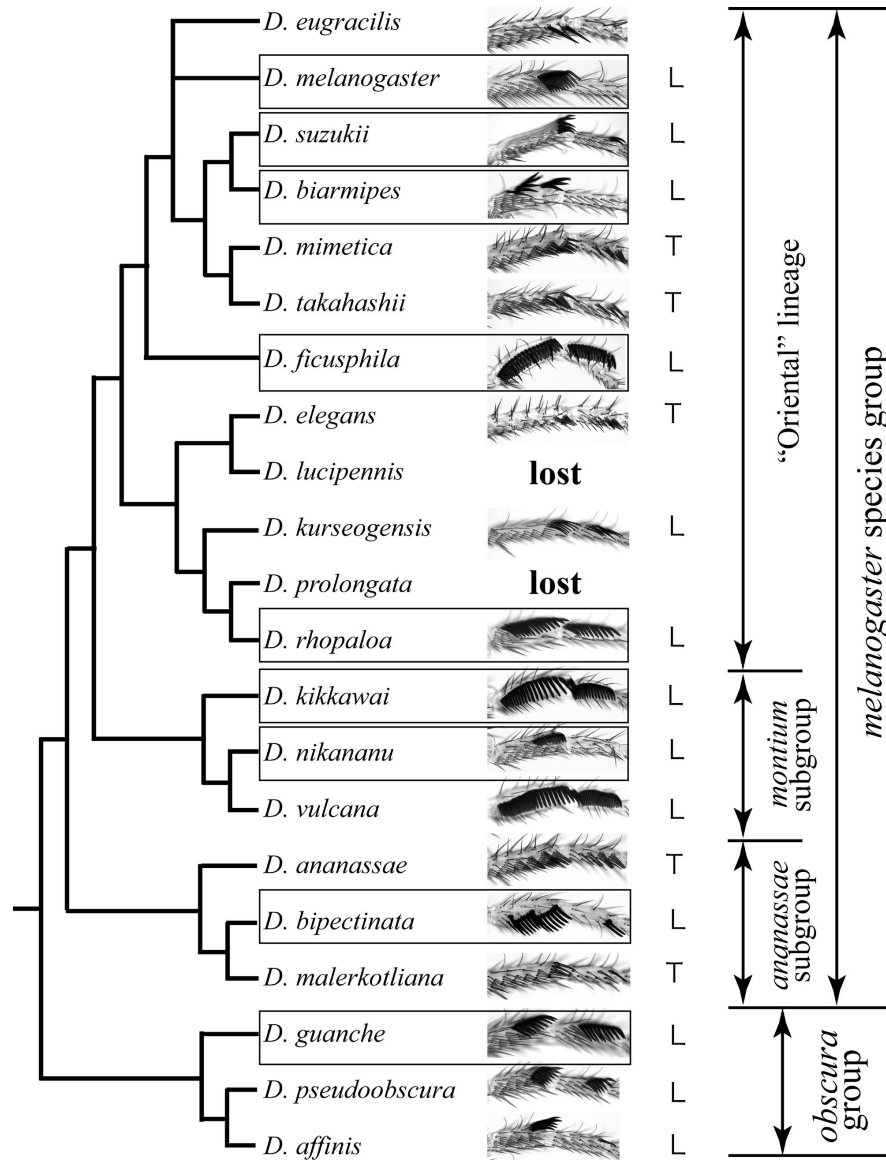


Figure 11. Morphology of sex comb in the *obscura* and *melanogaster* species groups

The morphological diversity of sex combs in the subgenera of *obscura* and *melanogaster* is illustrated above. “L” stands for longitudinal sex comb, and “T” stands for transverse sex comb. The species in boxes have a rotation process during development of their sex comb structure. The distribution of species with rotation is not restricted in certain clades but is along the phylogenetic tree. This figure was taken without modification from Kopp, 2011. This figure was reproduced with permission.

1.1.4 Summary

As mentioned before, the morphologies of sex combs differ significantly among the *Drosophila* species that are closely related (Atallah et al., 2009a). Even among species with similar sex comb orientation, development processes are very different, some having the rotation process and others pre-specified. There are four independent processes (leg development, bristle morphogenesis, sex-determination pathway and cross-regulation between SCR and DSX^M) that determine the presence and morphogenesis of sex combs. The model of a “positive feedback regulation loop” between SCR and DSX^M suggests that the interaction between SCR and DSX^M is crucial to the formation of sex combs (Kopp, 2011; Tanaka et al., 2009). This model provides an idea of how sex comb evolved during the evolution history (Kopp, 2011; Tanaka et al., 2009). The complexity of morphogenetic pathways and diversity of the sex comb rotation process makes the sex comb an important model of research in the development of evolutionary innovations.

1.2. Artificially selected traits are good targets to study the development of evolutionary innovations

1.2.1 Artificial selection and development

In evolutionary developmental biology research, artificially selected traits can be very useful models to study developmental perturbations or innovations (Beldade et al., 2002). Studying developmental processes of artificially-selected traits allows us to analyze how development introduces constraints onto the phenotypes (Beldade et al., 2002), especially to find out the properties required for morphology of repeated elements

(e.g. arthropod body bristles, vertebrate teeth). In addition, it also helps us to figure out how these elements respond to the environment and differentiate from each other during evolution (Beldade et al., 2002). For example, scientists have tried to explore the genetic correlations among wing patterns of butterflies by studying artificially selected eyespots of *Bicyclus anynana* (Beldade et al., 2002; Wagner, 2011). Such genetic analysis of artificially selected traits will help us understand adaptive evolution at the molecular level (Wagner, 2011). In general evolutionary innovations are due to alterations of the expression of pre-existing relevant regulatory networks (Wagner, 2011). For example, in the genome of modern maize, about 1200 genes have been affected due to prolonged periods of artificial selection (Wright et al., 2005). Furthermore, often those molecules whose expressions are altered are transcription factors (Wagner, 2011). For instance, *Distal-less (Dll)* controls the eyespot formation on the butterfly wings (Beldade et al., 2002; Wagner, 2011).

As mentioned before, sex comb represents a remarkable evolutionary innovation in *Drosophila* and is a good model to understand how such sex-specific innovations arise. The morphological differences of artificially selected sex combs are likely due to changes in gene expression via alteration of transcription factors that regulate sex comb development and formation. So far the research indicates that SCR and DSX^M may be two primary “suspects” (Kopp, 2011; Tanaka et al., 2011).

1.3. Project Objective

Artificially selected *Drosophila* bristles have been studied for many years. Most

studies have focused on abdominal bristles (Caballero et al., 1991). In this project, my focus is on the genes and proteins that are fundamental to the development of sex combs and how they may be affected by artificial selection.

The objective of my project is to discover how development constrains the response to artificial selection and whether there are any differences in key developmental gene expression between artificially selected lines and wildtype, in the development and formation of the sex comb.

The result of this study will help us elucidate the influence of artificial selection on the sex comb at the molecular level. DSX^M and SCR are two markers we will use to study developmental responses of the sex comb to artificial selection.

The hypothesis of my project is that artificial selection on sex comb bristle number has a direct influence on the *dsx* and/or *scr* expression on the forelegs of *D. melanogaster*. I will use artificially selected *Drosophila* lines of high sex comb number (Highline) and a low sex comb number (Lowline). The main assumption is that artificial selection will increase the expression of two genes (*dsx* and *scr*) in the Highline and reduce their expression in the Lowline. Compared to the wild type specifically, the forelegs (especially tarsus 1, where sex comb forms), there are more number of cells expressing the two genes in the Highline and less number of cells in the Lowline. In order to do this, I will trace the expression pattern of the DSX^M and SCR on forelegs at specific pupation stage (AP5) of three lines (Highline, Lowline and Wildtype) (Figure 12).

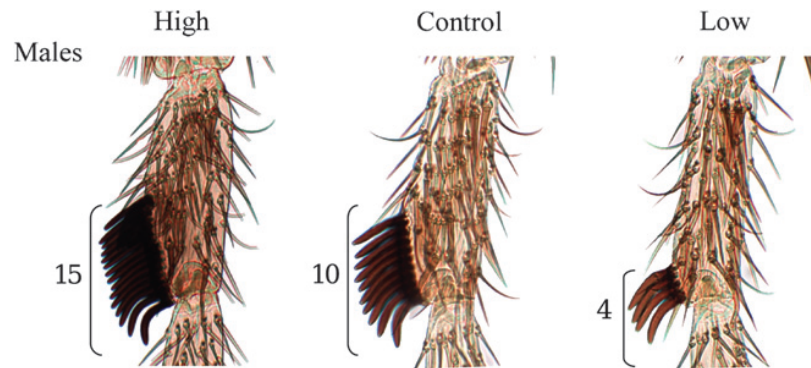


Figure 12. Sex comb morphology of Highline, Lowline and Control

The sex comb morphology of the three artificially selected lines (Highline, Lowline and Control) is presented above. The average number of the sex comb bristle numbers of each line is also presented: Highline, 15; Control, 10; and Lowline, 4. The figure was taken without modification from Ahuja and Singh, 2008. This figure was reproduced with permission.

Chapter 2. MATERIALS AND METHODS

2.1. Artificial selection

Protocols for artificial selection of *Drosophila* sex comb number, described below, are based on methods previously designed and published in the paper entitled “Variation and evolution of male sex combs in *Drosophila*: nature of selection response and theories of genetic variation for sexual traits” (Ahuja and Singh, 2008). All the selection experiments were done at room temperature (25°C) and flies were housed and raised on medium consisting of cornmeal, molasses and agar. Artificial selection experiments were done on the “base population” (Ahuja and Singh, 2008). In order to obtain a base population, thirty-two different *D. melanogaster* lines from different places were raised under standard lab circumstances for four generations. Around thirty males were collected for each line. The average sex comb bristle number from both forelegs of each male collected was recorded and the mean value of sex combs in each line was calculated. Three lines with the highest mean value of sex comb bristle number and three lines with the lowest mean value of sex comb bristle number were crossed. Approximate eighty offspring from each cross were picked and put together to breed. The population established after four generations of breeding is the “base population” needed for the artificial selection (Ahuja and Singh, 2008).

Artificial selections produced three different lines. The first line was selected for high sex comb bristle number (Highline, HL); the second line was selected for low sex comb bristle number (Lowline, LL) and a wildtype line was used as a control. In the first generation, approximately two hundred males were collected from the base population,

and their sex comb bristle numbers were scored. From these two hundred males, the highest scoring ten were chosen as parents for the Highline (HL). The lowest scoring ten individuals were chosen as parents for the Lowline (LL). For each line, males were mated with ten females that were collected randomly from the base population. Among the offspring of the first generation, ten most extreme males of each line were collected as parents for the next generation, mated with random females. In each of the following generations, one hundred males from each line were collected and scored. Among them, 10 most extreme males were selected to be parents for the next generation. The sex comb artificial selection was continued in both lines for twenty-four generations. There were two replicates of each line, high lines (High 1 and High 2) and low lines (Low 1 and Low 2) that were selected and maintained separately throughout the selections experiments. The data for the selection experiment and the development of these lines are shown in Figure 13.

After the 24th generation, both high and low lines were maintained for a time without selection before being subjected to selection once again until what was estimated to be the 96th generation of these lines. The selection was then continued until the 100th generation before relaxing selection again. The lines were maintained without selection for a period of one year before initiation of the final four rounds of selection for two years from June 11, 2011 to Mar 20, 2013 (Figure 13). During selection for generation 96 it was discovered that the Low 1 line was contaminated with wild type flies; therefore the Low 1 line was discarded. To replace the Low 1 line, the Low 2 line was split into two populations (Low 2A and Low 2B). Similarly, in March 2011 the High 2 line was

discarded due to the presence of a significant number of flies with low bristle number (Figure 13). Contamination was once again strongly suspected to be the cause. The symbol “*ns*” in Figure 15 stands for “non-selection”, which means, on June 11, 2012, High 1B was just maintained and not selected from the previous generation (Figure 13).

Artificial selections from generation 0 to 100, and selection prior to 2012 were done by Abha Ajuha (Ahuja and Singh, 2008) and Sogol Eizadshenass (Personal communication).

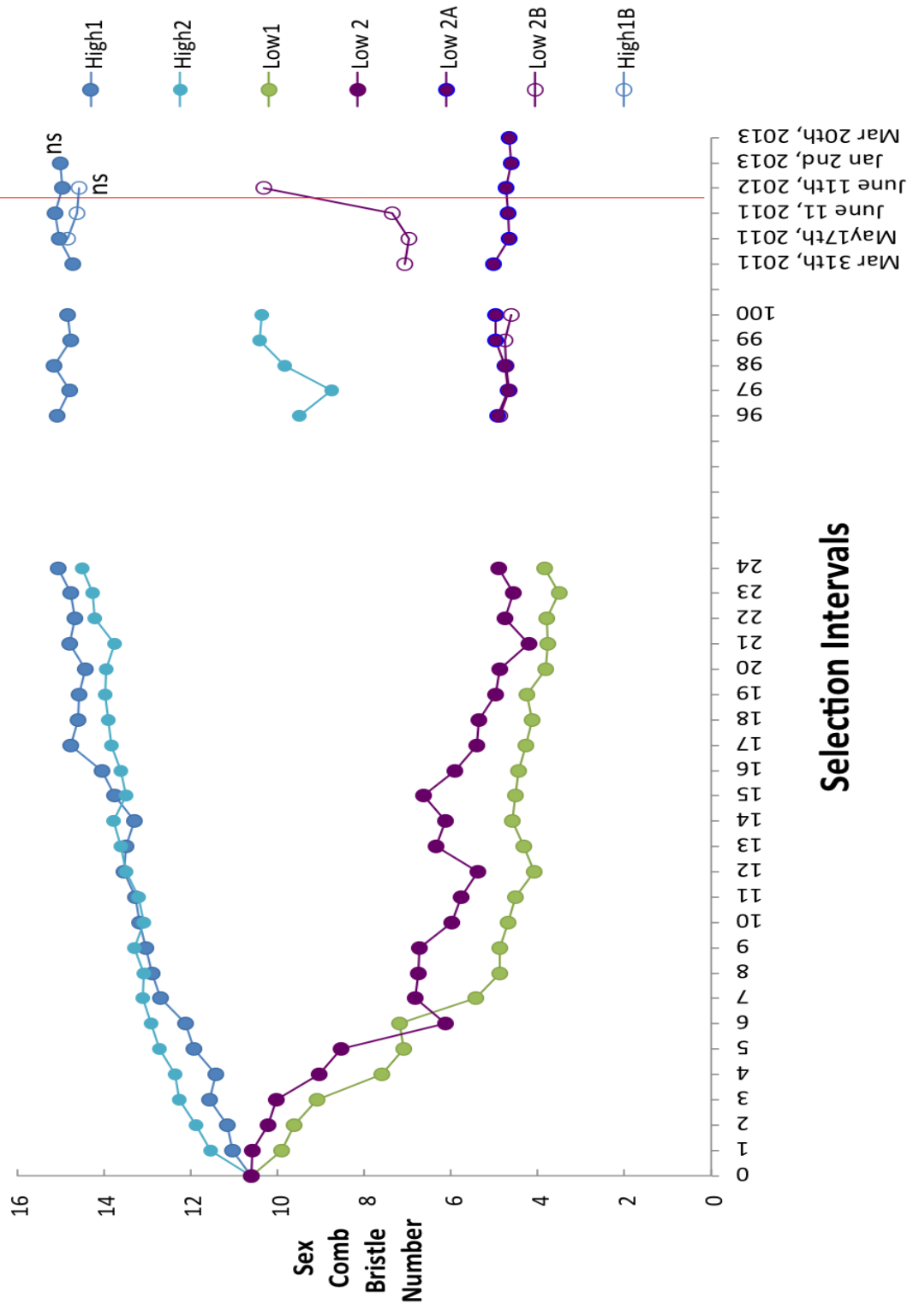


Figure 13. Selection experiment of sex comb bristle number.

The results of the selection experiments are shown in this figure. Low 1 was discarded at generation 96. In March 2011, the High 2 line was discarded. At generation 99, Low 2 was split into two populations (Low 2A and Low 2B) to replace Low 1. High 2 was discarded in May 2011. In May 2011, High 1 was split into two populations: High 1A and High 1B. High 1A and High 1 were represented by the same symbol in the figure. “ns” stands for *non-selection*. The last three rounds of selection (to the right of the red line) were finished by the author of this thesis.

2.2 Fly maintenance

The flies for the experiments were raised in *Drosophila* culture bottles at room temperature. The flies from different lines were kept in separate locations to avoid contaminations from each other. The flies were raised on medium consisting of cornmeal, molasses and agar. They were transferred to new bottles with fresh medium every 12-14 days. The medium was prepared by Sogol Eizadshenass and Jacqueline Thompson.

2.3 Antibody staining of DSX and SCR

Step 1: Collection of white prepupae

Prepupae refer to pupae that appear white in color (Held, 2010). This stage represents a stage when larvae stop moving and their pupal cases begin to form (Held, 2010). This white prepupal stage was determined to be 0 hours post pupation (AP0), $t=0$, for this study. Prepupae were collected using a wet, fine-haired brush and were sexed under the microscope by determining the presence of testes, which appear as two “black dots” on the dorsal side. Prepupae were incubated at 25°C to the specific desired time point, which in this study is five hours post pupation (AP5).

Step 2: Dissection, fixation and blocking

In order to prepare the pupae for fixation, the soft tissue of the pupae was removed from the puparium in 1X PBS. The posterior half of the abdomen was removed, and remaining region was fixed in 4% formaldehyde (from 20% formaldehyde solution diluted in 1X PBS) at room temperature (25°C) for 30 minutes. After fixation, the tissues

were first washed three times in 1X PBS followed by three consecutive washes in TNT solution (0.1 M Tris pH=7.4, 0.3 M NaCl, 0.5% Triton X-100) at room temperature (25°C). The recipe of TNT solution was obtained from Dr. Artyom Kopp's Lab, University of California Davis, CA, USA. The abdominal tissue was removed as much as possible without damaging the legs in order to expose the forelegs as much as possible to facilitate optimal staining. The remaining tissue was blocked in Image-iT FX signal enhancer solution (Catalog # I36933, Life technologies, Eugene, OR) at room temperature (25°C) for 30 minutes. The tissue was then washed in TNT solution 3 times.

Step 3. Antibody incubation and mounting

After being washed, the tissue was incubated at 4 °C overnight with primary antibody or antibodies, which were diluted in TNT solution at specific dilutions (as described below). The primary antibodies used in this investigation were rat *anti-Dsx^M*, at 1:100 dilution (Hempel and Oliver, 2007), and mouse *anti-Scr 6H4.1*, at 1:10 dilution (Glicksman and Brower, 1988; Tanaka et al., 2011). The rat *anti-Dsx^M* antibody was provided by Dr. Brian Oliver, Laboratory of Cellular and Developmental Biology, NIDDK, National Institutes of Health, MD, USA. The mouse *anti-Scr 6H4.1* antibody was purchased from the Developmental Studies Hybridoma Bank, University of Iowa, IA, USA. The next day, the tissue was washed in TNT solution 6 times. The tissue was then incubated with secondary antibody or antibodies, which were diluted in TNT solution, overnight at 4 °C. The secondary antibodies were donkey *anti-rat IgG* Alexa Fluor 488 and goat *anti-mouse IgG* Alexa Fluor 594 (Life technologies, Eugene, OR). The dilution

of secondary antibody was 1:200. The next day, the tissue was washed 6 times in TNT solution. After the washes, the stained samples were mounted on microscope slides using the Prolong Gold antifade-mounting reagent (Catalog # P36930, Life technologies, Eugene, OR). The slides were kept at 4°C before the fluorescent pictures were taken.

2.4 Fluorescent pictures modifications and analysis

Fluorescent pictures were taken on a Lecia DM6000 CS confocal microscope, using LAS AF software. Each leg sample was scanned at 8 equally spaced layers from top to bottom by the confocal microscope. Fluorescent pictures were taken separately for each layer. Then the pictures from all 8 layers were merged together to comprehensively record the fluorescent signal of the sample. The pictures were saved in “LIF” file format by the LAS AF software. They were later transformed into “TIFF” formats to be analyzed using the software packages, Image J and Adobe Photoshop.

The expression pattern was observed at the time point of AP5 (five hours post pupation) on the fluorescent pictures. The regions where DSX^M and SCR were expressed were demonstrated on the picture. The edges of the region where the proteins were expressed and the edges of the tarsal segments 1-4 were outlined in Image J. The outlined areas were then measured and recorded in pixel units using Adobe Photoshop. Expression Levels (EL) were then calculated for 1) EL of DSX^M in tarsus 1 and 2) EL of DSX^M in tarsus 2-4. EL in specific tarsal segments was estimated as the area where the protein (DSX^M) is expressed, divided by the area of the tarsal segment (see Figure 14). For instance, in Figure 14, the EL of DSX^M in tarsus 1 is equal to the area of the region where

DSX^M was expressed in tarsus 1 (outlined in red) divided by the area of tarsus 1 (outlined in blue). The EL in tarsus 2-4 is equal to the total area of the regions where DSX^M was expressed in tarsus 2-4 (outlined in yellow) divided by the area of the tarsus 2-4 (outline in purple).

Measurements of the DSX^M expression region

In order to measure the width of the area in which DSX^M is expressed, five vertical lines were drawn to divide the area into six equally spaced regions (illustrated by yellow lines in Figure 15) in Image J software. The lengths of the five different lines were measured and recorded in pixel units in Adobe Photoshop. The average of the five measurements was calculated and recorded as the width of the expressed area (see Figure 15). In Figure 15, the DSX^M expression region in tarsus 1 (bright green area) is outlined with white lines using Image J software. The 5 equally spaced yellow lines were drawn to measure the width of the expression pattern. Statistical analysis on the mean width was done using Statistix software. Similarly, DSX^M expression region in tarsus 2-4 was traced and outlined using Image J software. The total area of the DSX^M expression region in tarsus 2-4 was calculated and recorded in pixel units in Adobe Photoshop software. Then statistical analysis on the area of the DSX^M expression patterns was done using Statistix software. The expression pattern demarcations, measurement and calculation mentioned above were done repeatedly by one other individual (in this case Jacqueline Thompson) to obtain second unbiased measurements. The source of the pictures was not known to the analyzer.

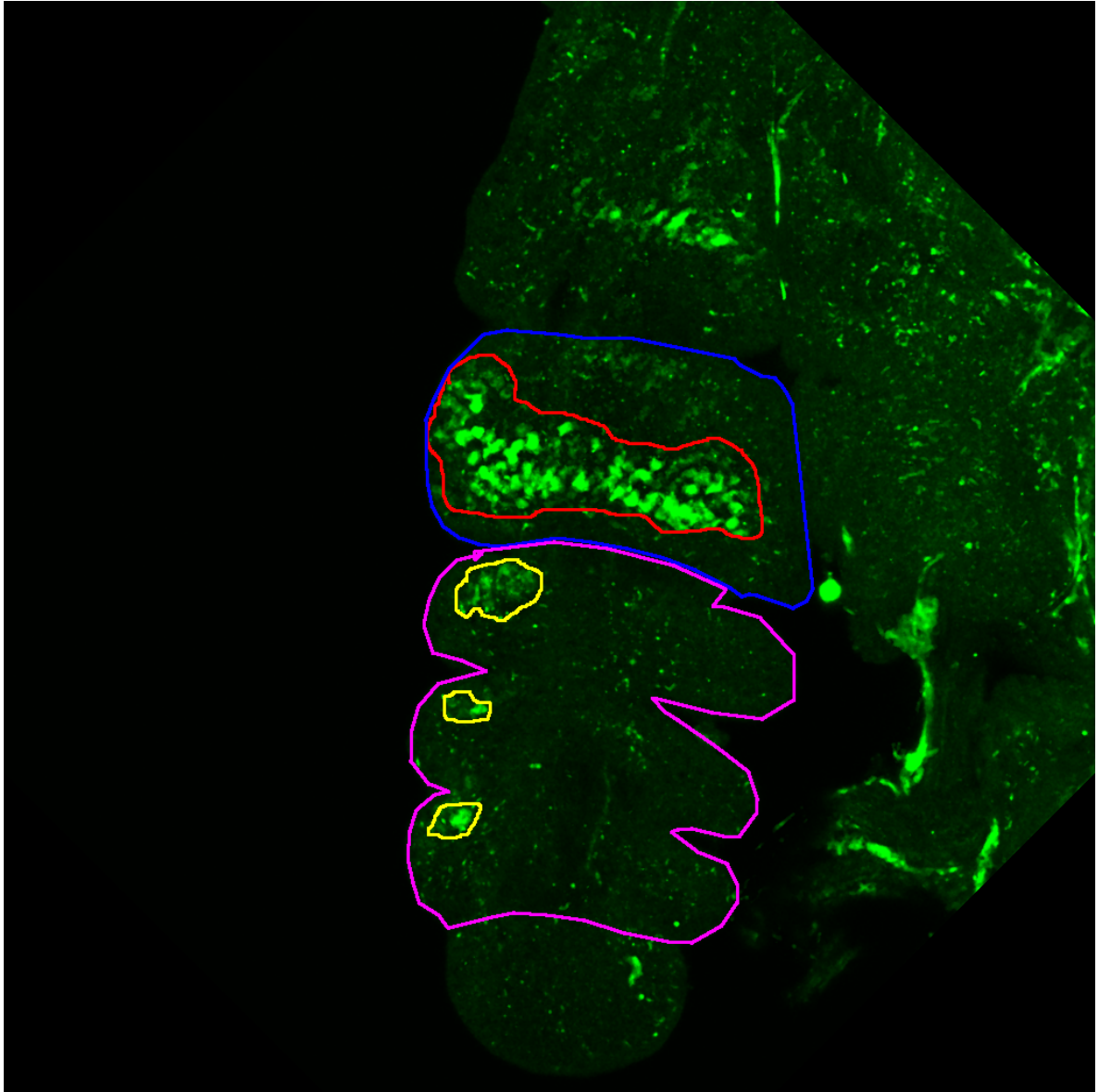


Figure 14. Example of the expression level (EL) calculation

DSX^M expressing region in tarsus 1 is outlined in red. Tarsus 1 is outlined in blue. DSX^M expressing area in tarsus 2-4 is outlined in yellow. Tarsus 2-4 is outlined in purple. EL of DSX^M in tarsus 1 is equal to the area of the region where DSX^M was expressed in tarsus 1 divided by the area of the tarsus 1. The EL in tarsus 2-4 is equal to the total area of the regions where DSX^M was expressed in tarsus 2-4 divided by the area of the tarsus 2-4.

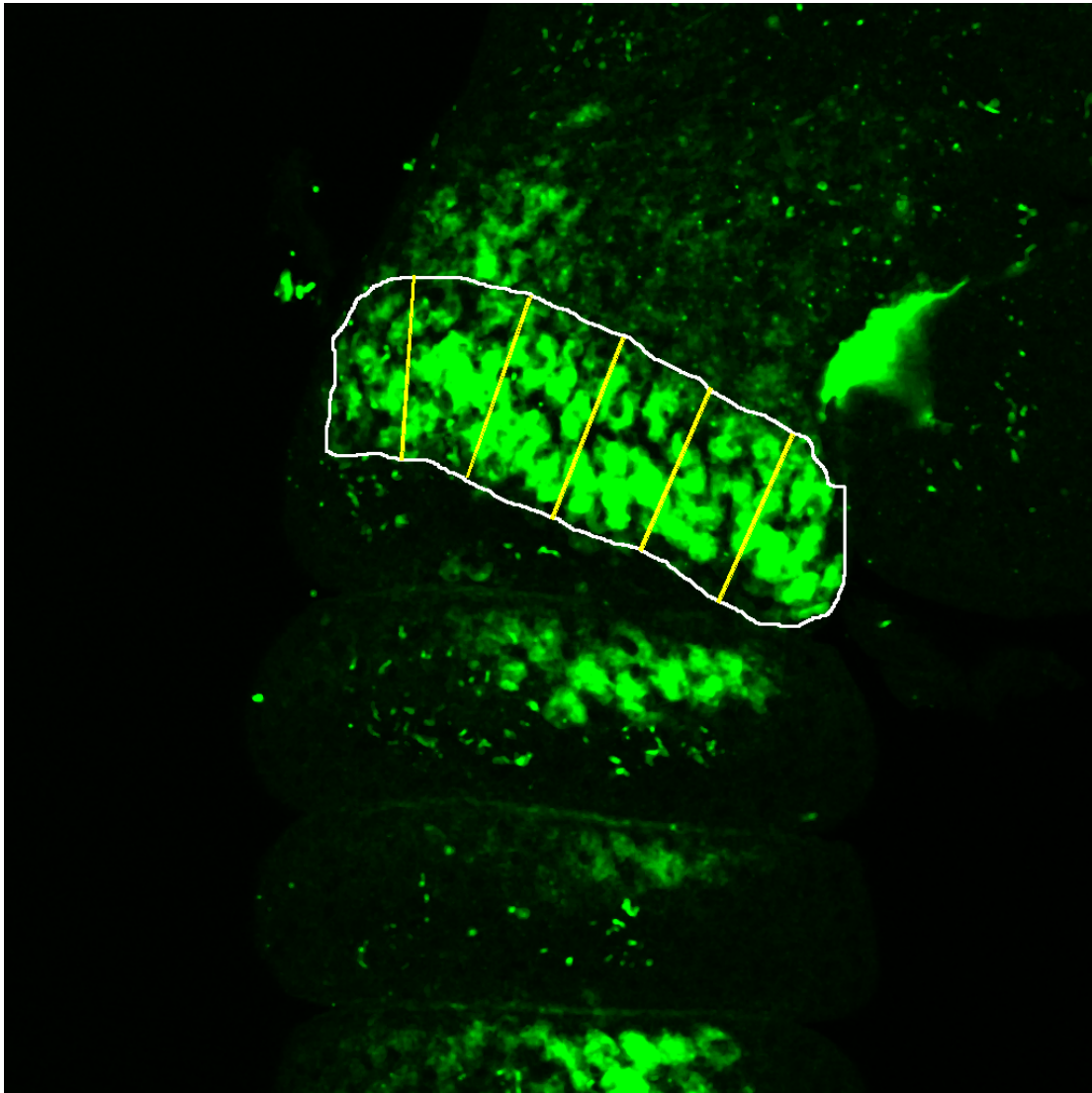


Figure 15. Example of the width of expression pattern measurement.

The bright green areas outlined in white represent the DSX^M expression region (in this case, in tarsus 1). 5 equally spaced yellow lines were drawn across the expression pattern to represent the widths of the expression pattern.

Chapter 3. RESULTS

Sex comb morphologies vary significantly among species of *Drosophila* (Atallah et al., 2009a), and these structures are thought to be under selection (Ahuja and Singh, 2008; Atallah et al., 2009a; Kopp, 2011; Tanaka et al., 2009; Tanaka et al., 2011). Despite years of research, the underlying developmental mechanisms that control the formation and development of sex comb still remain unclear but a few important proteins have been identified to be involved. Two transcriptional factors, *Doublesex* male isoform (DSX^M) and *Sexcombs reduced* (SCR), are considered important for the formation and development of the sex comb. Current models posit that the expression of DSX^M is activated by the SCR and, at the same time, SCR is also seems to be up-regulated by DSX^M from its default level (Kopp, 2011; Tanaka et al., 2011), leading to the speculation that there is “a positive regulation loop” between DSX^M and SCR (Kopp, 2011; Tanaka et al., 2011). Therefore, any mutations of DSX^M and SCR will be amplified by the positive regulation loop, which can in turn cause morphological changes in the species (Kopp, 2011). This positive regulation loop suggests that DSX^M and SCR expression maybe flexible and allows species to respond to selection pressure (Kopp, 2011). This model has not been empirically tested, which would be important to identify which one of these genes contributes most to the developmental flexibility (in response to selection) of the sex comb.

The rationale behind this thesis is that the positive feedback loop and relative roles of DSX^M and SCR in developmental flexibility of the sex comb can be investigated by identifying how each of these proteins responds to artificial selection. Accordingly the

objectives of this thesis were: a) to determine if developmental constraints in the sex combs respond to artificial selection, and b) to determine if artificial selection can be used to study the molecular basis of phenotypic plasticity of sex combs. In lines with these goals, two artificially selected lines of *D. melanogaster* that significantly differ in sex comb number (Highline and Lowline) were created. Highline and Lowline were investigated hoping that molecular differences in development of sex combs between these lines could be traced. The expression patterns of the two molecular markers DSX^M and SCR in the three different lines (Highline, Wildtype and Lowline) at early development stage (AP5, five hours post pupation) were studied using the immunofluorescent techniques.

3.1 Artificial selection

The last three rounds of artificial selections were completed by the author of this thesis (Figure 13). Lowline Low 2B was discarded after the selection on June 11, 2012 since the average bristle number of this line regressed towards the wild type phenotype with the grand average of 10.4 sex comb bristles (Figure 13). In order to keep the phenotype of low sex comb bristle number, the Lowline Low 2A was put under two more rounds of selection. The average bristle number of Low 2A was stabilized at 4.7 (Figure 13). For the Highline (High 1A), the sex comb was stabilized at 15.01 (Figure 13). Low 2A (Lowline) and High 1A (Highline) were the two lines used in the later immunofluorescent experiments.

3.2 Differential expression of DSX^M and SCR

3.2.1 SCR expression at AP5

Previous studies have shown that in pupal stage SCR expression is restricted to tarsus 1 and tibia in the foreleg (Kopp, 2011; Tanaka et al., 2011). Furthermore, SCR is only expressed in the positions where the transverse rows and the sex comb are formed (Kopp, 2011; Tanaka et al., 2011). In order to identify whether there are any developmental differences in the sex combs of the two artificially selected lines (Highline and Lowline) and Wildtype line, we used immunofluorescent methods to determine the expression pattern of SCR. All experiments were conducted on samples 5 hours post pupation (AP5), which represents a much earlier developmental stage than previous studies. Confocal images taken at AP5 revealed that the artificially selected lines and Wildtype are in fact very similar in their SCR expression pattern during this early stage of development (Figure 16 and 17). We found no detectable difference in the expression pattern of SCR between the three lines. These results indicated that artificial selection did not detectably alter SCR expression patterns at early stages of development (AP5).

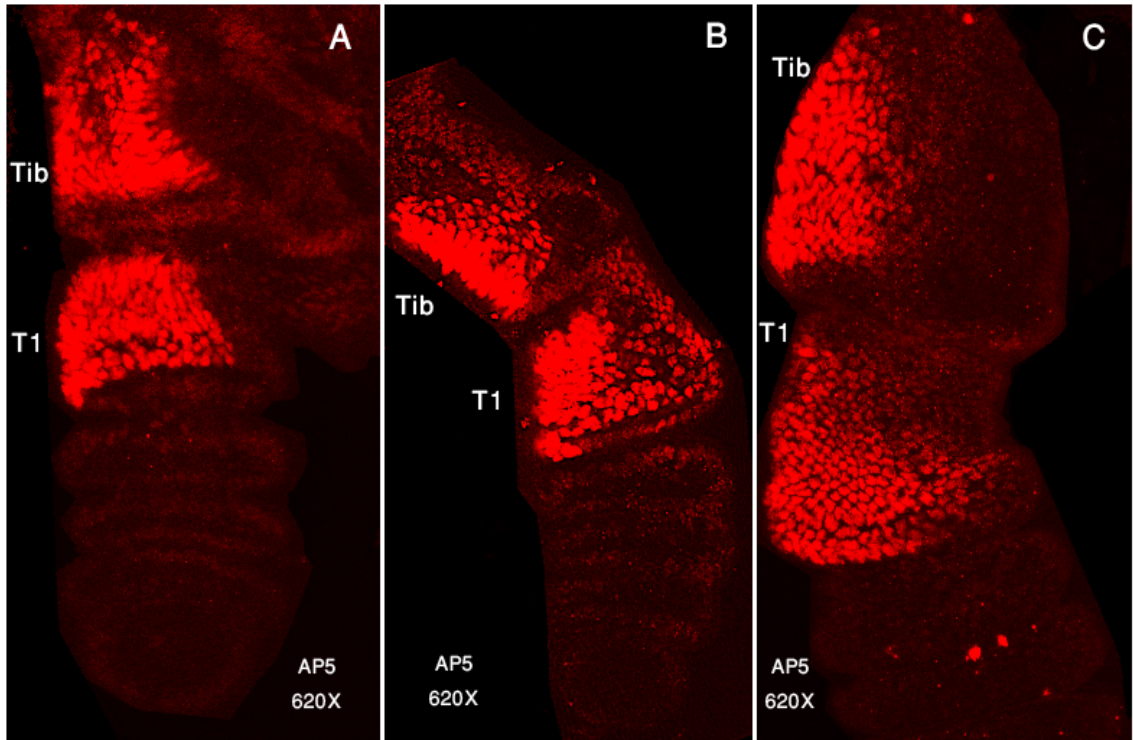


Figure 16. Comparison of the expression pattern of SCR on the forelegs

The expression pattern of SCR is compared among the three lines: Highline (A), Wildtype (B) and Lowline (C). All the pictures were taken at AP5 (five hours post pupation) and the magnifications of the pictures were 620X. T1 stands for tarsus 1, and Tib stands for the tibia. Among the three lines, there was no detectable difference of SCR expression pattern on the forelegs.

3.2.2 DSX^M Expression at AP5

At 5 hours post pupation (AP5) DSX^M expression can be seen all along the tarsal segments, from tarsus 1 to tarsus 4, however, DSX^M expression appears to be at its most intense level in tarsus 1 (medial view) (Figure 17 A, B and C). These results are also consistent with the findings of Tanaka et al., 2011. A large area of DSX^M expression is evident in the distal portion of tarsus 1, and along the joint between tarsus 1 and tarsus 2 (Figure 17 A, B and C). In comparison to tarsus 1, DSX^M is in small clusters of cells in tarsus 2-4 (Figure 17 A, B and C). Our results indicated striking differences in the expression pattern for DSX^M between the two artificially selected lines and Wildtype. We found that the expression pattern for DSX^M, varied between artificially selected lines in all of the tarsal segments expressing DSX^M but the most remarkable difference in expression is seen in tarsus 1 (Figure 17 A, B and C).

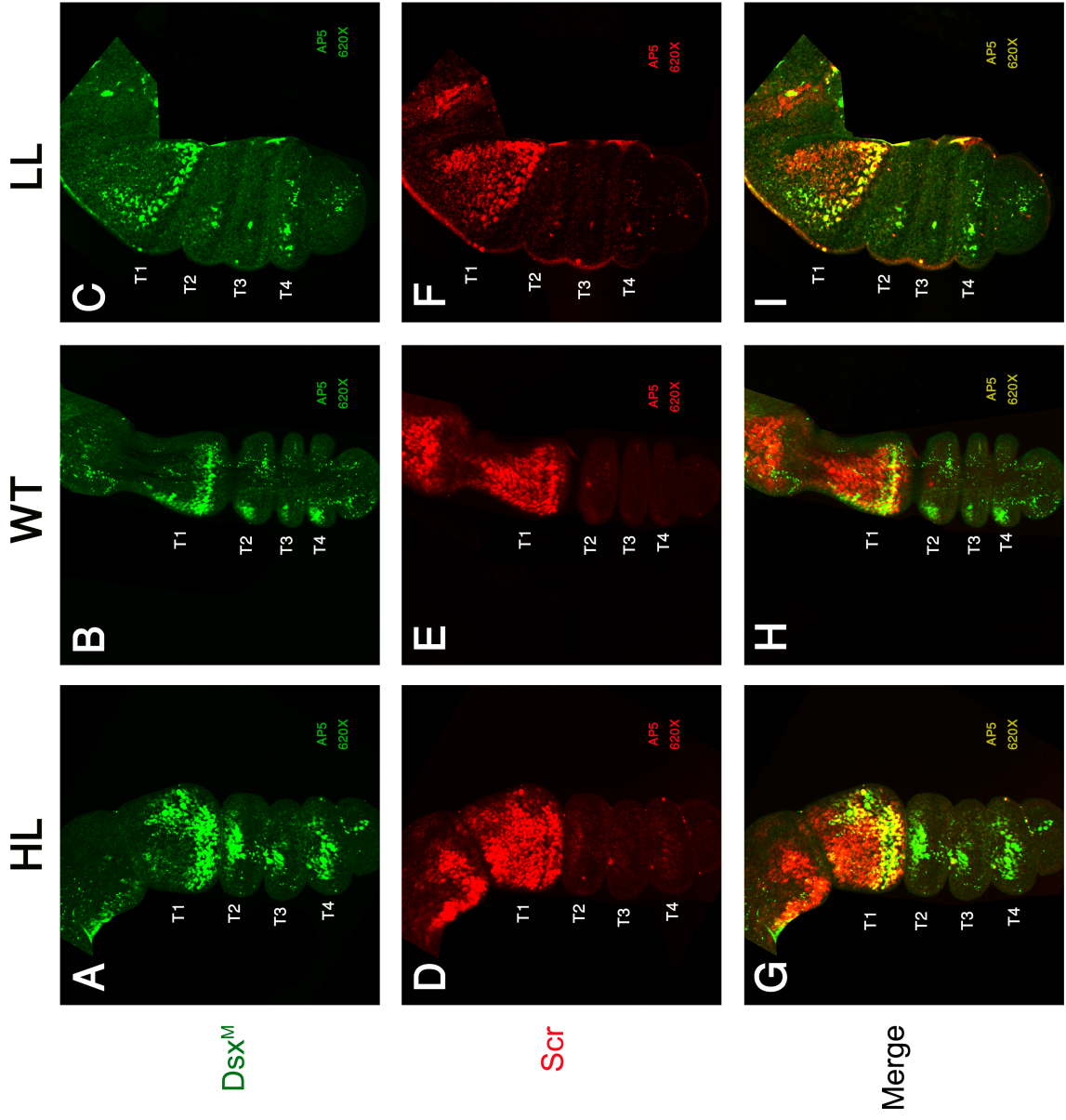


Figure 17. Comparison of the expression pattern of DSX^M and SCR on the forelegs
All the pictures were from AP5 and the magnifications of all the pictures were 620X. “T” stands for tarsus or tarsal segment. All pictures were taken from the medial view of the foreleg.

3.2.3 DSX^M expression on tarsus 1

Our findings on the differences in expression pattern of DSX^M were quite interesting particularly in tarsus 1 where DSX^M is expressed at highest levels and spatial area. Analysis of the expression pattern in the foreleg of Highline as seen in Figure 18A, clearly shows that the area of cells expressing DSX^M occupy nearly half of the first tarsal segment's medial surface. DSX^M expression is observed as a concave area of bright green stained cells (Figure 17 A). In the Lowline DSX^M expression is dramatically lower, occupying a much smaller area of the tarsus 1 medial surface (Figure 17 C). We also calculated the differences in expression levels of DSX^M on tarsus 1 (as described in the methods Chapter 2.4) between the artificially selected lines. The expression levels (EL) analysis on tarsus 1 was only applied to the three samples presented in Figure 17 A, B and C. Expression levels are summarized in Figure 18. The expression level of DSX^M is highest in Highline (46.7%), followed by Wildtype (34.7%) and is least in Lowline (25.9%, see Figure 19). These results suggest that the artificial selection produced over 20% difference in expression levels of DSX^M between Lowline and Highline.

In order to further verify the spatial variation in DSX^M expression between Highline, Wildtype and Lowline, we measured the width of the DSX^M expression pattern in tarsus 1 between three different lines (as described in the methods Chapter 2.4). The widths of the DSX^M expression region at five different positions across the area of tarsus 1 where DSX^M is expressed were measured. The mean value (average width) of the five measurements was calculated and recorded (Figure S1-S33, Table 1 and Table S1). A Shapiro-Wilk's Normality Test was used to test the distribution of the mean values of the

samples within each line. The Shapiro-Wilk's Normality Test is a statistical test that determines whether the samples are normally distributed or not. The null hypothesis (H_0) of the Shapiro-Wilk's Normality test is that the group of samples are from a normally distributed population (Shapiro and Wilk, 1965). If the P-Value obtained from the Normality test is greater than the confidence level alpha ($\alpha=0.05$), then we do not reject that null hypothesis that the samples come from a normally distributed population (Shapiro and Wilk, 1965). Based on the result of the Shapiro-Wilk's Normality test, the P-Values of the Normality test for the mean values within each line were 0.7902 for Highline, 0.7919 for Wildtype and 0.1676 for Lowline. All the P-Values are greater than confidence level alpha ($\alpha=0.05$) (Table 2). The null hypothesis of the Shapiro-Wilk's Normality test was not able to be rejected (Table 2).

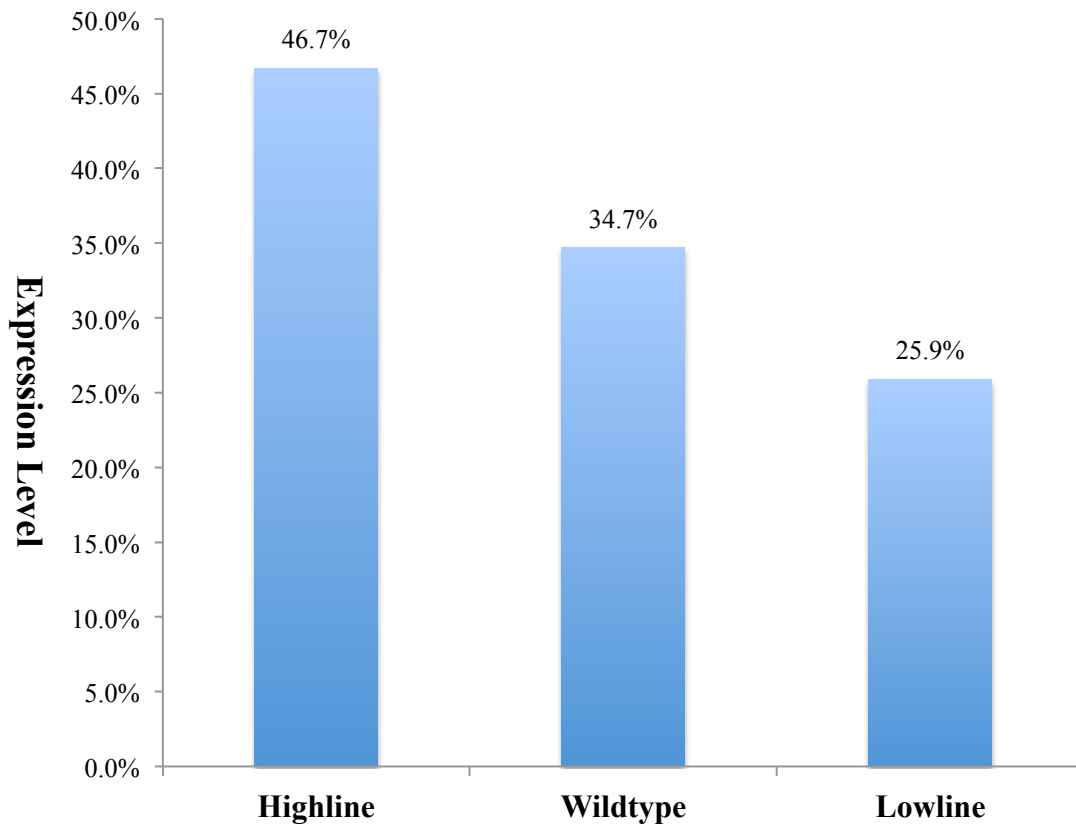


Figure 18. DSX^M expression level on tarsus 1

Summary of the results of the DSX^M expression level on tarsus 1 of the three samples shown in Figure 17. The expression level in Highline is significantly higher than the Lowline.

Highline		Wild type		Lowline	
Fig S1	107.726	Fig S16	72.114	Fig S25	65.614
Fig S2	105.076	Fig S17	75.100	Fig S26	60.976
Fig S3	97.534	Fig S18	75.540	Fig S27	64.848
Fig S4	95.434	Fig S19	64.290	Fig S28	82.060
Fig S5	82.802	Fig S20	84.400	Fig S29	51.798
Fig S6	92.172	Fig S21	57.672	Fig S30	55.624
Fig S7	70.420	Fig S22	54.028	Fig S31	60.336
Fig S8	87.716	Fig S23	74.492	Fig S32	53.070
Fig S9	92.020	Fig S24	90.812	Fig S33	64.132
Fig S10	91.834				
Fig S11	76.570				
Fig S12	82.104				
Fig S13	81.804				
Fig S14	71.396				
Fig S15	80.360				
	87.665 (mean)		72.050 (mean)		62.051 (mean)
	11.172 (SDV)		11.852 (SDV)		9.058 (SDV)

Table 1. Mean and standard deviation of the average width of DSX^M expression pattern in tarsus 1 for three lines: Highline, Wildtype and Lowline. Each datum represents a mean of 5 measurements of the width of DSX^M expression pattern in tarsus 1. Each datum comes from a different leg. Every leg is from a different fly. The unit is pixel.

Variable	N	W	P
Highline	15	0.9657	0.7902
Wildtype	9	0.9594	0.7919
Lowline	9	0.8827	0.1676

Table 2. Shapiro-Wilk's Normality Test for the data from Table 1.

The W-Values and P-Values of Shapiro-Wilk's Normality Test are presented above. The W-Value is the test statistic of the Shapiro-Wilk's Normality Test. Since P-Values of the three lines are all greater than 0.05, all three lines are normally distributed.

Since the null hypothesis of the Shapiro-Wilk's Normality test for the mean values were failed to be rejected, and the mean values were independent of each other (from different tissue), a one-way analysis of variance (one-way ANOVA) test was used to investigate whether there were any statistical differences among the three different lines. The one-way ANOVA test is a statistical test used to compare the means of two or more groups of independent samples (Christensen, 1996). The null hypothesis (H_0) of the one-way ANOVA test is that the samples in different sample groups share the same mean values (Christensen, 1996). If the P-Value obtained from the one-way ANOVA test is greater than the alpha level (0.05 in this experiment), then the null hypothesis is rejected, which means that there is a significant difference between the mean values of the different sample groups (Christensen, 1996). The results of the one-way ANOVA are summarized in Table 3. The result shows that P-Value of the ANOVA test is 0.0000 (Table 3), indicating that DSX^M spatial expression pattern in tarsus varies significantly across the three lines (Table 3). Following the one-way ANOVA test, the Tukey's Honest Significant Difference (HSD) test and Least Significant Difference (LSD) comparison test were performed in order to analyze the data further. Tukey's HSD comparison test and LSD comparison test are both used in conjunction with the ANOVA test to find out the sample group with the means that are significantly different from other sample groups (Christensen, 1996). The results of Tukey's and LSD tests will classify the sample groups into different homogeneous groups, with different symbols (e.g. "A", "B", "C" and so on) (Christensen, 1996). The sample groups within the same classification have no statistical differences between each other and groups within different classifications are

significantly different (Christensen, 1996). The alpha value of the Tukey's HSD comparison is 0.05 ($\alpha=0.05$) (Table 4). The result of the Tukey's test for the mean value of the DSX^M expression region widths in tarsus 1 is summarized in Table 4. The homogeneous classification for Highline is classified as group "A", while Wildtype and Lowline are both grouped as "B" (Table 4). A similar classification and comparison result were also obtained by the LSD test (Table 5). Based on the Tukey's and LSD classification, for the mean value of the widths of the DSX^M expression region in tarsus 1, Highline is deemed significantly different from Wildtype and Lowline. However, there is no significant difference between Wildtype and Lowline.

Data of Table 1 was plotted into a bar graph based on the data distribution within each line (Figure 19). X-axis of the graph is the mean width, and Y-axis is the number of observation. The green bars represent Lowline, the red bars represent Wildtype, and the blue bars represent Highline (Figure 19). The bar representing the highest distribution is shifted from left to right along X-axis (from Lowline- Wildtype- Highline) (Figure 19). Our statistical analyses of expression level (Table 3-5, Figure 19) and spatial expression patterns of DSX^M in tarsus 1 (Figure 17 A, B and C) quite clearly show that, compared to Lowline, DSX^M is expressed at higher levels and in a larger area of tarsus 1 in Highline. DSX^M expression in Lowline tarsus 1 is restricted to a relatively small spatial area. These results clearly show that artificial selection has significantly altered the expression patterns of DSX^M in tarsus 1 of *D. melanogaster*.

Source	DF	SS	MS	F	P
Between	2	3926.72	1963.36	16.7	0.0000
Within	30	3527.58	117.59		
Total	32	7454.30			

Variable	N	Mean	SE
Highline	15	87.665	2.7998
Lowline	9	62.051	3.6146
Wildtype	9	72.050	3.6146

Table 3. One-Way ANOVA for the average width of DSX^M expression pattern in tarsus 1 of Highline, Lowline and Wildtype

The F- Value is 16.7 and P is 0.0000, which means there is a significant difference among the average width of the three lines. DF: Degree of Freedom. SS: Sum of Squares. MS: Mean Square. SE: Standard Error. N: sample size of each group. “Between” represents the results between sample groups. “Within” represents the results within the sample group.

Variable	Mean	Homogeneous Groups
Highline	87.665	A
Wildtype	72.050	B
Lowline	62.051	B

Alpha

0.05

There are 2 groups (Wildtype and Lowline) in which the means are not significantly different from one another.

Table 4. Tukey's HSD All-Pairwise Comparisons Test for the average width of DSX^M expression pattern in tarsus 1 (Highline, Lowline and Wildtype).

The Alpha value is 0.05. The homogeneous classification for highline is A and for Wildtype and Lowline is B. Based on the classification, highline is significantly different with Wildtype and Lowline. However, there is no significant difference between Wildtype and Lowline.

Variable	Mean	Homogeneous Groups
Highline	87.665	A
Wildtype	72.050	B
Lowline	62.051	B

Alpha 0.05

There are 2 groups (Wildtype and Lowline) in which the means are not significantly different from one another.

Table 5. LSD All-Pairwise Comparisons Test for the average width of DSX^M expression pattern in tarsus 1 (Highline, Lowline and Wildtype)

The Alpha value is 0.05. The homogeneous classification for highline is A and for Wildtype and Lowline is B. Based on the classification, Highline is significantly different with Wildtype and Lowline. However, there is no significantly difference between Wildtype and Lowline.

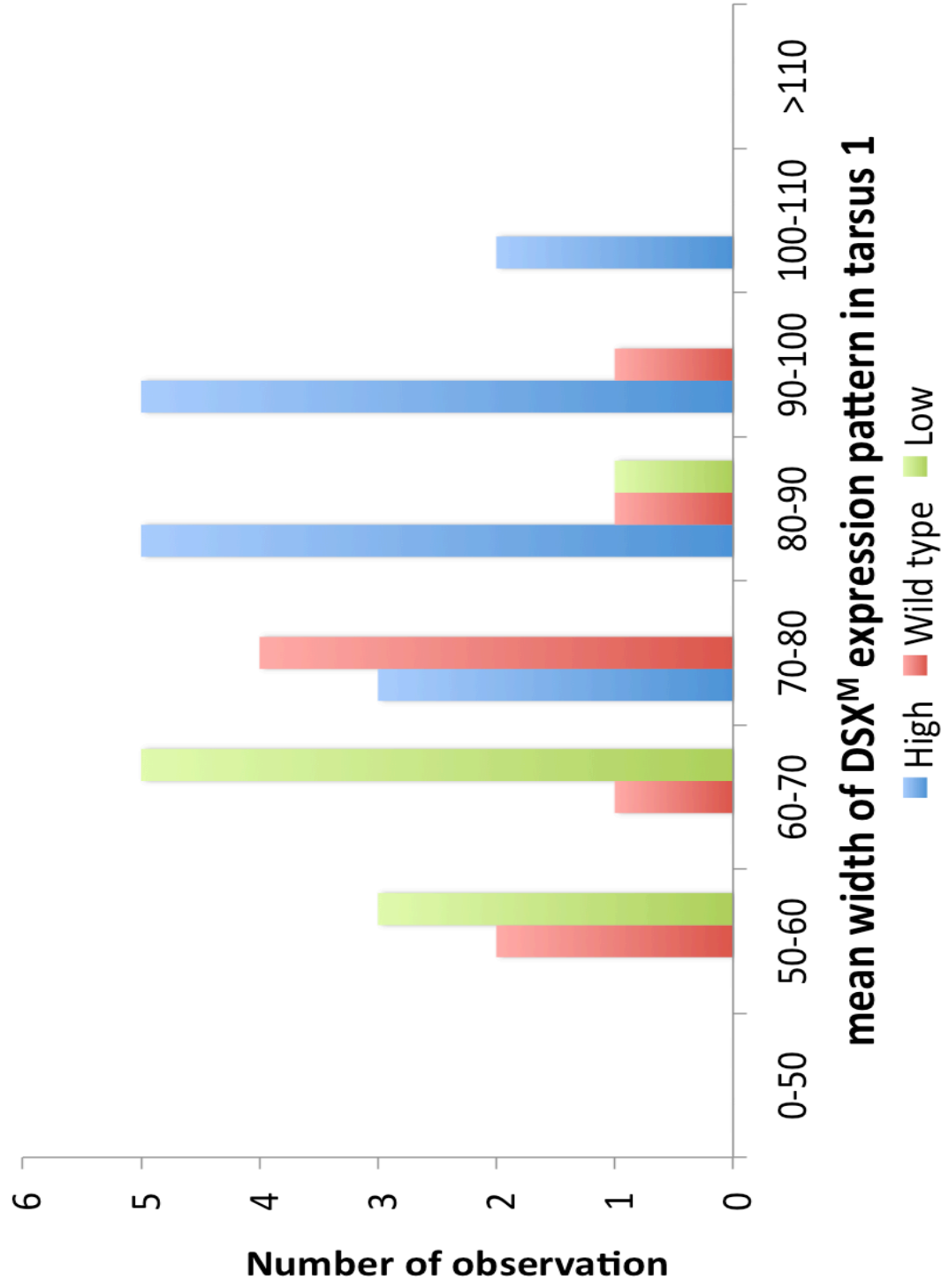


Figure 19. Distribution of the mean width of the DSX^M expression pattern on tarsus 1

In the graph, the green bars represent Lowline, the red bars represent Wildtype and the blue bars represent Highline. X-axis is the mean width (unit: pixels), and Y-axis is the number of observation. Compared the sample distribution of Lowline and the sample distribution of Highline, the highest appearance is shifted from left to the right (from the interval 60-70 to the intervals 80-90 and 90-100). There is a significant difference between the distribution of Lowline and Highline.

3.2.4 DSX^M expression on tarsus 2-4

DSX^M expression can be detected in several big clusters of cell on the tarsus 2 to tarsus 4 in Highline (Figure 17 A). In comparison, DSX^M expression is significantly reduced on the tarsus 2 to tarsus 4 of Lowline samples (Figure 17 C). In Lowline tarsus 2-4 of the foreleg (medial view), very few cells express DSX^M compared to Highline (Figure 17 C, Figure 20). As for tarsus 1, we made similar calculations of DSX^M expression level (EL) on tarsus 2-4. The expression levels (EL) analysis on tarsus 2-4 was only applied to the three samples presented in Figure 17 A, B and C. Our results indicate that the DSX^M expression level on tarsal segments 2-4 is 12.7% in highline, 8.4% in Wildtype, and 2.4% in Lowline (Figure 21). DSX^M expression level is more than five times higher in Highline compared to Lowline.

We also measured the area of the region expressing DSX^M on tarsus 2-4 among three lines (as described in the methods Chapter 2.4) (Figure S1-S33, Table 6 and Table S1). The Shapiro-Wilk's Normality Test was performed upon the data from Table 6 to test the distribution of value of the expression area within each line (Table 7). Since the P-Values of the three lines for the Normality Test (0.2949 for Highline, 0.7517 for Wildtype and 0.4373 for Lowline) are all greater than the critical value, 0.05, the null hypothesis can not be rejected that these data (expression area in tarsus 2-4) are from normally distributed populations (Table 7). A one-way ANOVA test was performed to test the significances (Table 8). Results of the ANOVA test indicate that there is a significant difference between the three lines (0.0015, $P < 0.05$) (Table 8). The Tukey's HSD comparison and the LSD comparison tests verify that for DSX^M expression area in

tarsus 2-4, Lowline is significantly lower than Highline and Wildtype, but there are no significant differences between Highline and Wildtype (Table 9 and 10). We reached a similar conclusion when the data from Table 6 was plotted into a bar graph (Figure 22). Here, the bars representing highest distribution shifted from left to right along X-axis (from Lowline- Wildtype- Highline) (Figure 22). Combining the results of the statistical analysis and the distribution graph, it can be inferred that the area of the DSX^M expression region in tarsus 2-4 in Lowline is significantly smaller than the area in Highline. Thus, there is significant alteration of the expression region of DSX^M in tarsus 2-4. An artificial selection had a direct influence on the DSX^M expression in the forelegs of *D. melanogaster*.

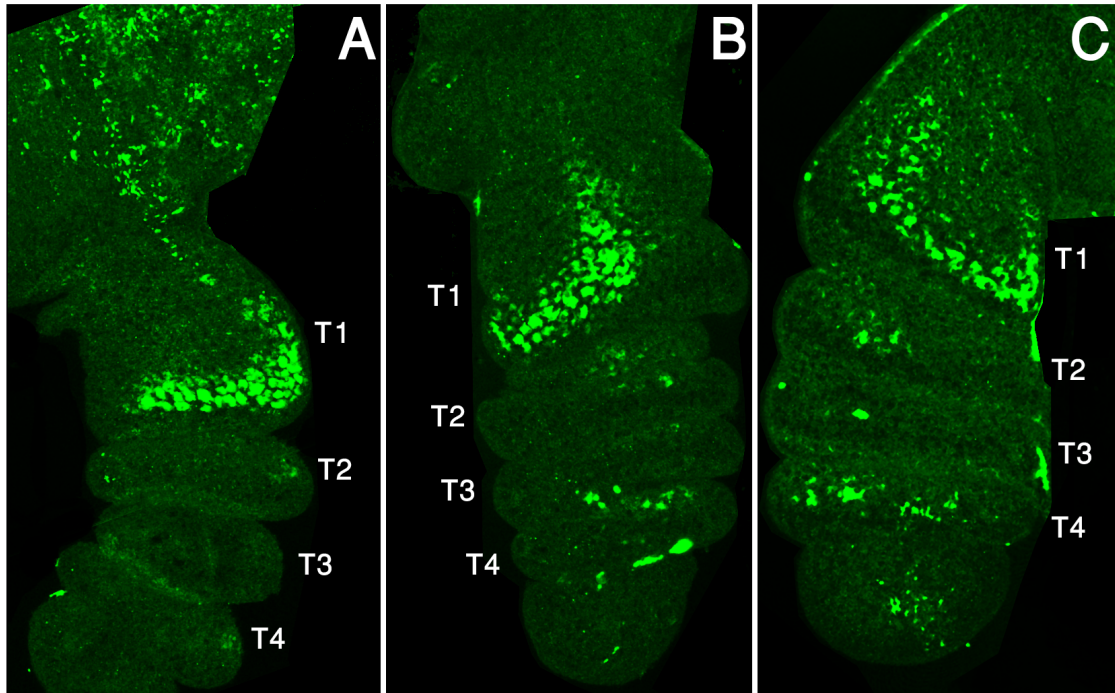


Figure 20. DSX^M expression in Lowline

The Lowline DSX^M expressions of the three different samples (A, B and C) are shown in this figure. All the pictures were taken at AP5 and the magnifications of all the pictures were 620X. “T” stands for the tarsus. “T1” stands for tarsus 1 and so on. A, B, C, are all medial view picture of Lowline foreleg. It can be detected that the DSX^M expression is very limited in ts2-ts4. The DSX^M expression is reduced in ts2-ts4 compared to Highline.

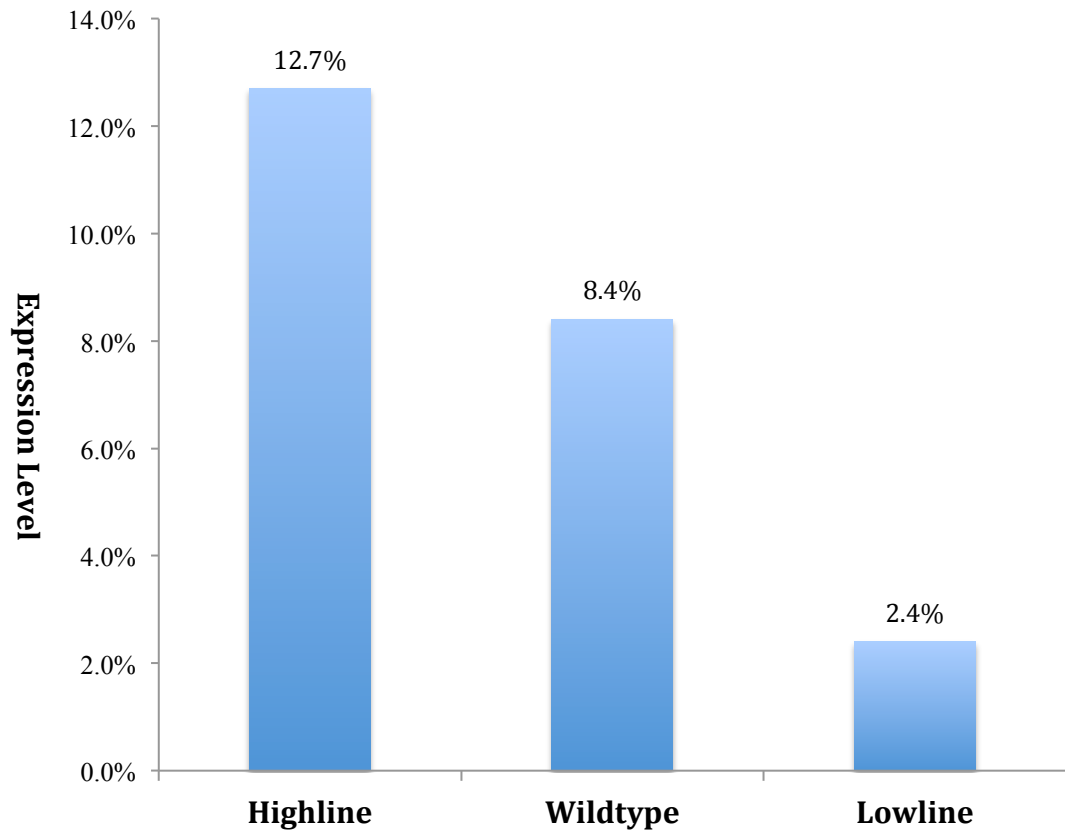


Figure 21. DSX^M expression level on tarsus 2- 4.

Summary of the results of the DSX^M expression level on tarsus 2-4 of the three samples is shown in Figure 18. The expression level in Highline is significantly higher than the Lowline.

	Highline	Wild type	Lowline
Fig S1	15344.64	Fig S16	1916.93
Fig S2	4663.30	Fig S17	6147.07
Fig S3	14635.00	Fig S18	11575.30
Fig S4	12570.63	Fig S19	10349.57
Fig S5	7225.34	Fig S20	14782.46
Fig S6	3723.26	Fig S21	5584.90
Fig S7	11040.77	Fig S22	4478.98
Fig S8	6460.42	Fig S23	8616.96
Fig S9	6294.53	Fig S24	2294.78
Fig S10	7391.23		
Fig S11	5621.76		
Fig S12	5861.38		
Fig S13	9612.29		
Fig S14	2027.52		
Fig S15	2838.53		
	7687.37 (mean)	7305.22 (mean)	1788.93 (mean)
	4118.36 (SDV)	4352.56 (SDV)	1120.75 (SDV)

Table 6. Mean value and standard deviation of the area of DSX^M expression pattern in tarsus 2-4 for three lines: Highline, Wildtype and Lowline. Each data represents the area of DSX^M expression pattern in tarsus 2-4. Each data comes from a different leg. Every leg is from a different fly. The unit is pixel.

Variable	N	W	P
Highline	15	0.9323	0.2949
Wildtype	9	0.9556	0.7517
Lowline	9	0.9252	0.4373

Table 7. Shapiro-Wilk's Normality Test for the data from Table 6.

The W-Values and P-Values of Shapiro-Wilk's Normality Test are presented above. The W-Value is the test statistic of the Shapiro-Wilk's Normality Test. Since P -Values of the three lines are all greater than 0.05, all three lines are normally distributed.

Source	DF	SS	MS	F	P
Between	2	2.176E+08	1.088E+08	8.18	0.0015
Within	30	3.991E+08	1.330E+07		
Total	32	6.167E+08			

Variable	N	Mean	SE
Highline	15	7687.4	941.7
Lowline	9	1788.9	1215.7
Wildtype	9	7305.2	1215.7

Table 8. One-Way AOVVA test for the area of DSX^M expression pattern in tarsus 2-4 of Highline, Lowline and Wildtype

The F-Value is 8.18 and P- Value is 0.0015, which means there is a significant difference among the data of the three lines. DF: Degree of Freedom. SS: Sum of Squares. MS: Mean Square. SE: Standard Error. N: sample size of each group. “Between” stands for the results between sample groups. “Within” stands for the results within the sample group.

Variable	Mean	Homogeneous Groups
Highline	7687.4	A
Wildtype	7305.2	A
Lowline	1788.9	B

Alpha

0.05

There are 2 groups (Highline and Wildtype) in which the means are not significantly different from one another.

Table 9. Tukey's HSD All-Pairwise Comparisons Test for the area of DSX^M expression pattern in tarsus 2-4 (Highline, Lowline and Wildtype)

The Alpha-Value is 0.05. The homogeneous classification for Highline and Wildtype is A and for Lowline is B. Based on the classification, Lowline is significantly different with Wildtype and Highline. However, there is no significant difference between Wildtype and Highline.

Variable	Mean	Homogeneous Groups
Highline	7687.4	A
Wildtype	7305.2	A
Lowline	1788.9	B

Alpha 0.05

There are 2 groups (Highline and Wildtype) in which the means are not significantly different from one another.

Table 10. LSD All-Pairwise Comparisons Test for the area of DSX^M expression pattern in tarsus 2-4 (Highline, Lowline and Wildtype)

The Alpha-Value is 0.05. The homogeneous classification for Highline and Wildtype is A and for Lowline is B. Based on the classification, Lowline is significantly different with Wildtype and Highline. However, there is no significant difference between Wildtype and Highline.

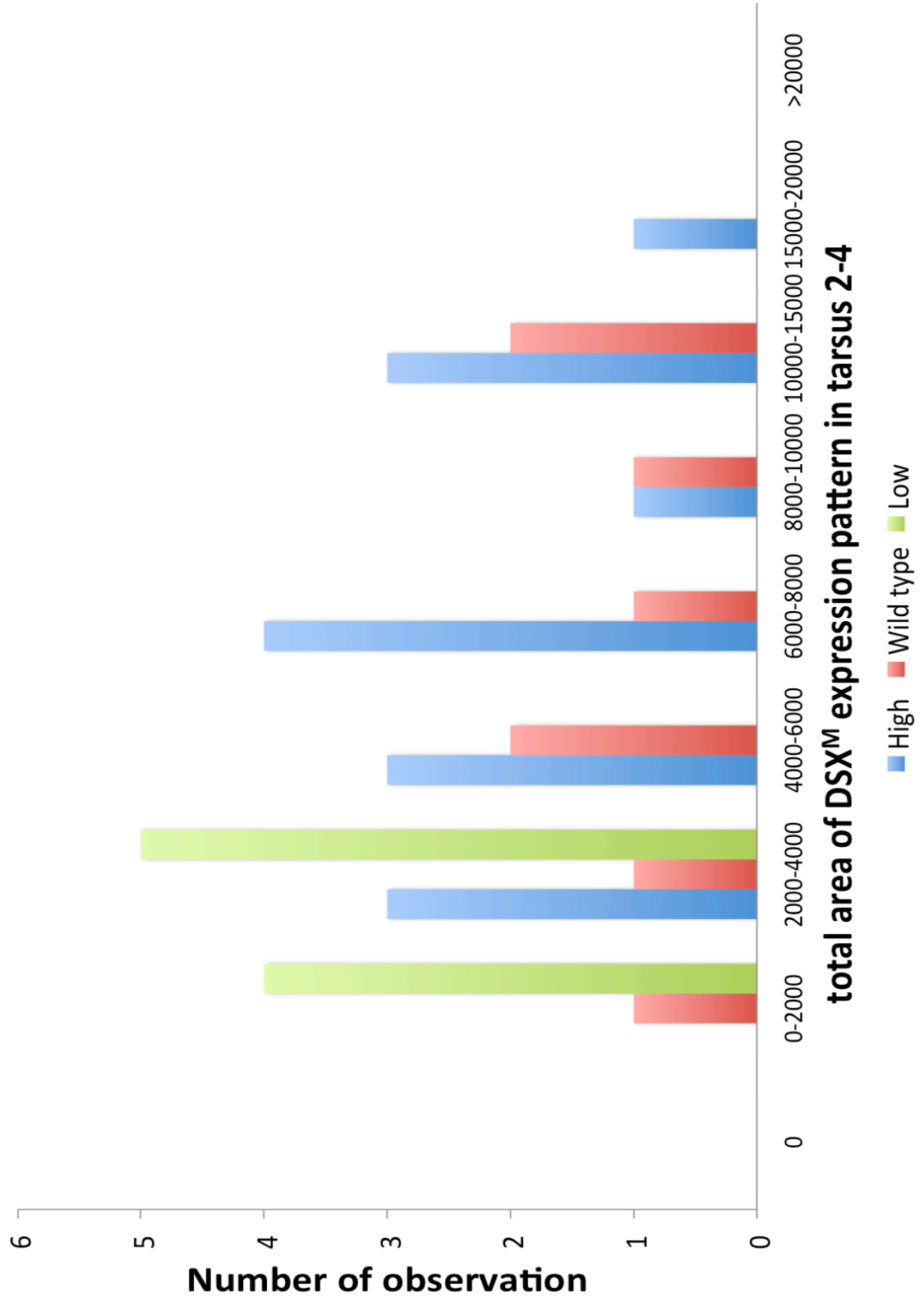


Figure 22. Distribution of the area of the DSX^M expression pattern on tarsus 2-4

In the graph, the green bars represent Lowline, the red bars represent Wildtype and the blue bars represent Highline. X-axis is the expression area measured (unit: pixels), and Y-axis is the number of observation. Compared the sample distribution of Lowline and the sample distribution of Highline, the highest appearance is shifted from left to right (from the interval 2,000-4,000 to the interval 6,000-8,000). There is a significant difference between the distribution of Lowline and Highline.

3.2.5 Expression patterns of SCR and DSX^M

Thus far, we have examined the expression patterns of SCR and DSX^M separately, and have also measured the DSX^M expression region independently. However, in order to have a comprehensive idea of the boundaries of the expression patterns of SCR and DSX^M and the manner in which they are regulated, we needed to merge the expression patterns together and study the two markers together. Previous studies indicate that, at AP16, DSX^M is expressed in sex comb precursor cells on tarsus 1, but SCR expression is nonexistent in sex comb precursor cells (Tanaka et al., 2011). However, SCR is expressed at a very high level in the epidermal cells that are adjacent to the sex comb bristles or precursor cells (Figure 7) (Tanaka et al., 2011). Putative sex comb precursor cells can be identified at AP16 based on both DSX^M and SCR expression patterns (Figure 7) (Tanaka et al., 2011). The results for AP5 are presented in Figure 17 G, H and I, where the green color area denotes expression of DSX^M, the red area represents expression of SCR. The yellow area is indicative of the regions where the expression of DSX^M and SCR overlap. In tarsus 1, DSX^M is expressed in the distal portion, and SCR is expressed all over the tarsus 1. In Highline, when the expression patterns of DSX^M and SCR are merged, the specific expression pattern correlates to the pattern of the sex comb precursor cells. The expression of the “precursor cells” is visible at the distal portion of tarsus 1 (the “green line” beneath in the “yellow region”, see Figure 17 G). However, this phenomenon is not found in Wildtype and Lowline (Figure 17 H and I). Since there is no solid evidence indicating that cell fate on the foreleg is determined at AP5, it cannot be concluded that the “green line” on Highline picture represents sex comb precursor cells. Furthermore,

this pattern (“green line” beneath in the “yellow region”) was not repeated in Wildtype and Lowline pictures. Therefore, the “green line” expressed might simply be due to the spreading of the DSX^M expression region.

Chapter 4. DISCUSSION

Evolutionary innovations represent the evolution of the new relationships among previously unconnected genes or alterations in the regulations of gene(s) within existing genetic networks (Carroll, 2005, 2008; Kopp, 2011; Wagner, 2011). There are many changes and modifications of the gene networks underlying the formation and development of morphological novelties (Lowe et al., 2011). The quest to better understand the cellular and molecular mechanism underlying the development of such evolutionary innovations is the core of evolution-development research (evo-devo) (Carroll, 2005, 2008; Kopp, 2011; Wagner, 2011). Understanding the molecular basis of sexually dimorphic traits and their subsequent sex-specific diversification is a particularly interesting area of evo-devo research (Kopp, 2011). In *Drosophila*, one such sex-specific character is the sex comb (Kopp, 2011). The sex comb is one of the most remarkable examples of a rapidly evolving male-specific trait (Atallah et al., 2009a; Atallah et al., 2009b; Kopp, 2011; Tanaka et al., 2011). Several studies have been done on the development of sex comb using wildtype lines and mutation lines as the target models (Tanaka et al., 2009; Tanaka et al., 2011). All of these studies focused on the late stages of development (16 hours post pupation, AP16), when the sex comb rotation process starts (Atallah et al., 2009a; Atallah et al., 2009b; Tanaka et al., 2009; Tanaka et al., 2011).

However, to better understand the molecular basis of sex-specific development and diversification it might be useful to begin at an early stage before the sex-specific trait has been genetically determined. An additional dimension can be added by artificially selected lines. This would make it possible to dissect the regulatory controls that are under selection for the elaboration of the trait under question, in this case the sex comb.

This thesis presents an improvement to the evo-devo research since to date no study has implemented these ideas that: SCR expression varies subtly between artificially selected lines and wild type. Previous studies have pointed toward two important *D. melanogaster* genes, *Doublesex* (*dsx*) and *Sexcomb reduced* (*Scr*) that control the development of the male sex comb (Kopp, 2011). The objective of this investigation was to examine the gene expression of the male isoform of *Doublesex* (DSX^M) and *Sexcombs reduced* (SCR) in Wildtype and in artificially selected lines (Highline and Lowline) at the early pupal stage (AP5). Our results provide a test of the validity of Kopp's model, the "positive feedback loop" (Kopp, 2011; Tanaka et al., 2011) between SCR and DSX^M during development. This research specifically shows that much of the regulatory perturbation is observed in DSX^M and not in SCR, unlike described in previous models predicted by Kopp, 2011.

4.1 Experimental investigation of innovation

4.1.1 Significance of selection lines in studying the developmental genetics of evolutionary innovations

Since the genetic variance of the evolutionary innovation can be preserved by artificial selection (Ahuja and Singh, 2008), this makes it a good model to study the development of sex comb. Studying the development process of an artificially selected trait provides an approach to analyze how developmental perturbations introduce biases into regulatory networks (Beldade et al., 2002). It also helps to identify how evolutionary innovations respond to environmental conditions and how they differentiate during evolution. The underlying idea applied in this research is the expectation that high and low lines reflect natural morphologies that have diverged across species. It should therefore allow us to dissect the genetic basis of such morphological divergence.

4.1.2 Role of macro- vs. micro-mutations in evolutionary innovation

Some genetic mutations cause dramatic phenotypic changes of sex comb. For example, *D. melanogaster* individuals with the mutation *bab*^{PR72} (compromises both BAB protein isoforms' function) have ectopic sex comb on tarsus 2 (Couderc et al., 2002; Godt et al., 1993). These mutations are called “macro-mutations”. They significantly change the morphology of the individuals carrying them. At the same time, macro-mutations in gene regulatory networks also cause morphological divergence of species by interrupting the gene expression during development. For example, the morphological divergence of the larva trichome pattern in different *Drosophila* species is mainly caused by the genetic changes of three upstream enhancers of the gene, *shavenbaby* (*svb*) (McGregor et al., 2007). However, most of the time macro-mutations do not persist since individuals with macro-mutations have much lower fitness and will be eliminated by the natural selection.

Compared to macro-mutations, there is another type of genetic alteration called “micro-mutations”. The genetic variation underlying artificial selections is mainly produced by micro-mutations.

4.2 Main findings of this investigation and its significance

4.2.1 Predominant expression divergence in DSX^M underlies divergent sex comb morphologies.

We used immunofluorescent technique (antibody staining) to trace and compare the expression of two markers, DSX^M and SCR, in the forelegs in three different lines (Highline, Wildtype and Lowline). The main finding of this research is that the expression region of DSX^M on the foreleg is altered by the artificial selection. The expression region of SCR has minor difference among three lines. The SCR expression is preserved consistently between the artificially selected lines.

Fluorescent pictures of DSX^M antibody staining among three different lines (Highline, Wildtype and Lowline) indicate that the width of the *Doublesex* male isoform (DSX^M) expression region in tarsus 1 of the foreleg in Highline is significantly greater than that in Lowline. In tarsus 2-4, the area of the DSX^M expression region in Highline is significantly larger than in Lowline, this means comparing to Lowline, there are more cells expressing DSX^M on the foreleg in Highline.

4.2.2 Role of DSX and SCR in an interactive model

As mentioned before, DSX^M and SCR are crucial to the sex comb bristle cells determination and development (Kopp, 2011; Tanaka et al., 2011). The sex comb formation and development can be affected by manipulating the expression of DSX^M and SCR (Kopp, 2011; Tanaka et al., 2011). No sex comb will be formed if either of these two transcription factors is knocked out (Struhl, 1982; Tanaka et al., 2011). On the other hand, it has been shown that DSX^M and SCR overexpression leads to the ectopic sex comb formation in tarsus 2-4 in the forelegs (Kopp, 2011; Tanaka et al., 2011). According to Kopp (2011), there is a strong correlation between the formation and morphology of sex comb and the expression of both SCR and DSX (Kopp, 2011; Tanaka et al., 2011). The expression of DSX^M is activated by the SCR and, at the same time, SCR is also elevated by DSX^M prior and during sex combs rotation (Figure 14) (Kopp, 2011; Tanaka et al., 2011). It has been suggested that, in the common ancestor of *D. melanogaster* and *D. obscura*, a positive regulation loop of SCR and DSX^M was recruited into the putative sex comb region, resulting the origination of the sex comb (Kopp, 2011; Tanaka et al., 2011). The loop is a prerequisite of the sex comb formation in evolution (Kopp, 2011; Tanaka et al., 2011). During evolution, any genetic alterations on either of these genes will be exaggerated by the positive-regulation loop and lead to morphological changes of the sex comb (Kopp, 2011; Tanaka et al., 2011). We expected that there might be some differences of the SCR and DSX^M expression regions or patterns among the three lines (Highline, Wildtype and Lowline). However, the results were not consistent with the expectations described above. Based on the result of antibody staining, artificial selection on sex comb bristle numbers directly perturbed DSX^M expression, but the SCR

expression level and pattern remain unchanged between all three lines. There was no solid evidence to suggest that in Highline the SCR expression region was expanded. There was also no sign of decreased SCR expression in Lowline. It is noteworthy that development did constrain the DSX^M or SCR expression response to artificial selection in *D. melanogaster*.

We hypothesize three major reasons why SCR expression was not up or down regulated between the three different lines: 1) SCR is not the sole determining factor for specifying sex comb bristle numbers. During the development, SCR expression level and area of expression are fixed in *D. melanogaster*. SCR expression is similar between the artificial selected lines. It is highly possible that SCR expression is independent of DSX^M and has no flexibility to respond to selection pressure. This view is partially supported by a recently published study that demonstrated SCR expression on the male foreleg is similar in the *D. melanogaster* Wildtype line and the male *dsx^M-deficiency* line (Devi and Shyamala, 2013). Still, it has also been shown that SCR is essential to the formation of sex comb, since sex comb is completely absent in the *D. melanogaster* male individual with *Scr-null* mutation (Randsholt and Santamaria, 2008; Struhl, 1982; Tanaka et al., 2011); considering these data, we hypothesize that while SCR is essential to determine the development of the sex comb, SCR is probably not responsible for determining sex comb bristle number. Present studies only indicate that the positive feedback and regulation loop between SCR and DSX^M is crucial to the “formation” of sex comb. The specific pattern and orientation of the sex comb bristles are mediated by the downstream factors, which are co-regulated by the SCR and DSX^M. As DSX^M expression is altered in

the artificially selected lines, the expression of some unknown downstream determination factors are also perturbed. Compared to SCR, the unknown downstream determination factors make more contributions to the sex comb bristle number variation. 2) It is possible SCR expression is elevated in Highline, but the area of the expression region is not changed. In other words, the expression level in each cell is increased. In future studies, the Quantitative (real-time) Reverse-Transcription PCR (qRT-PCR) technique may be utilized to investigate the actual expression level among the three different lines. 3) It is possible that artificial selection not only perturbed DSX^M expression, but also influenced some other SCR repressors. As DSX^M expression is increased, some unknown downstream SCR repressors are activated and enhanced. It is possible that the elevated SCR repressors limit SCR expression level and region. For example, like *sex combs distal* (SCD) (Randsholt and Santamaria, 2008). SCD is a dose-dependent SCR repressor. Males with two copies of SCD have smaller sex combs, than wildtype (Randsholt and Santamaria, 2008). SCD is expressed in tarsal segment in the foreleg; the expression of SCD helps to delimit the distal boundary of the SCR expression region at the joint between tarsus 1 and 2 (Randsholt and Santamaria, 2008). It is possible that in Highline the SCD expression is elevated in tarsus 1. Consequently, the elevated SCD counteract the influence of the increased DSX^M and maintain the SCR expression at the normal level. For Lowline, it is the opposite way.

4.2.3 Significance of this investigation

Our research is unique and has three significant advantages: 1) Previous studies on the developmental mechanisms of sex comb used the *D. melanogaster* Wildtype lines and mutation lines as the target models (Tanaka et al., 2009; Tanaka et al., 2011). In our research, the artificial selected lines were used as target models. Our results have demonstrated that some of the genes that control the formation of sex comb, manifest some expression flexibility in response to artificial selection during the development (e.g. DSX^M). Nevertheless, the flexibility is constrained by the development, because development introduces constraints into the sexual trait evolution. 2) Previous studies focused on the late stage of the development (16 hours post pupation, AP16) when the sex comb rotation process starts (Atallah et al., 2009a; Atallah et al., 2009b; Tanaka et al., 2009; Tanaka et al., 2011). Our research focused on the early stage of the pupation period (5 hours post pupation, AP5). The results from our research indicate that the artificial selection has affected the drosophila development process at the period of very early stages after pupation. 3) Our research provides additional evidence to give complete of Kopp's model on SCR and DSX^M interaction loop. Even though our results contradict some hypothesis and expectation derived from the Kopp's model, we provide an approach to test the validity of the cross regulation loop model during the development.

Chapter 5. CONCLUSION AND FUTURE DIRECTION

Our results indicate that the expression region of DSX^M in Highline is significantly higher than the expression region in Lowline, and the expression region of SCR has no appreciate differences among three lines (Highline, Wildtype and Lowline).

DSX^M expression was altered by artificial selection, but the SCR expression was not. DSX^M expression manifests some flexibility to adapt to the environmental condition changes and the pressure of the selection force. Since there is no significant difference between Wildtype and Lowline for the width of the DSX^M expression region in tarsus 1, and no significant difference between Wildtype and Highline for DSX^M expression area in tarsus 2-4, it can be concluded that the flexibility of DSX^M expression is constrained by development. Our research provides an approach to test the validity of the model of cross-regulation loop between SCR and DSX^M during the development proposed by Kopp, 2011; Tanaka et al., 2011.

We believe future studies should focus on two parts: first, to use the quantitative RT-PCR technique to accurately determine the actual expression levels of both DSX^M and SCR among the three lines (Highline, Wildtype and Lowline). Based on quantitative data from PCR experiments, we can have a definitive answer about the SCR expression in the three lines. We can comprehensively measure the response of SCR to the artificial selection. Second, we should investigate the SCR and DSX^M expression in two other kinds of mutation lines: the mutated *D. melanogaster* line with ectopic sex comb structure (gain function mutation) and the line with compromised sex comb (loss function mutation). The gain and loss of function mutations are both macro-mutations. Combining the data of the macro-mutation with the data from artificial selection (micro-mutation), we might produce a novel and comprehensive model of SCR- DSX^M cross regulation loop. Furthermore the expression differences between these two genes can be measured in

wild type species with varied morphologies to understand if similar regulatory processes are responsible for divergent sex comb morphologies.

Transcriptomic and epigenetic methods using next generation sequencing can be used to clarify the involvement of all genes responsible for sex comb and bristle number development as well as the role of micro RNAs that may control gene regulation. These approaches will greatly enhance our understanding of factors that control major evolutionary innovations, such as sex combs.

REFERENCES

- Ahuja, A., and Singh, R.S. (2008). Variation and evolution of male sex combs in *Drosophila*: nature of selection response and theories of genetic variation for sexual traits. *Genetics* 179, 503-509.
- Atallah, J., Liu, N.H., Dennis, P., Hon, A., Godt, D., and Larsen, E.W. (2009a). Cell dynamics and developmental bias in the ontogeny of a complex sexually dimorphic trait in *Drosophila melanogaster*. *Evolution & Development* 11, 191-204.
- Atallah, J., Liu, N.H., Dennis, P., Hon, A., and Larsen, E.W. (2009b). Developmental constraints and convergent evolution in *Drosophila* sex comb formation. *Evolution & Development* 11, 205-218.
- Atallah, J., Watabe, H., and Kopp, A. (2012). Many ways to make a novel structure: a new mode of sex comb development in Drosophilidae. *Evolution & Development* 14, 476-483.
- Baker, B.S., Taylor, B.J., and Hall, J.C. (2001). Are Complex Behaviors Specified by Dedicated Regulatory Genes? Reasoning from *Drosophila*. *Cell* 105, 13-24.
- Barmina, O., and Kopp, A. (2007). Sex-specific expression of a HOX gene associated with rapid morphological evolution. *Developmental Biology* 311, 277-286.
- Bate, M., and Martinez Arias, A. (1991). The embryonic origin of imaginal discs in *Drosophila*. *Development* 112, 755-761.
- Beldade, P., Koops, K., and Brakefield, P.M. (2002). Modularity, individuality, and evo-devo in butterfly wings. *Proceedings of the National Academy of Sciences* 99, 14262-14267.
- Burtis, K.C., and Baker, B.S. (1989). *Drosophila doublesex* gene controls somatic sexual differentiation by producing alternatively spliced mRNAs encoding related sex-specific polypeptides. *Cell* 56, 997-1010.
- Caballero, A., Toro, M.A., and López-Fanjul, C. (1991). The response to artificial selection from new mutations in *Drosophila melanogaster*. *Genetics* 128, 89-102.
- Carroll, S.B. (2005). Evolution at Two Levels: On Genes and Form. *PLoS Biol* 3, e245.
- Carroll, S.B. (2008). Evo-Devo and an Expanding Evolutionary Synthesis: A Genetic Theory of Morphological Evolution. *Cell* 134, 25-36.
- Christensen, R. (1996). One-Way ANOVA. In *Plane Answers to Complex Questions: The Theory of Linear Models* (Springer New York), pp. 112-114.

- Christiansen, A.E., Keisman, E.L., Ahmad, S.M., and Baker, B.S. (2002). Sex comes in from the cold: the integration of sex and pattern. *Trends in Genetics* 18, 510-516.
- Condic, M.L., Fristrom, D., and Fristrom, J.W. (1991). Apical cell shape changes during *Drosophila* imaginal leg disc elongation: a novel morphogenetic mechanism. *Development* 111, 23-33.
- Cook, R. (1977). Behavioral role of the sexcombs in *Drosophila melanogaster* and *Drosophila simulans*. *Behavior genetics* 7, 349-357.
- Couderc, J.-L., Godt, D., Zollman, S., Chen, J., Li, M., Tiong, S., Cramton, S.E., Sahut-Barnola, I., and Laski, F.A. (2002). The *bric à brac* locus consists of two paralogous genes encoding BTB/POZ domain proteins and acts as a homeotic and morphogenetic regulator of imaginal development in *Drosophila*. *Development* 129, 2419-2433.
- Coyne, J.A. (1985). Genetic studies of three sibling species of *Drosophila* with relationship to theories of speciation. *Genetics Research* 46, 169-192.
- Devi, T., and Shyamala, B.V. (2013). Male- and female-specific variants of *doublesex* gene products have different roles to play towards regulation of *Sex combs reduced* expression and sex comb morphogenesis in *Drosophila*. *J Biosci* 38, 455-460.
- Erdman, S.E., Chen, H.-J., and Burtis, K.C. (1996). Functional and Genetic Characterization of the Oligomerization and DNA Binding Properties of the *Drosophila* Doublesex Proteins. *Genetics* 144, 1639-1652.
- Fabre, C.C.G., Casal, J., and Lawrence, P.A. (2008). The abdomen of *Drosophila*: does planar cell polarity orient the neurons of mechanosensory bristles? *Neural Development* 3, 12.
- Ferveur, J.-F., Stortkuhl, K.F., Stocker, R.F., and Greenspan, R.J. (1995). Genetic feminization of brain structures and changed sexual orientation in male *Drosophila*. *Science* 267, 902+.
- Fristrom, D. (1988). The cellular basis of epithelial morphogenesis. A review. *Tissue and Cell* 20, 645-690.
- García-Bellido, A., and de Celis, J.F. (2009). The Complex Tale of the achaete–scute Complex: A Paradigmatic Case in the Analysis of Gene Organization and Function During Development. *Genetics* 182, 631-639.
- Gho, M., Bellaiche, Y., and Schweisguth, F. (1999). Revisiting the *Drosophila* microchaete lineage: a novel intrinsically asymmetric cell division generates a glial cell. *Development* 126, 3573-3584.

- Glicksman, M.A., and Brower, D.L. (1988). Expression of the Sex combs reduced protein in *Drosophila* larvae. *Developmental Biology* 127, 113-118.
- Godt, D., Couderc, J.L., Cramton, S.E., and Laski, F.A. (1993). Pattern formation in the limbs of *Drosophila*: *bric a brac* is expressed in both a gradient and a wave-like pattern and is required for specification and proper segmentation of the tarsus. *Development* 119, 799-812.
- Hannah-Alava, A. (1958). Developmental genetics of the posterior legs in *Drosophila melanogaster*. *Genetics* 43, 878-905.
- Hedley, M.L., and Maniatis, T. (1991). Sex-specific splicing and polyadenylation of *dsx* pre-mRNA requires a sequence that binds specifically to *tra-2* protein in vitro. *Cell* 65, 579-586.
- Held, L.I. (1991). Bristle patterning in *Drosophila*. *BioEssays* 13, 633-640.
- Held, L.I. (2010). How does *Scr* cause first legs to deviate from second legs? *Drosophila Information Service* 93, 132-146.
- Hempel, L., and Oliver, B. (2007). Sex-specific Doublesex^M expression in subsets of *Drosophila* somatic gonad cells. *BMC Developmental Biology* 7, 113.
- Hu, Y.-G., and Toda, M.J. (2001). Polyphyly of *Lordiphosa* and its relationships in Drosophilinae (Diptera: Drosophilidae). *Systematic Entomology* 26, 15-31.
- Kojima, T. (2004). The mechanism of *Drosophila* leg development along the proximodistal axis. *Development, Growth & Differentiation* 46, 115-129.
- Kopp, A. (2011). *Drosophila* sex combs as a model of evolutionary innovations. *Evolution & Development* 13, 504-522.
- Lecuit, T., and Cohen, S.M. (1997). Proximal-distal axis formation in the *Drosophila* leg. *Nature* 388, 139-145.
- Lowe, C.B., Kellis, M., Siepel, A., Raney, B.J., Clamp, M., Salama, S.R., Kingsley, D.M., Lindblad-Toh, K., and Haussler, D. (2011). Three Periods of Regulatory Innovation During Vertebrate Evolution. *Science* 333, 1019-1024.
- McGregor, A.P., Orgogozo, V., Delon, I., Zanet, J., Srinivasan, D.G., Payre, F., and Stern, D.L. (2007). Morphological evolution through multiple cis-regulatory mutations at a single gene. *Nature* 448, 587-590.
- Meier, N., Käppeli, S.C., Hediger Niessen, M., Billeter, J.-C., Goodwin, S.F., and Bopp, D. (2013). Genetic Control of Courtship Behavior in the Housefly: Evidence for a Conserved Bifurcation of the Sex-Determining Pathway. *PLoS ONE* 8, e62476.

- Mirth, C., and Akam, M. (2002). Joint Development in the *Drosophila* Leg: Cell Movements and Cell Populations. *Developmental Biology* 246, 391-406.
- Ng, C., and Kopp, A. (2008). Sex Combs are Important for Male Mating Success in *Drosophila melanogaster*. *Behavior Genetics* 38, 195-201.
- Pattatucci, A.M., Otteson, D.C., and Kaufman, T.C. (1991). A functional and structural analysis of the *Sex combs reduced* locus of *Drosophila melanogaster*. *Genetics* 129, 423-441.
- Randsholt, N.B., and Santamaria, P. (2008). How *Drosophila* change their combs: the Hox gene *Sex combs reduced* and sex comb variation among *Sophophora* species. *Evolution & Development* 10, 121-133.
- Robinett, C.C., Vaughan, A.G., Knapp, J.-M., and Baker, B.S. (2010). Sex and the Single Cell. II. There Is a Time and Place for Sex. *PLoS Biol* 8, e1000365.
- Scott, K., Brady Jr, R., Cravchik, A., Morozov, P., Rzhetsky, A., Zuker, C., and Axel, R. (2001). A Chemosensory Gene Family Encoding Candidate Gustatory and Olfactory Receptors in *Drosophila*. *Cell* 104, 661-673.
- Shapiro, S.S., and Wilk, M.B. (1965). An analysis of variance test for normality (complete samples). *Biometrika* 52, 591-611.
- Shroff, S., Joshi, M., and Orenic, T.V. (2007). Differential Delta expression underlies the diversity of sensory organ patterns among the legs of the *Drosophila* adult. *Mechanisms of Development* 124, 43-58.
- Soler, C., Daczewska, M., Da Ponte, J.P., Dastugue, B., and Jagla, K. (2004). Coordinated development of muscles and tendons of the *Drosophila* leg. *Development* 131, 6041-6051.
- Southworth, J.W., and Kennison, J.A. (2002). Transvection and Silencing of the *Scr* Homeotic Gene of *Drosophila melanogaster*. *Genetics* 161, 733-746.
- Struhl, G. (1982). Genes controlling segmental specification in the *Drosophila* thorax. *Proceedings of the National Academy of Sciences* 79, 7380-7384.
- Sturtevant, A.H. (1970). Studies on the bristle pattern of *Drosophila*. *Developmental Biology* 21, 48-61.
- Tanaka, K., Barmina, O., and Kopp, A. (2009). Distinct developmental mechanisms underlie the evolutionary diversification of *Drosophila* sex combs. *Proceedings of the National Academy of Sciences of the United States of America* 106, 4764-4769.

- Tanaka, K., Barmina, O., Sanders, L.E., Arbeitman, M.N., and Kopp, A. (2011). Evolution of sex-specific traits through changes in HOX-dependent *doublesex* expression. *PLoS Biol* 9, e1001131.
- Taylor, J., and Adler, P.N. (2008). Cell rearrangement and cell division during the tissue level morphogenesis of evaginating *Drosophila* imaginal discs. *Developmental Biology* 313, 739-751.
- von Kalm, L., Fristrom, D., and Fristrom, J. (1995). The making of a fly leg: A model for epithelial morphogenesis. *BioEssays* 17, 693-702.
- Wagner, A. (2011). The molecular origins of evolutionary innovations. *Trends in Genetics* 27, 397-410.
- Wright, S.I., Bi, I.V., Schroeder, S.G., Yamasaki, M., Doebley, J.F., McMullen, M.D., and Gaut, B.S. (2005). The Effects of Artificial Selection on the Maize Genome. *Science* 308, 1310-1314.

Appendix- Supplementary Figures and Tables

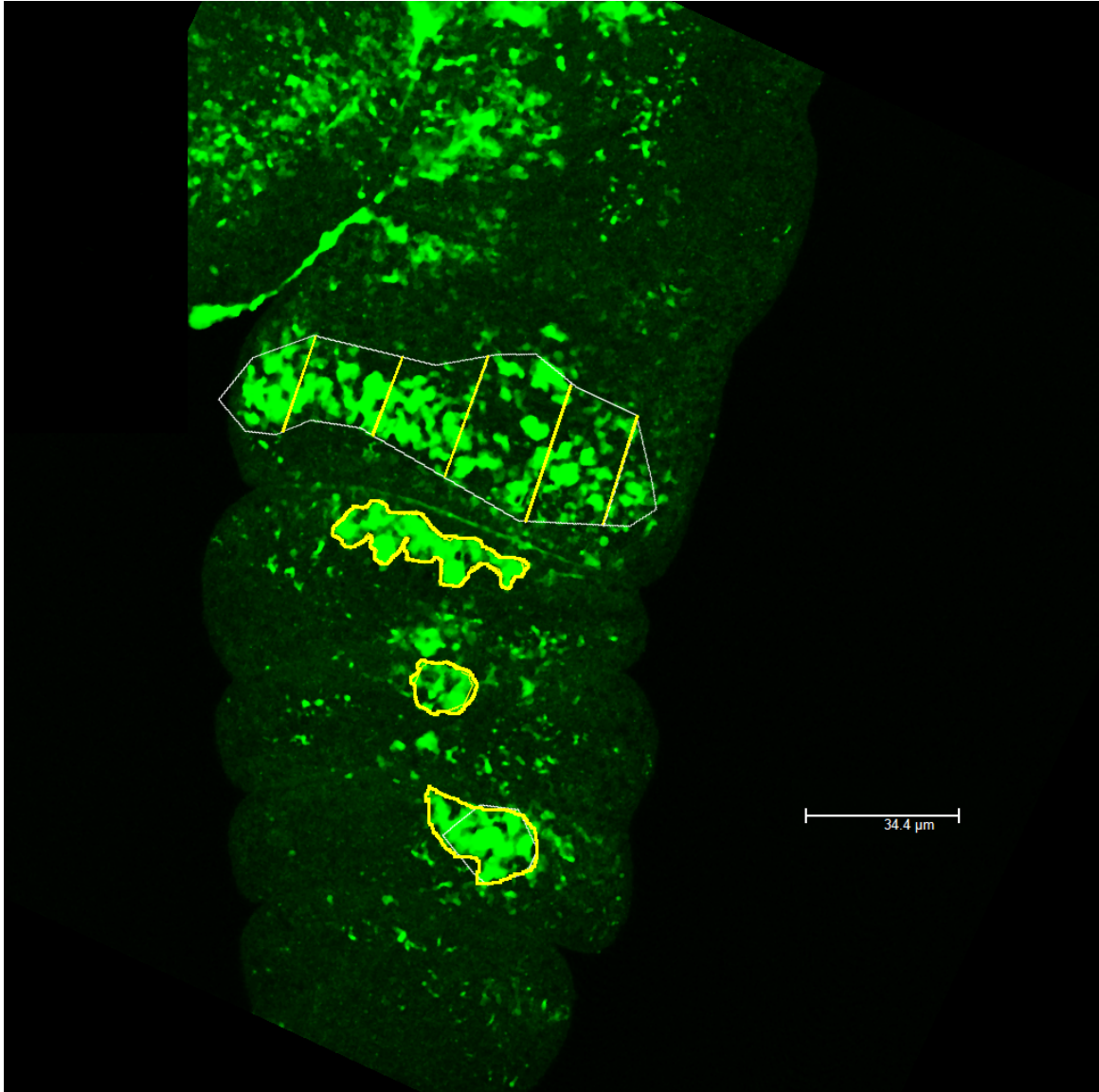


Figure S1. DSX^M expression on foreleg of Highline

The white perimeter depicts the DSXM expression pattern in tarsus 1. The five yellow line segments in tarsus represent the width of the expression pattern at five different places. The DSX^M expression area in tarsus 2-4 is depicted by yellow perimeter. The scale bar is provided.

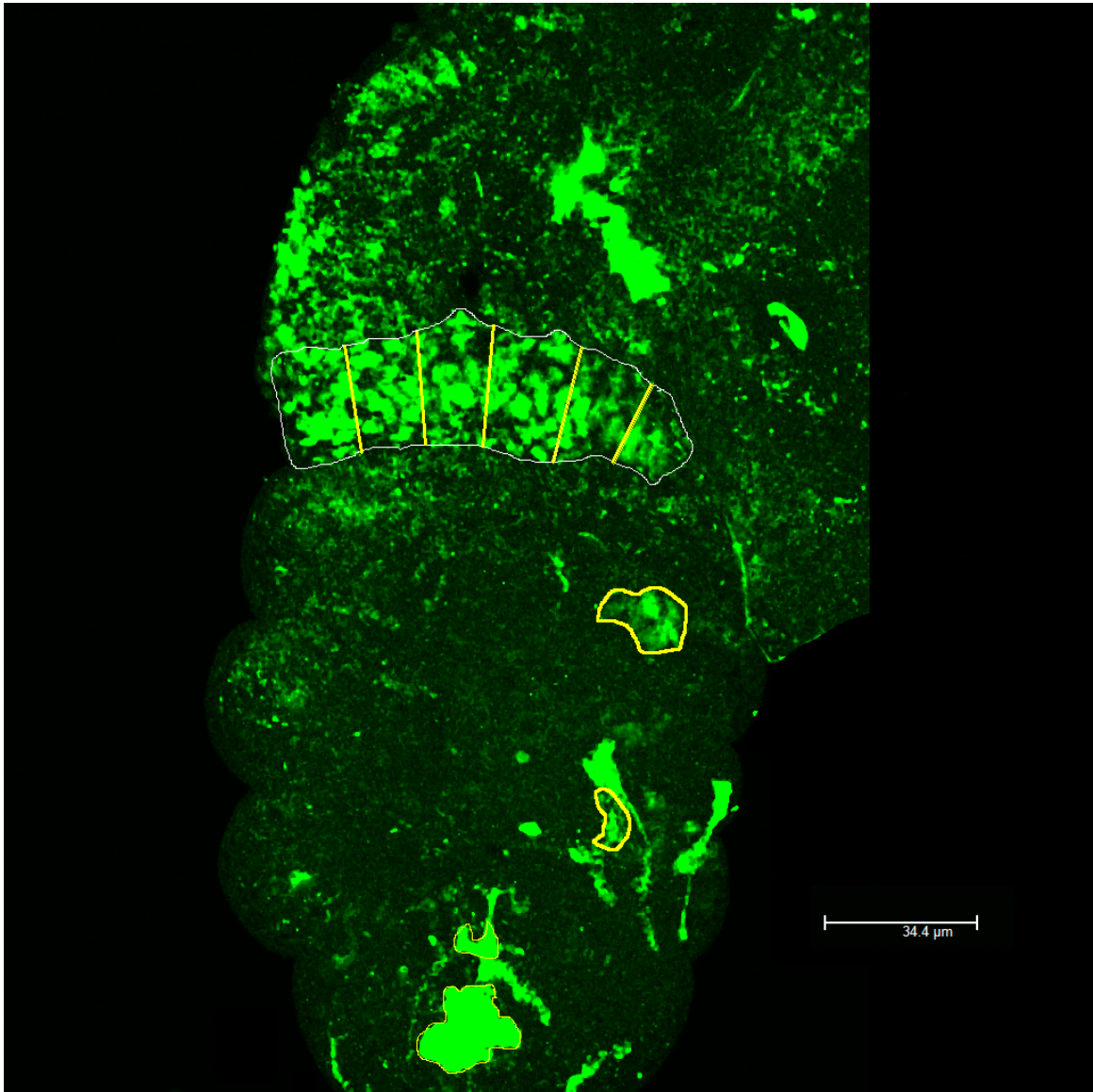


Figure S2. DSX^M expression on foreleg of Highline

The white perimeter depicts the DSX^M expression pattern in tarsus 1. The five yellow line segments in tarsus represent the width of the expression pattern at five different places. The DSX^M expression area in tarsus 2-4 is depicted by yellow perimeter. The scale bar is provided.

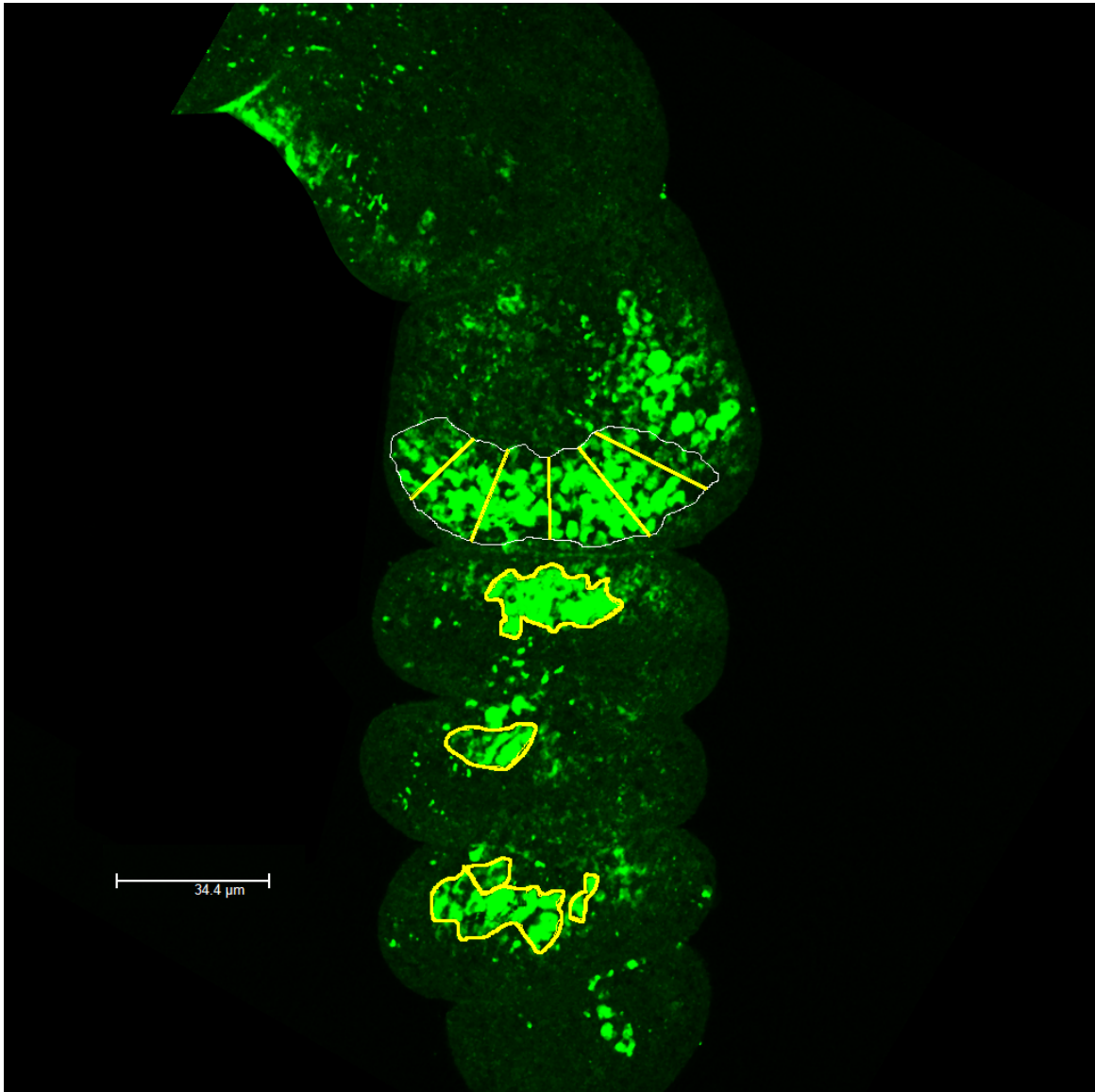


Figure S3. DSX^M expression on foreleg of Highline

The white perimeter depicts the DSX^M expression pattern in tarsus 1. The five yellow line segments in tarsus represent the width of the expression pattern at five different places. The DSX^M expression area in tarsus 2-4 is depicted by yellow perimeter. The scale bar is provided.

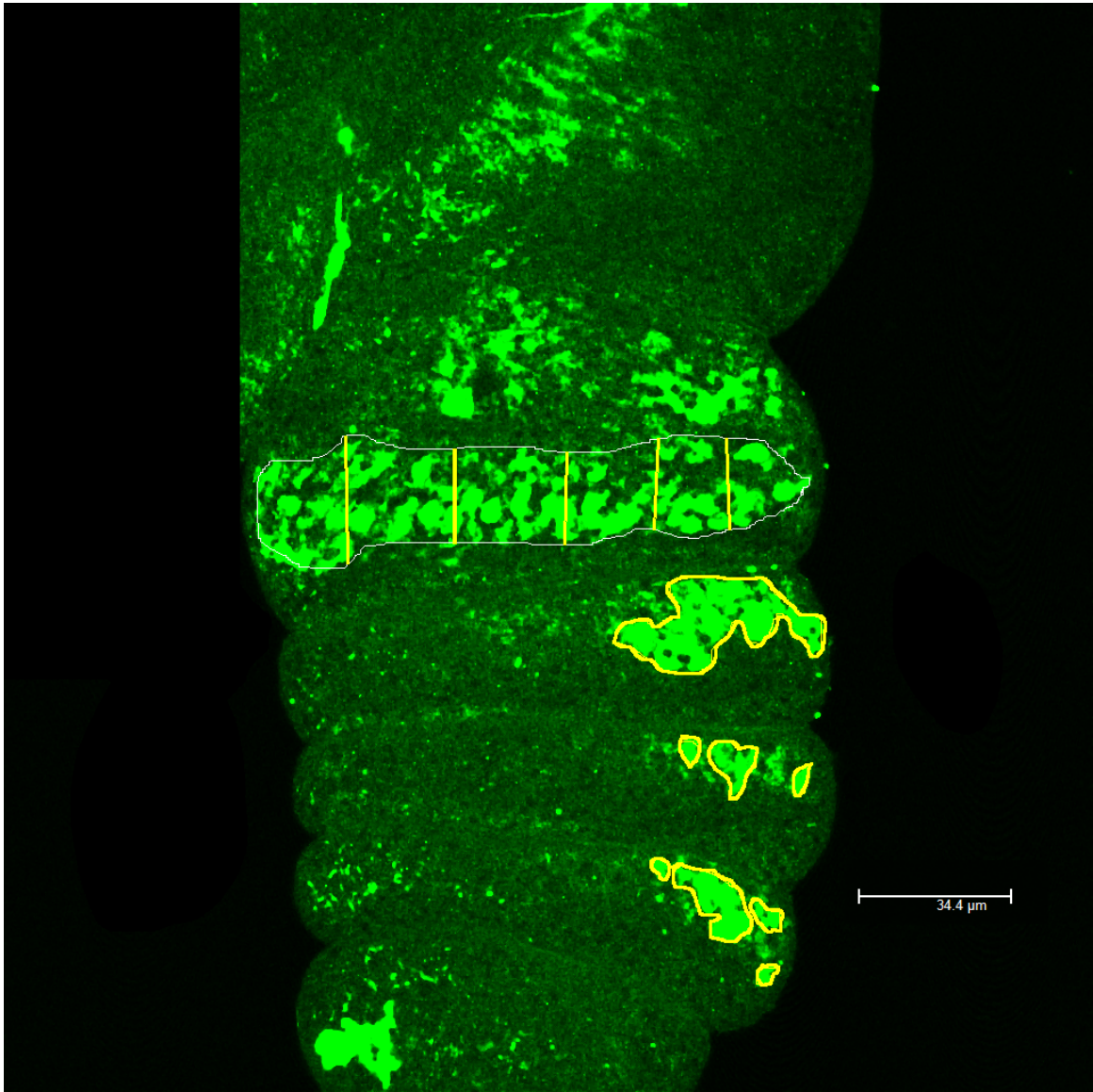


Figure S4. DSX^M expression on foreleg of Highline

The white perimeter depicts the DSXM expression pattern in tarsus 1. The five yellow line segments in tarsus represent the width of the expression pattern at five different places. The DSX^M expression area in tarsus 2-4 is depicted by yellow perimeter. The scale bar is provided.



Figure S5. DSX^M expression on foreleg of Highline

The white perimeter depicts the DSXM expression pattern in tarsus 1. The five yellow line segments in tarsus represent the width of the expression pattern at five different places. The DSX^M expression area in tarsus 2-4 is depicted by yellow perimeter. The scale bar is provided.

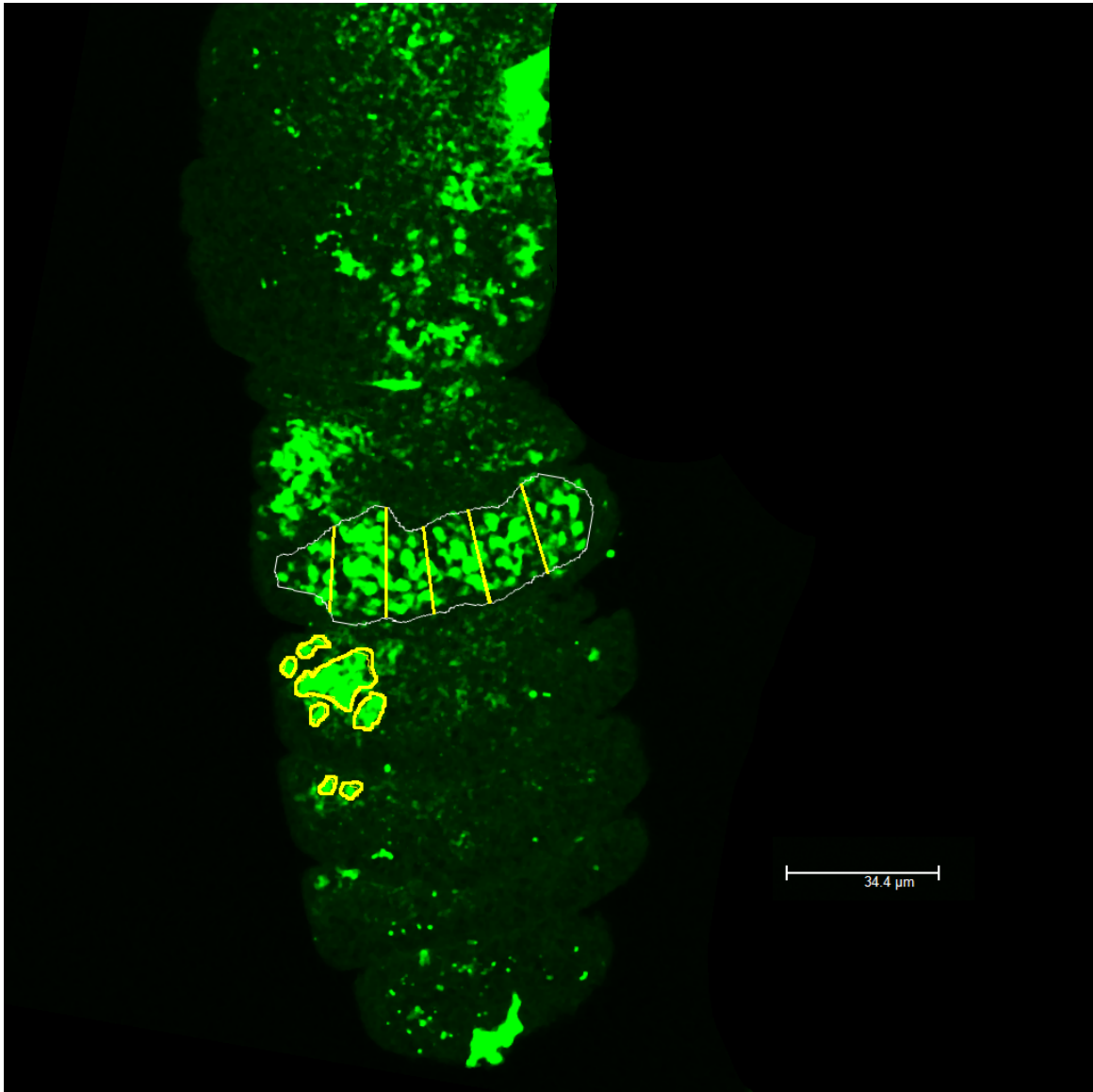


Figure S6. DSX^M expression on foreleg of Highline

The white perimeter depicts the DSX^M expression pattern in tarsus 1. The five yellow line segments in tarsus represent the width of the expression pattern at five different places. The DSX^M expression area in tarsus 2-4 is depicted by yellow perimeter. The scale bar is provided.



Figure S7. DSX^M expression on foreleg of Highline

The white perimeter depicts the DSXM expression pattern in tarsus 1. The five yellow line segments in tarsus represent the width of the expression pattern at five different places. The DSX^M expression area in tarsus 2-4 is depicted by yellow perimeter. The scale bar is provided.

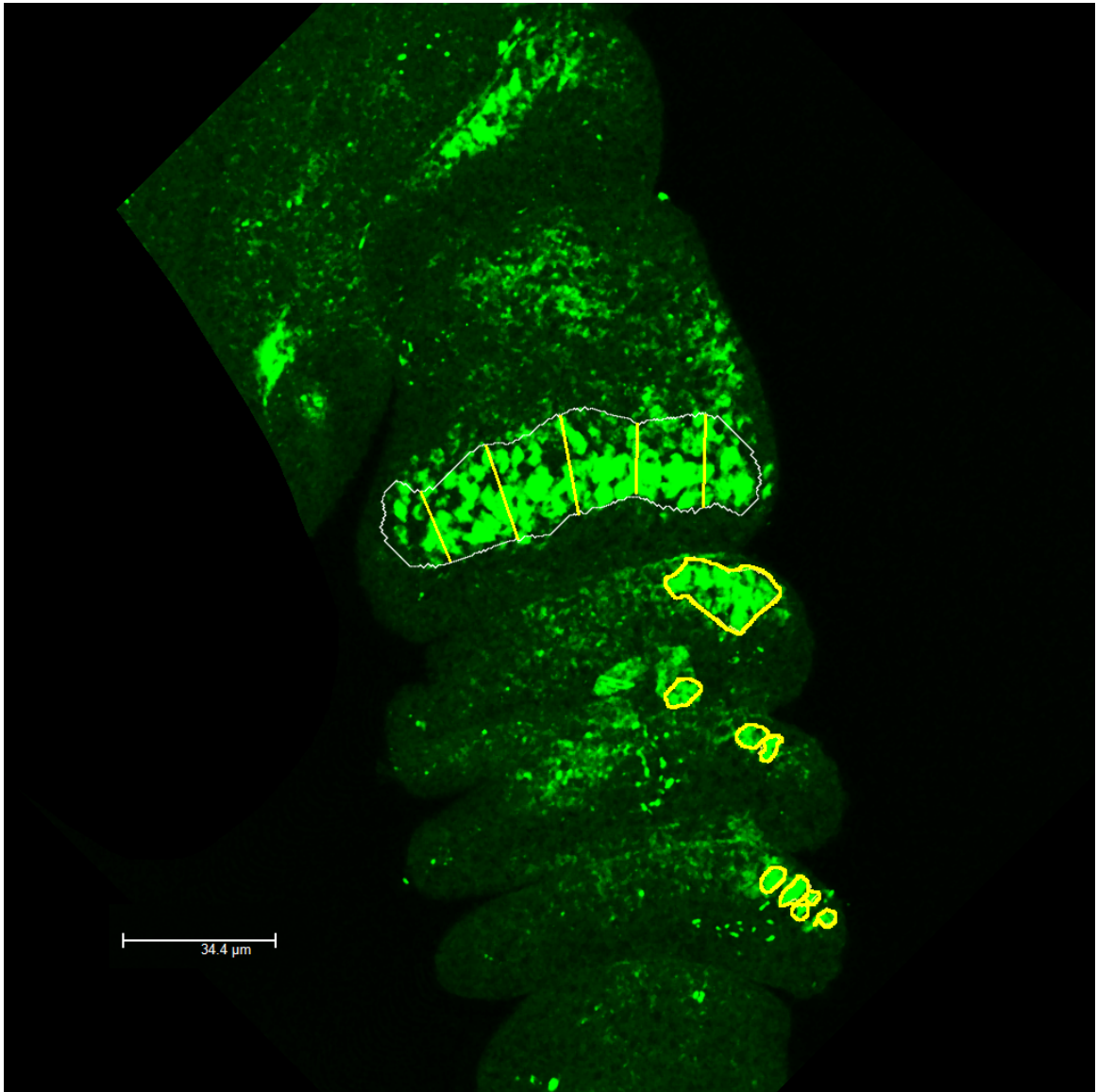


Figure S8. DSX^M expression on foreleg of Highline

The white perimeter depicts the DSX^M expression pattern in tarsus 1. The five yellow line segments in tarsus represent the width of the expression pattern at five different places. The DSX^M expression area in tarsus 2-4 is depicted by yellow perimeter. The scale bar is provided.

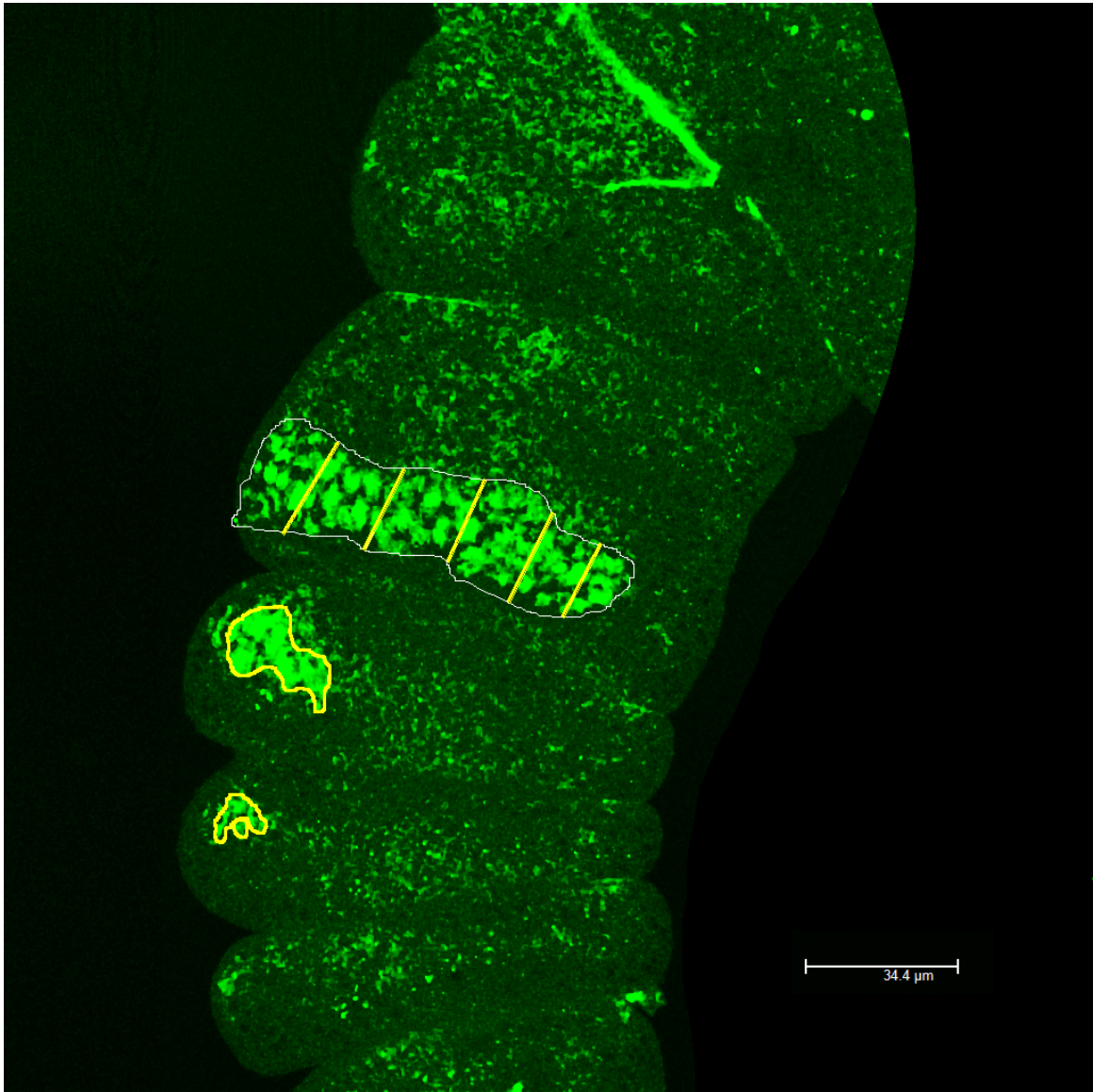


Figure S9. *DSX^M* expression on foreleg of Highline

The white perimeter depicts the *DSX^M* expression pattern in tarsus 1. The five yellow line segments in tarsus represent the width of the expression pattern at five different places. The *DSX^M* expression area in tarsus 2-4 is depicted by yellow perimeter. The scale bar is provided.

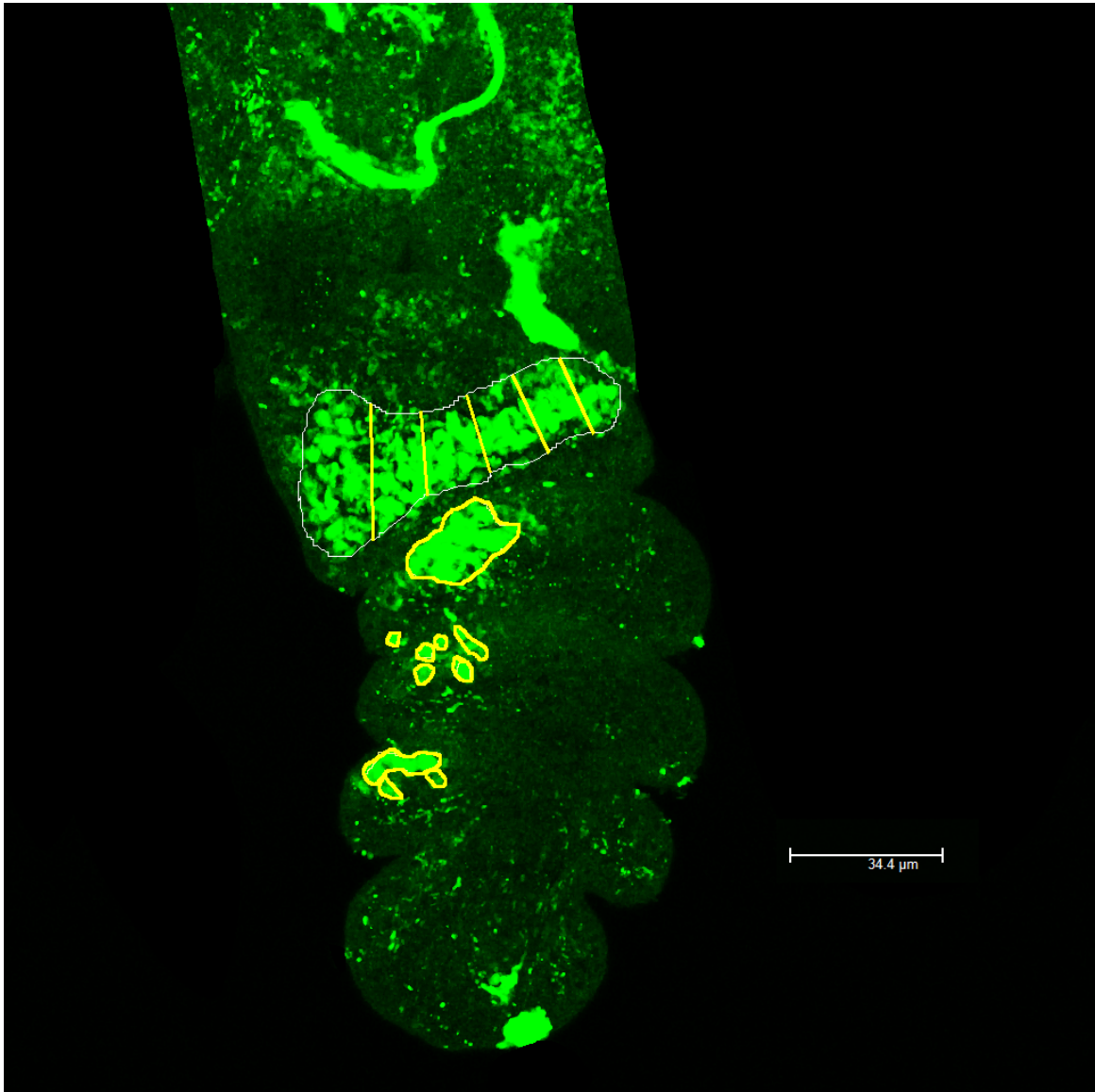


Figure S10. *DSX^M* expression on foreleg of Highline

The white perimeter depicts the *DSX^M* expression pattern in tarsus 1. The five yellow line segments in tarsus represent the width of the expression pattern at five different places. The *DSX^M* expression area in tarsus 2-4 is depicted by yellow perimeter. The scale bar is provided.



Figure S11. *DSX^M* expression on foreleg of Highline

The white perimeter depicts the *DSX^M* expression pattern in tarsus 1. The five yellow line segments in tarsus represent the width of the expression pattern at five different places. The *DSX^M* expression area in tarsus 2-4 is depicted by yellow perimeter. The scale bar is provided.

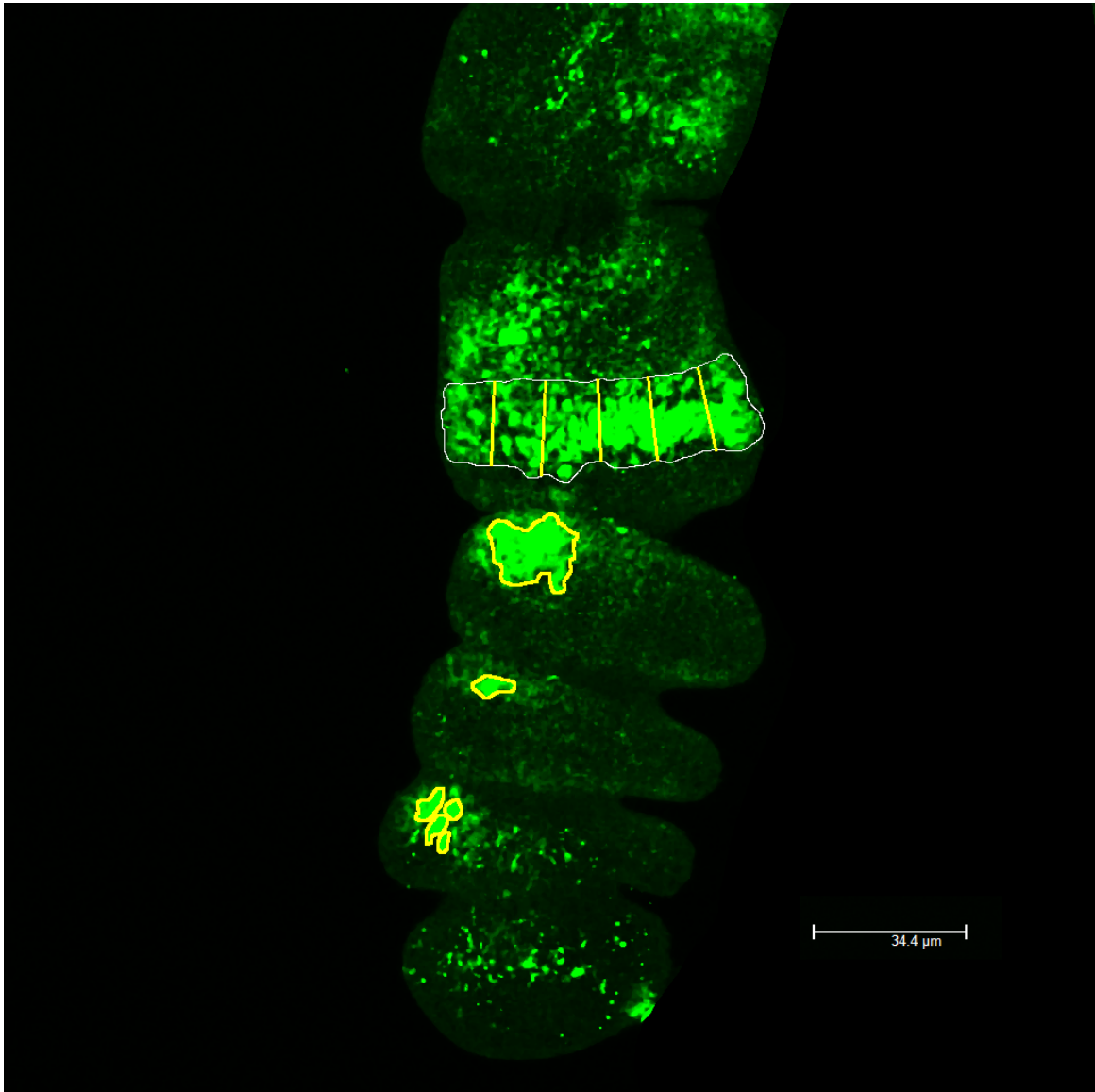


Figure S12. DSX^M expression on foreleg of Highline

The white perimeter depicts the DSX^M expression pattern in tarsus 1. The five yellow line segments in tarsus represent the width of the expression pattern at five different places. The DSX^M expression area in tarsus 2-4 is depicted by yellow perimeter. The scale bar is provided.



Figure S13. DSX^M expression on foreleg of Highline

The white perimeter depicts the DSXM expression pattern in tarsus 1. The five yellow line segments in tarsus represent the width of the expression pattern at five different places. The DSX^M expression area in tarsus 2-4 is depicted by yellow perimeter. The scale bar is provided.



Figure S 14. *DSX^M* expression on foreleg of Highline

The white perimeter depicts the *DSX^M* expression pattern in tarsus 1. The five yellow line segments in tarsus represent the width of the expression pattern at five different places. The *DSX^M* expression area in tarsus 2-4 is depicted by yellow perimeter. The scale bar is provided.

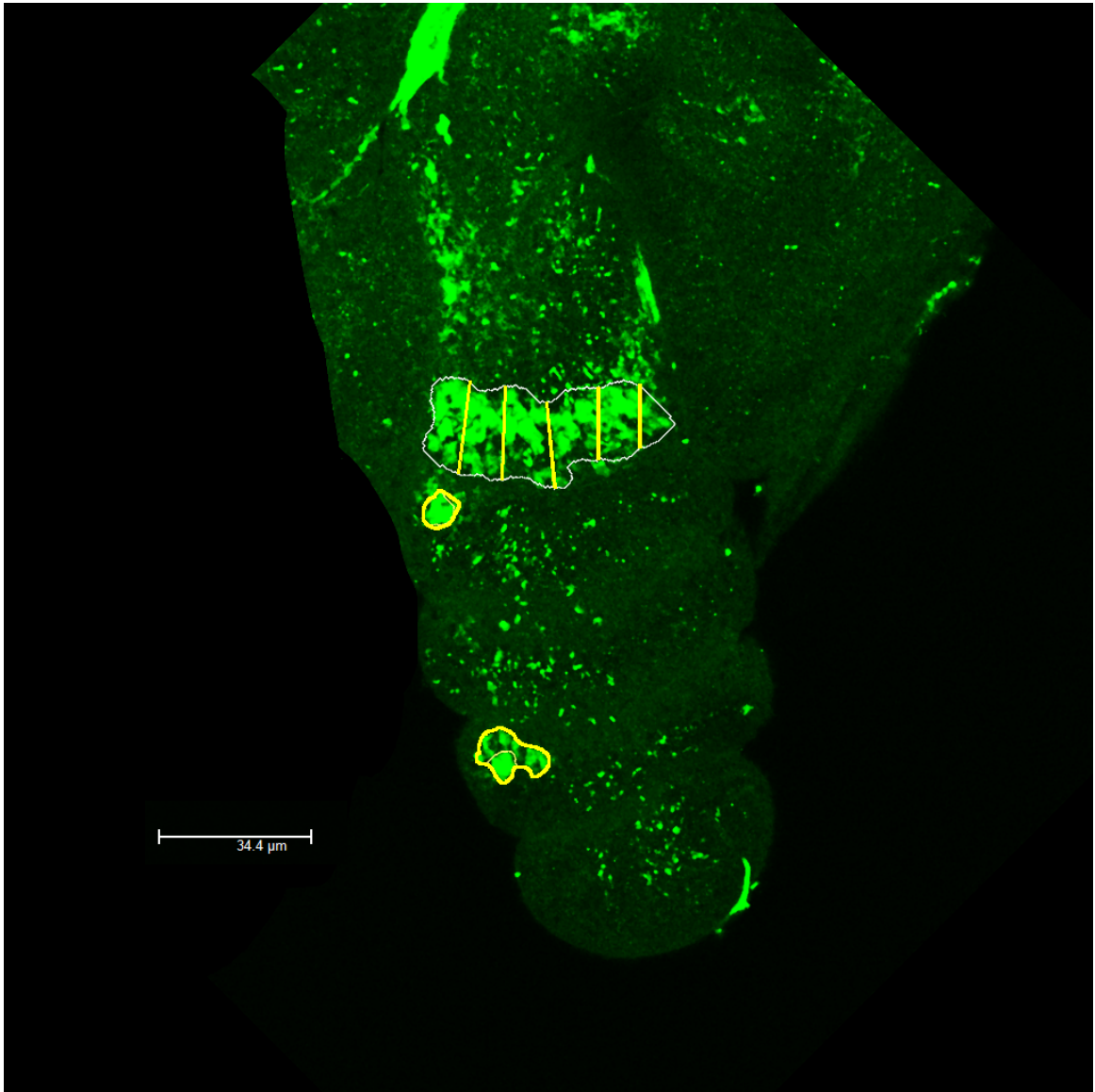


Figure S15. DSX^M expression on foreleg of Highline

The white perimeter depicts the DSXM expression pattern in tarsus 1. The five yellow line segments in tarsus represent the width of the expression pattern at five different places. The DSX^M expression area in tarsus 2-4 is depicted by yellow perimeter. The scale bar is provided.



Figure S16. DSX^M expression on foreleg of Wildtype

The white perimeter depicts the DSX^M expression pattern in tarsus 1. The five yellow line segments in tarsus represent the width of the expression pattern at five different places. The DSX^M expression area in tarsus 2-4 is depicted by yellow perimeter. The scale bar is provided.

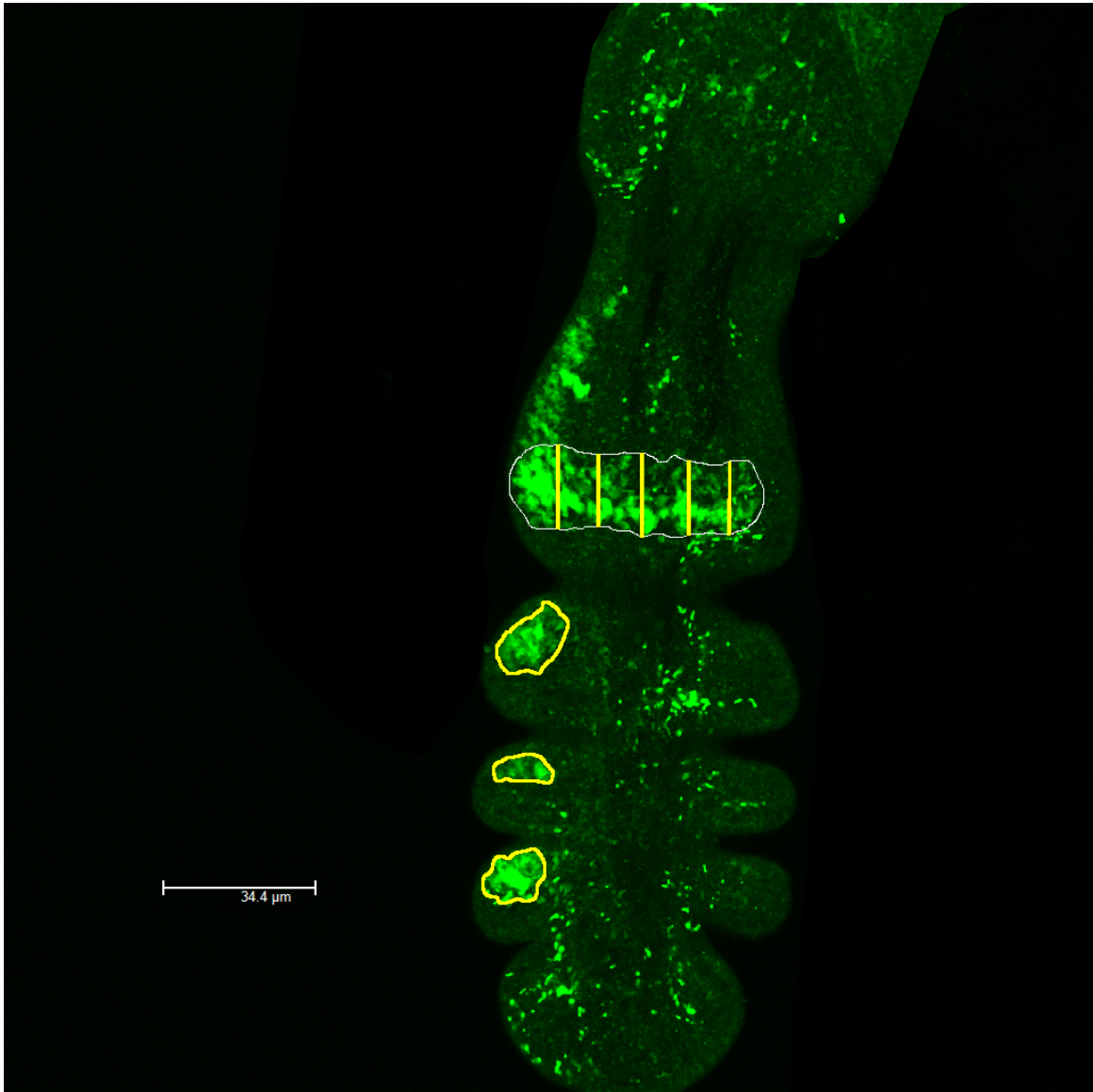


Figure S17. DSX^M expression on foreleg of Wildtype

The white perimeter depicts the DSXM expression pattern in tarsus 1. The five yellow line segments in tarsus represent the width of the expression pattern at five different places. The DSX^M expression area in tarsus 2-4 is depicted by yellow perimeter. The scale bar is provided.

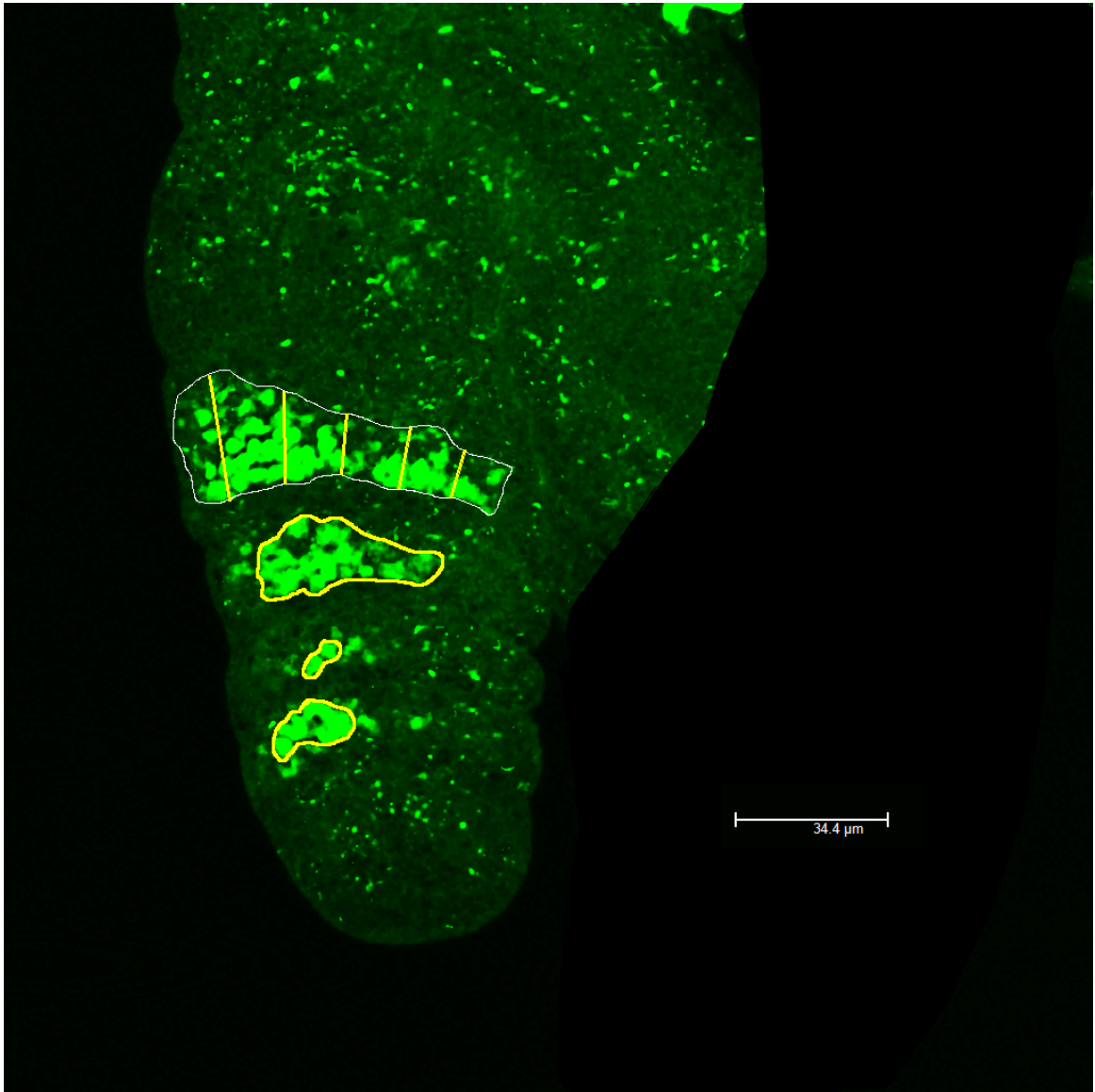


Figure S18. DSX^M expression on foreleg of Wildtype

The white perimeter depicts the DSX^M expression pattern in tarsus 1. The five yellow line segments in tarsus represent the width of the expression pattern at five different places. The DSX^M expression area in tarsus 2-4 is depicted by yellow perimeter. The scale bar is provided.

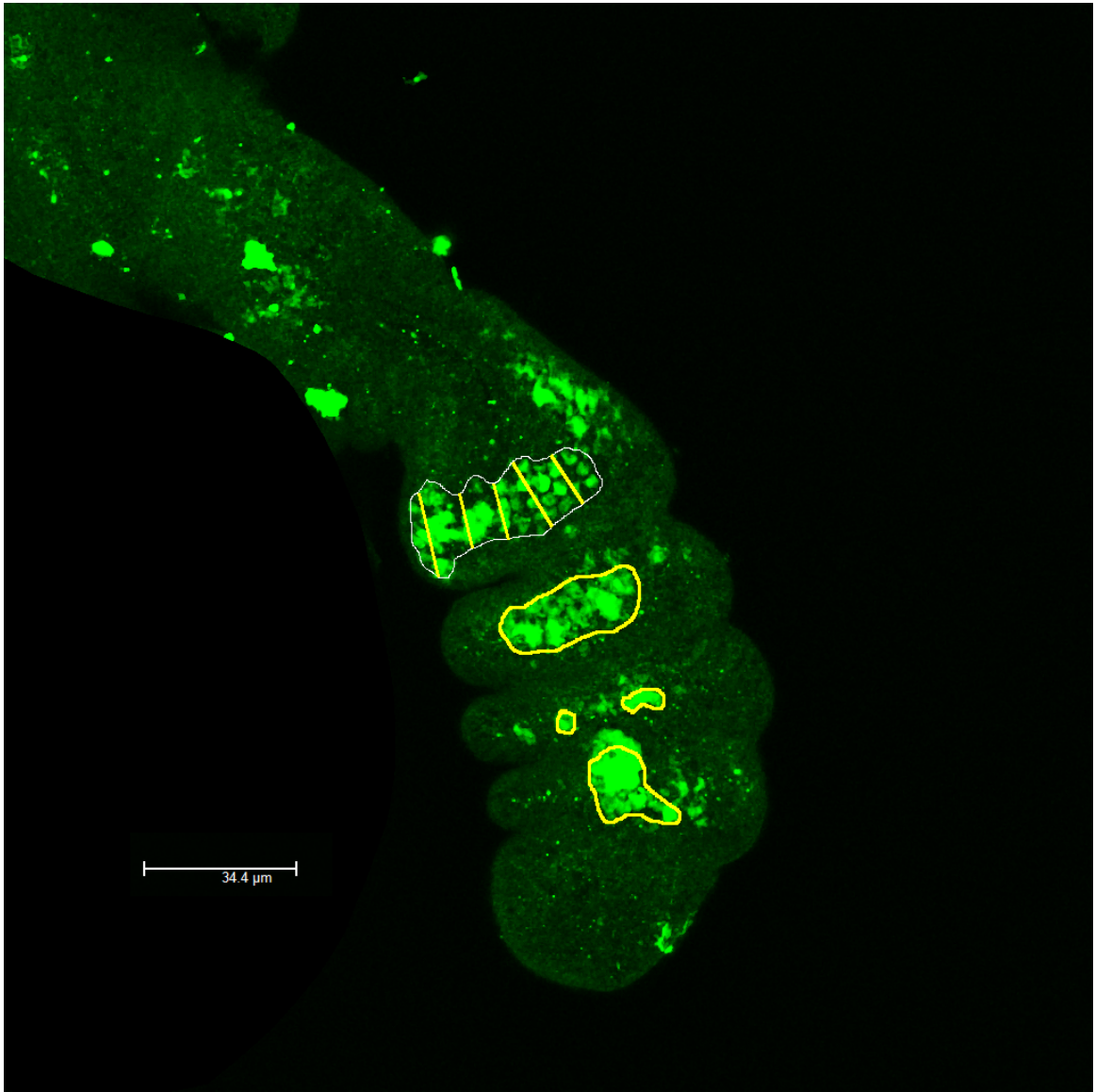


Figure S19. DSX^M expression on foreleg of Wildtype

The white perimeter depicts the DSXM expression pattern in tarsus 1. The five yellow line segments in tarsus represent the width of the expression pattern at five different places. The DSX^M expression area in tarsus 2-4 is depicted by yellow perimeter. The scale bar is provided.

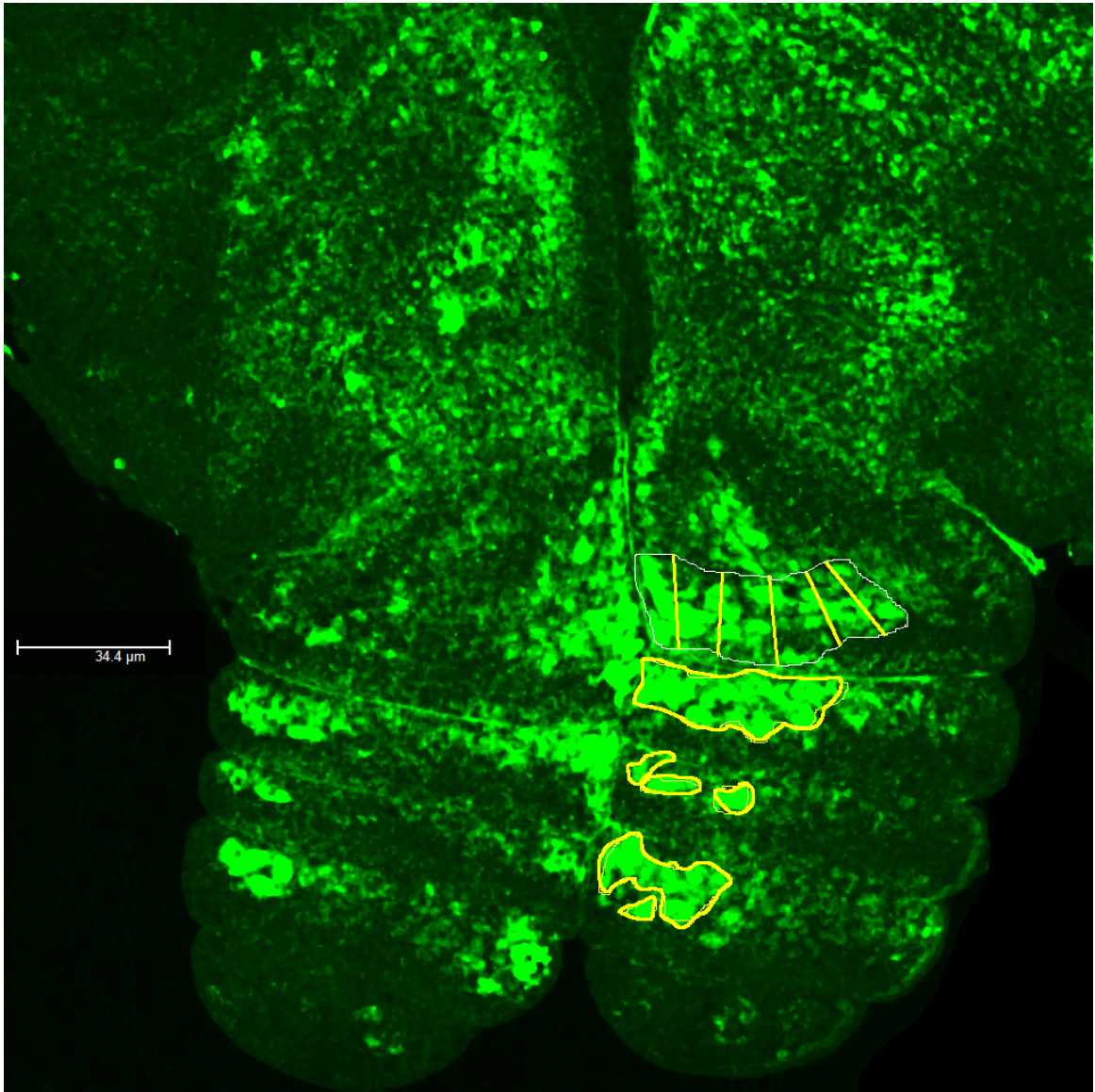


Figure S20. DSX^M expression on foreleg of Wildtype

The white perimeter depicts the DSXM expression pattern in tarsus 1. The five yellow line segments in tarsus represent the width of the expression pattern at five different places. The DSX^M expression area in tarsus 2-4 is depicted by yellow perimeter. The scale bar is provided.

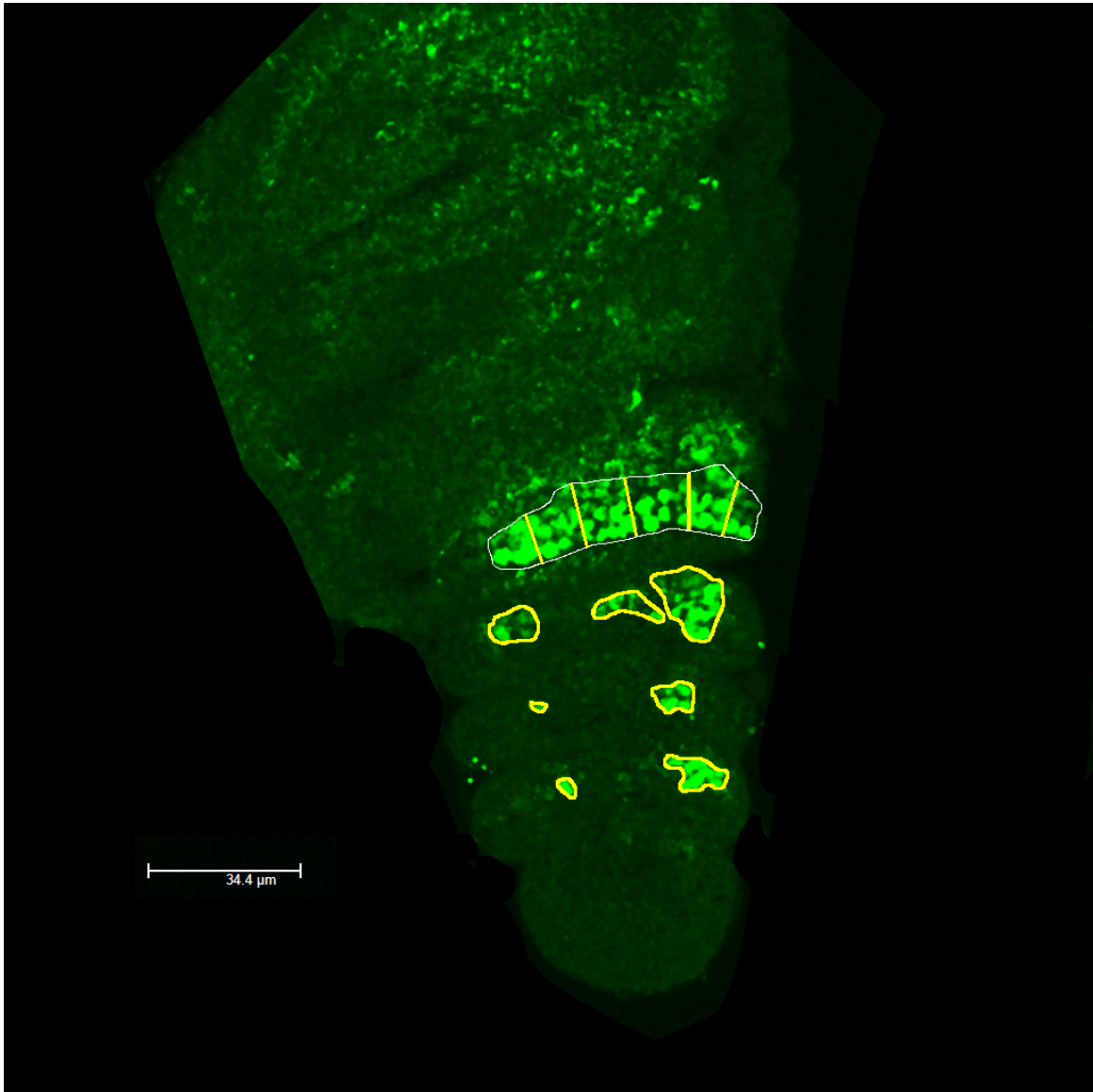


Figure S21. DSX^M expression on foreleg of Wildtype

The white perimeter depicts the DSXM expression pattern in tarsus 1. The five yellow line segments in tarsus represent the width of the expression pattern at five different places. The DSX^M expression area in tarsus 2-4 is depicted by yellow perimeter. The scale bar is provided.

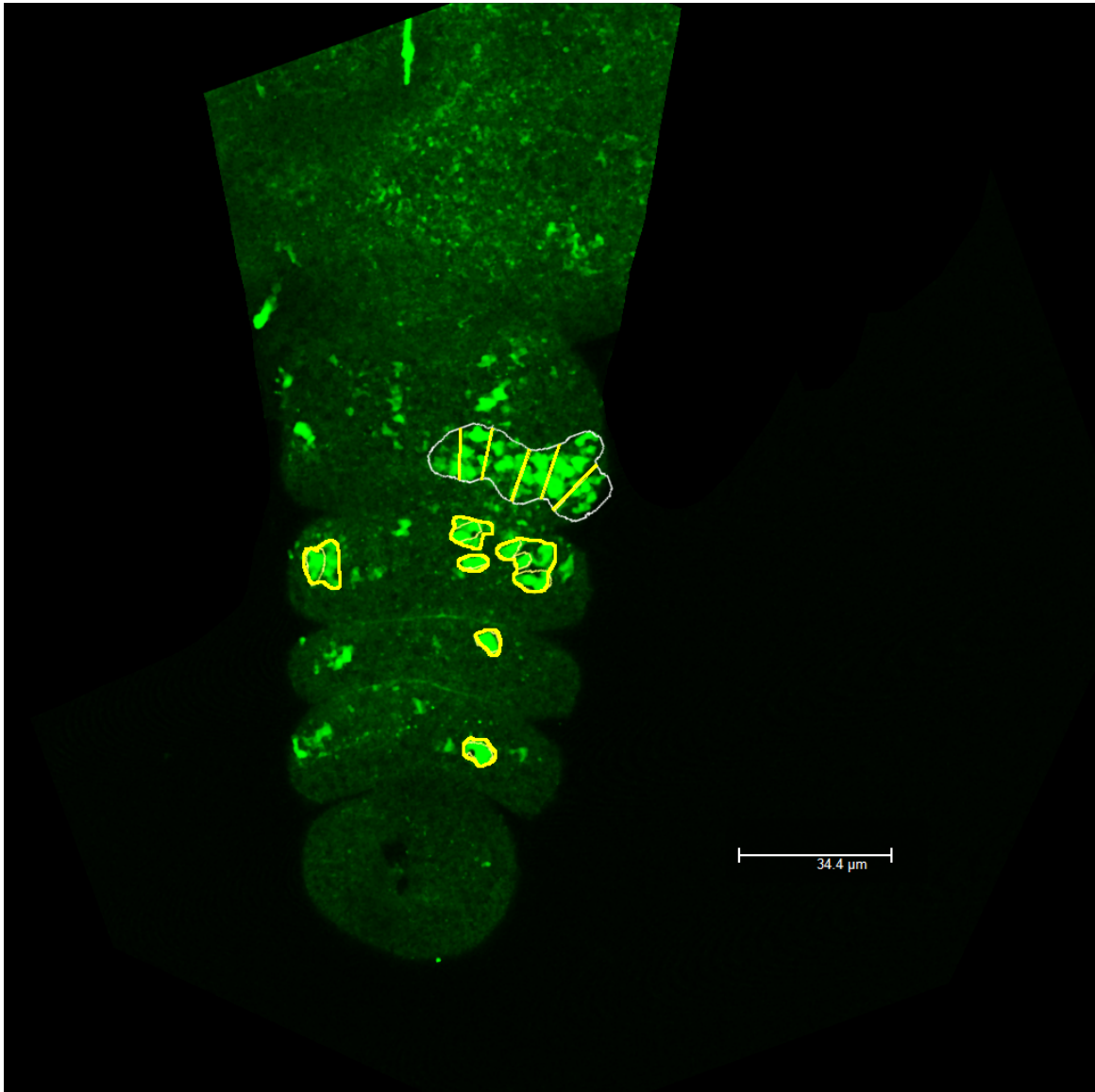


Figure S22. DSX^M expression on foreleg of Wildtype

The white perimeter depicts the DSX^M expression pattern in tarsus 1. The five yellow line segments in tarsus represent the width of the expression pattern at five different places. The DSX^M expression area in tarsus 2-4 is depicted by yellow perimeter. The scale bar is provided.

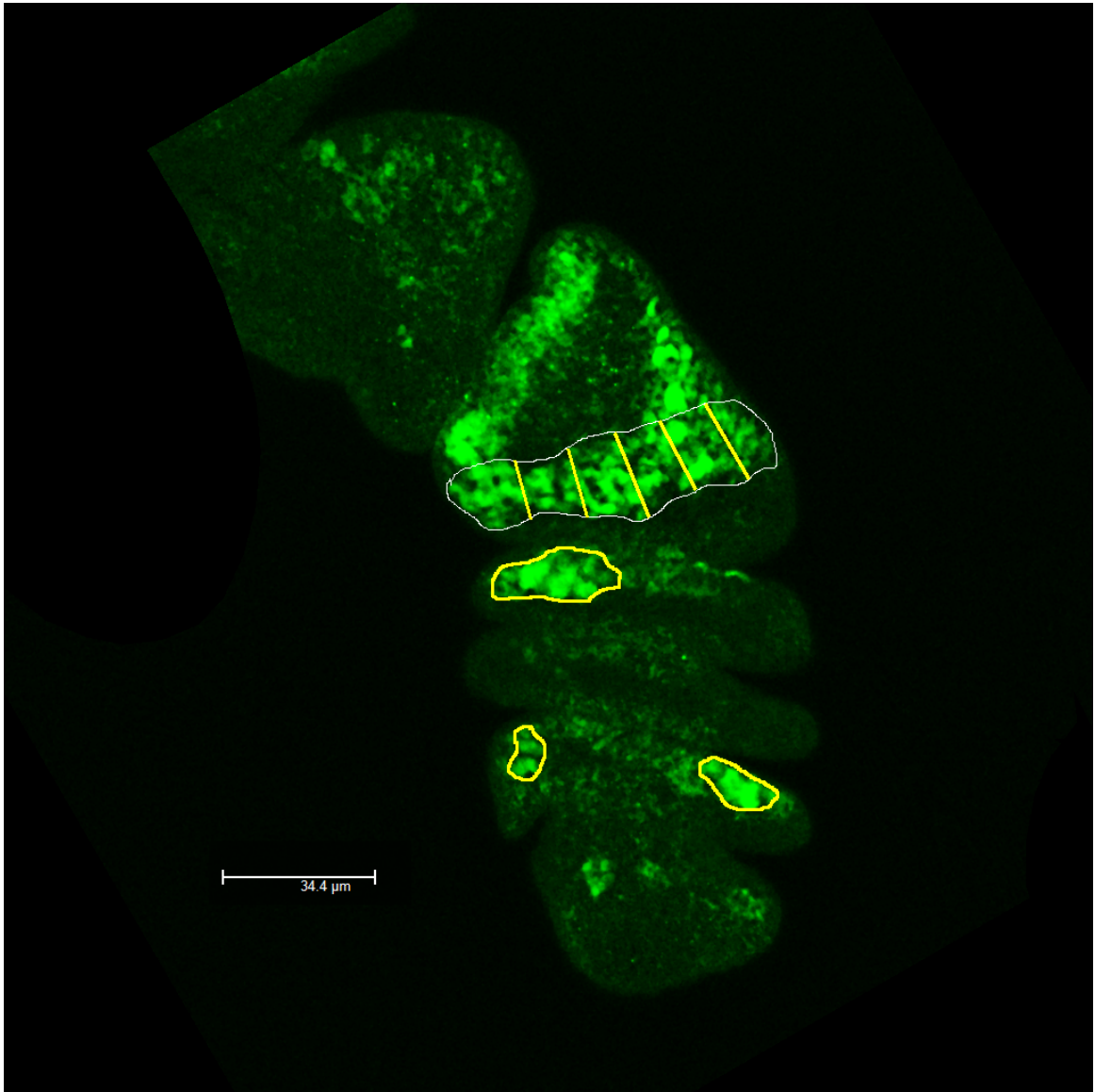


Figure S23. DSX^M expression on foreleg of Wildtype

The white perimeter depicts the DSXM expression pattern in tarsus 1. The five yellow line segments in tarsus represent the width of the expression pattern at five different places. The DSX^M expression area in tarsus 2-4 is depicted by yellow perimeter. The scale bar is provided.

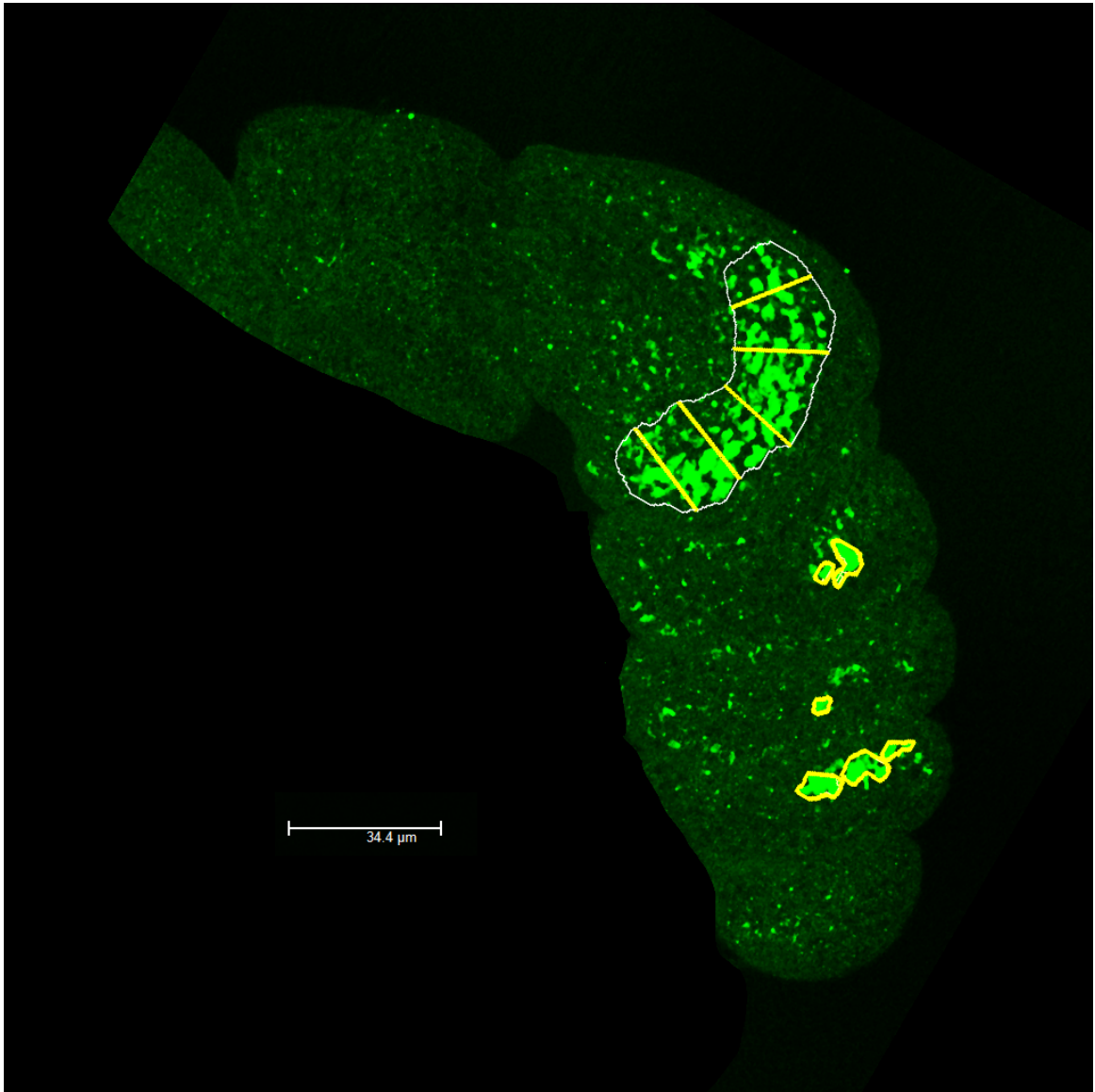


Figure S24. DSX^M expression on foreleg of Wildtype

The white perimeter depicts the DSXM expression pattern in tarsus 1. The five yellow line segments in tarsus represent the width of the expression pattern at five different places. The DSX^M expression area in tarsus 2-4 is depicted by yellow perimeter. The scale bar is provided.



Figure S25. DSX^M expression on foreleg of Lowline

The white perimeter depicts the DSXM expression pattern in tarsus 1. The five yellow line segments in tarsus represent the width of the expression pattern at five different places. The DSX^M expression area in tarsus 2-4 is depicted by yellow perimeter. The scale bar is provided.



Figure S26. DSX^M expression on foreleg of Lowline

The white perimeter depicts the DSXM expression pattern in tarsus 1. The five yellow line segments in tarsus represent the width of the expression pattern at five different places. The DSX^M expression area in tarsus 2-4 is depicted by yellow perimeter. The scale bar is provided.

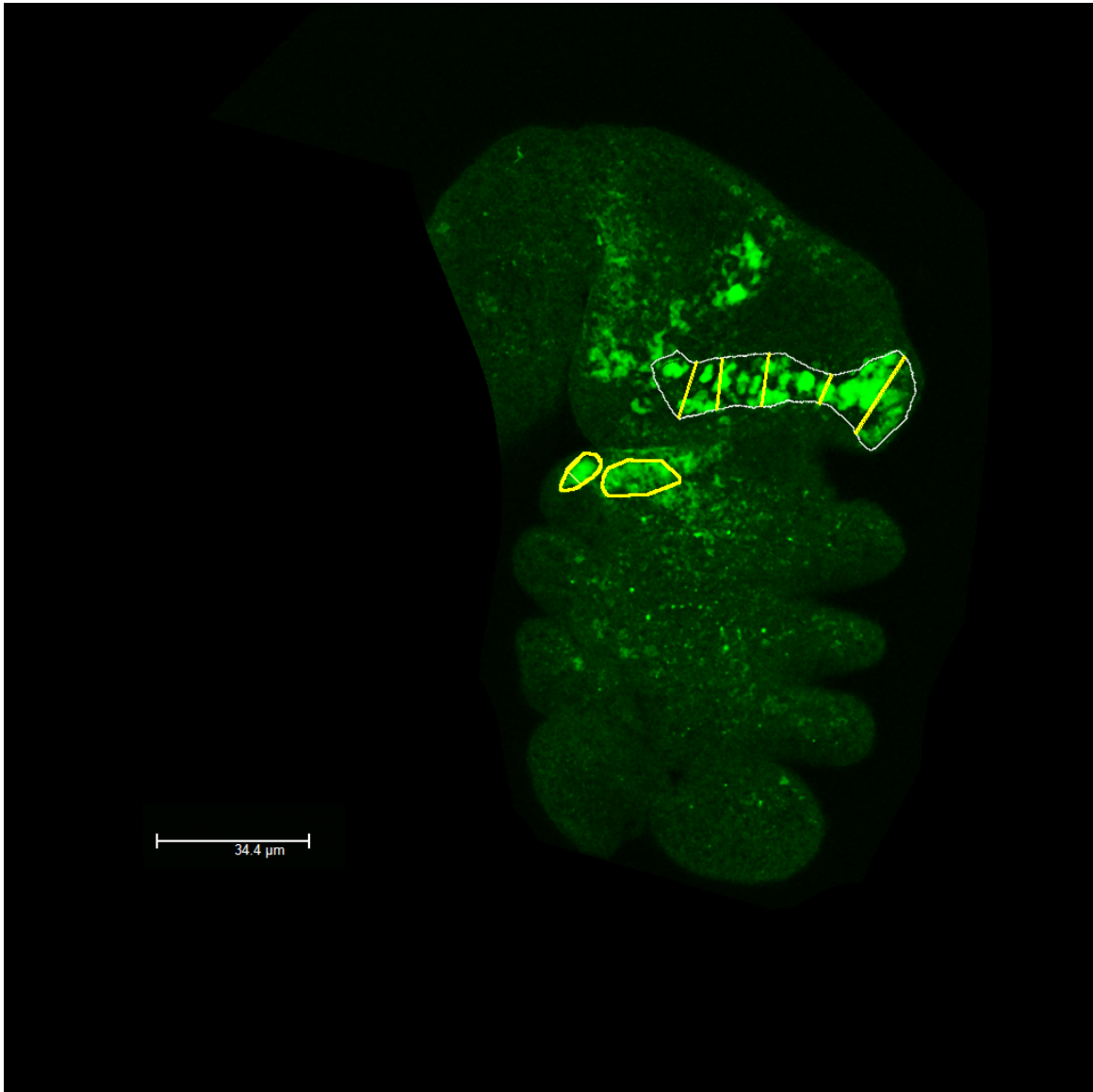


Figure S27. DSX^M expression on foreleg of Lowline

The white perimeter depicts the DSXM expression pattern in tarsus 1. The five yellow line segments in tarsus represent the width of the expression pattern at five different places. The DSX^M expression area in tarsus 2-4 is depicted by yellow perimeter. The scale bar is provided.

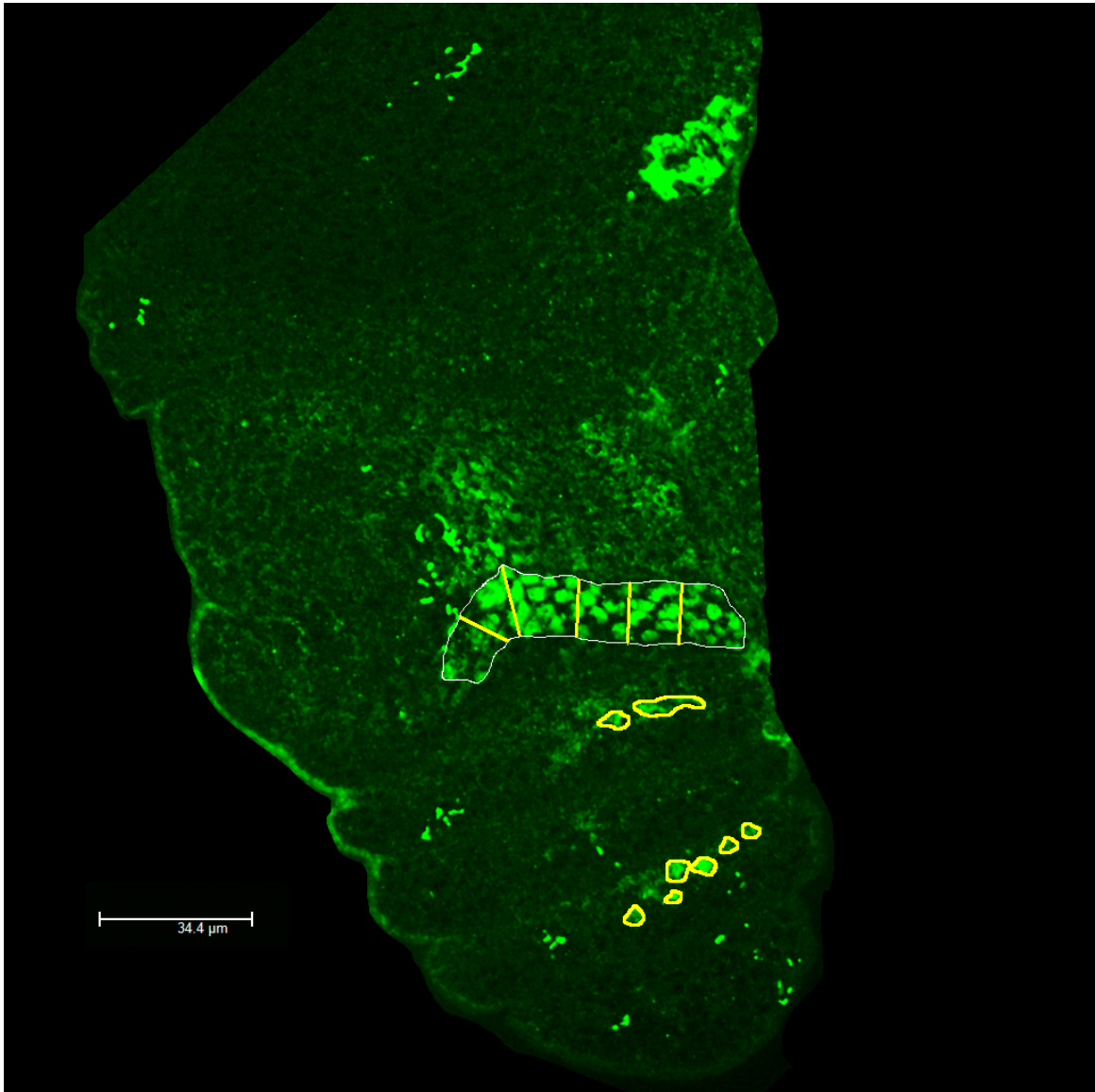


Figure S28. DSX^M expression on foreleg of Lowline

The white perimeter depicts the DSXM expression pattern in tarsus 1. The five yellow line segments in tarsus represent the width of the expression pattern at five different places. The DSX^M expression area in tarsus 2-4 is depicted by yellow perimeter. The scale bar is provided.



Figure S29. DSX^M expression on foreleg of Lowline

The white perimeter depicts the DSXM expression pattern in tarsus 1. The five yellow line segments in tarsus represent the width of the expression pattern at five different places. The DSX^M expression area in tarsus 2-4 is depicted by yellow perimeter. The scale bar is provided.



Figure S30. DSX^M expression on foreleg of Lowline

The white perimeter depicts the DSXM expression pattern in tarsus 1. The five yellow line segments in tarsus represent the width of the expression pattern at five different places. The DSX^M expression area in tarsus 2-4 is depicted by yellow perimeter. The scale bar is provided.

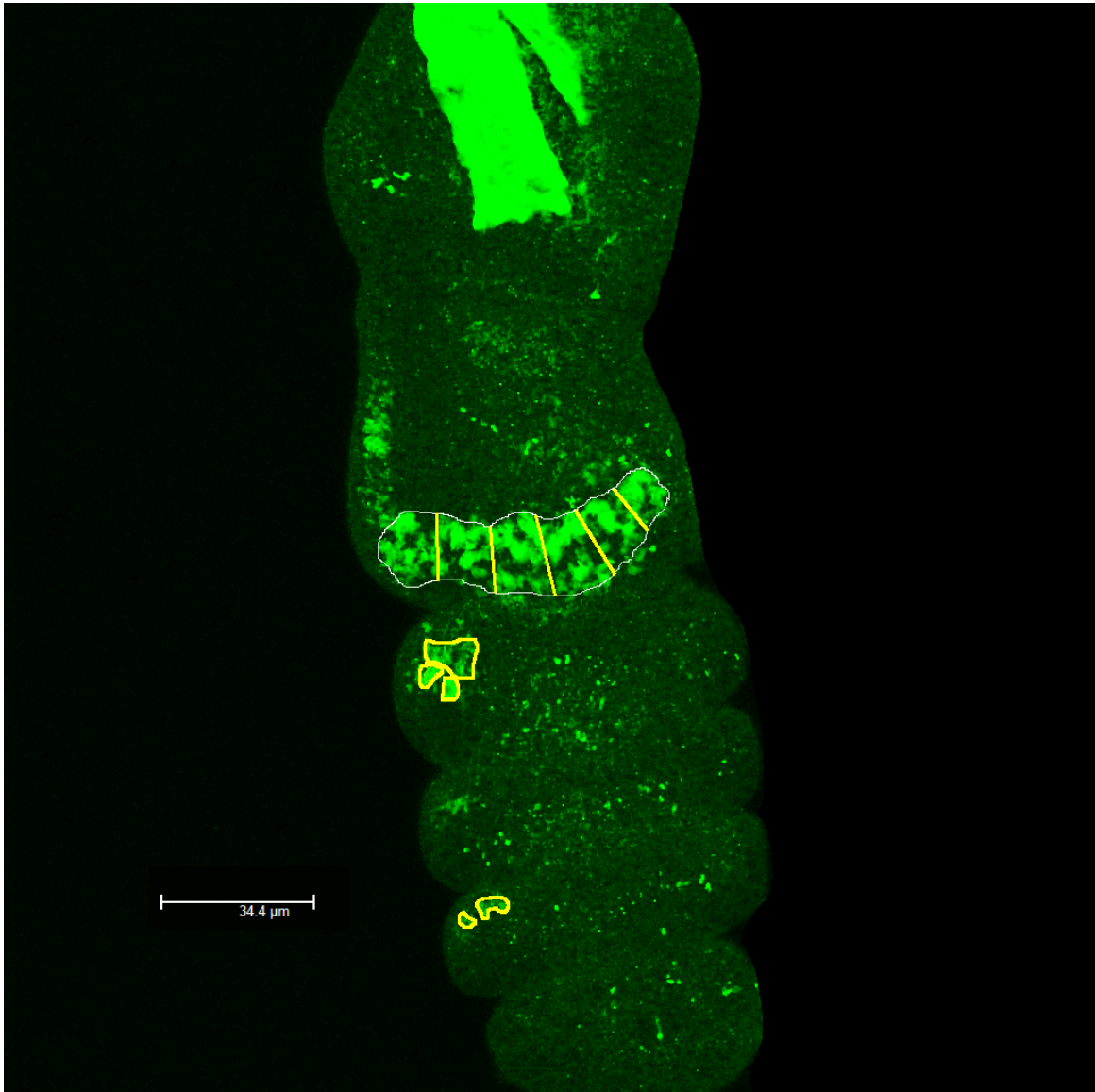


Figure S31. DSX^M expression on foreleg of Lowline

The white perimeter depicts the DSX^M expression pattern in tarsus 1. The five yellow line segments in tarsus represent the width of the expression pattern at five different places. The DSX^M expression area in tarsus 2-4 is depicted by yellow perimeter. The scale bar is provided.

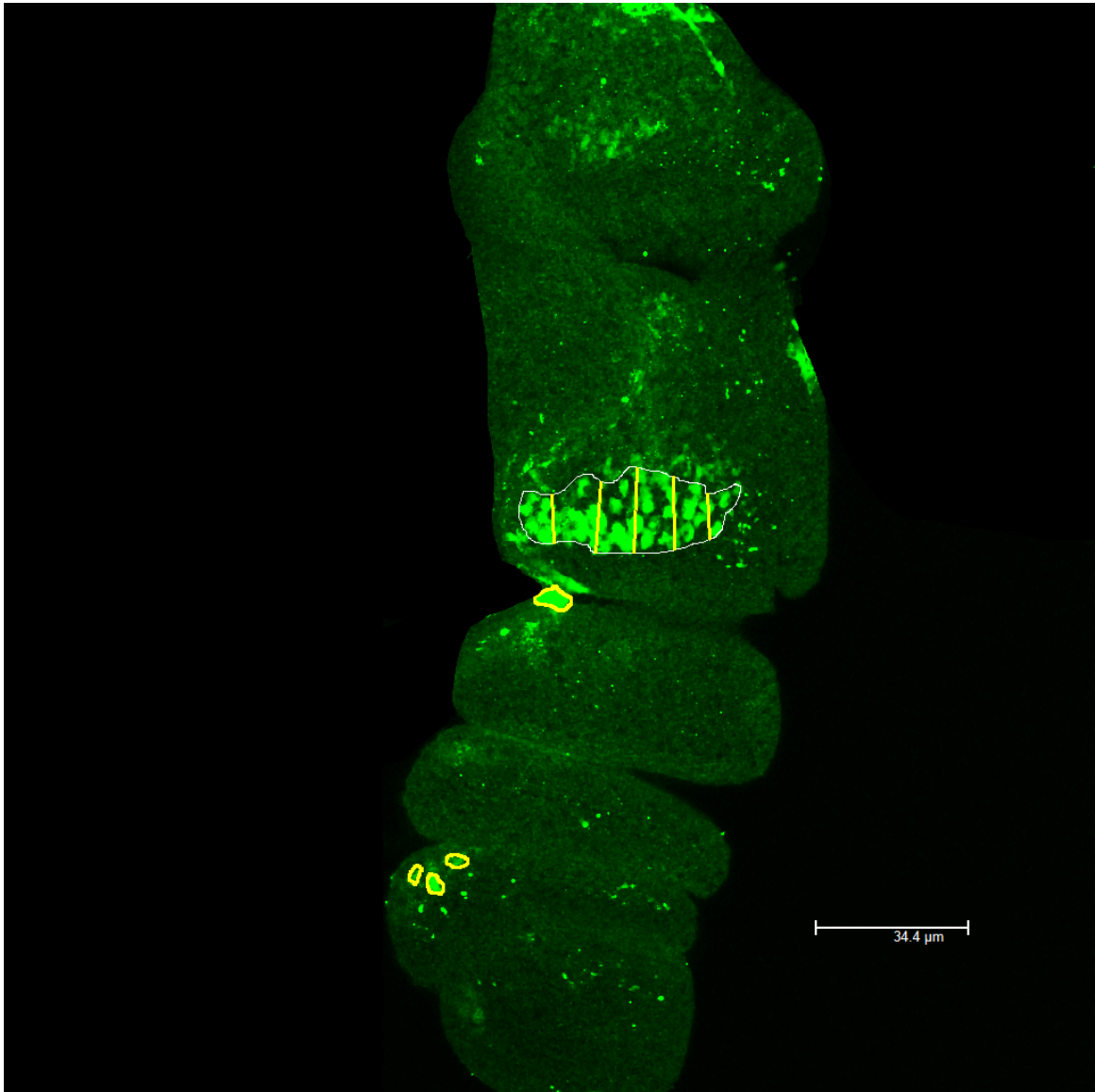


Figure S32. DSX^M expression on foreleg of Lowline

The white perimeter depicts the DSXM expression pattern in tarsus 1. The five yellow line segments in tarsus represent the width of the expression pattern at five different places. The DSX^M expression area in tarsus 2-4 is depicted by yellow perimeter. The scale bar is provided.

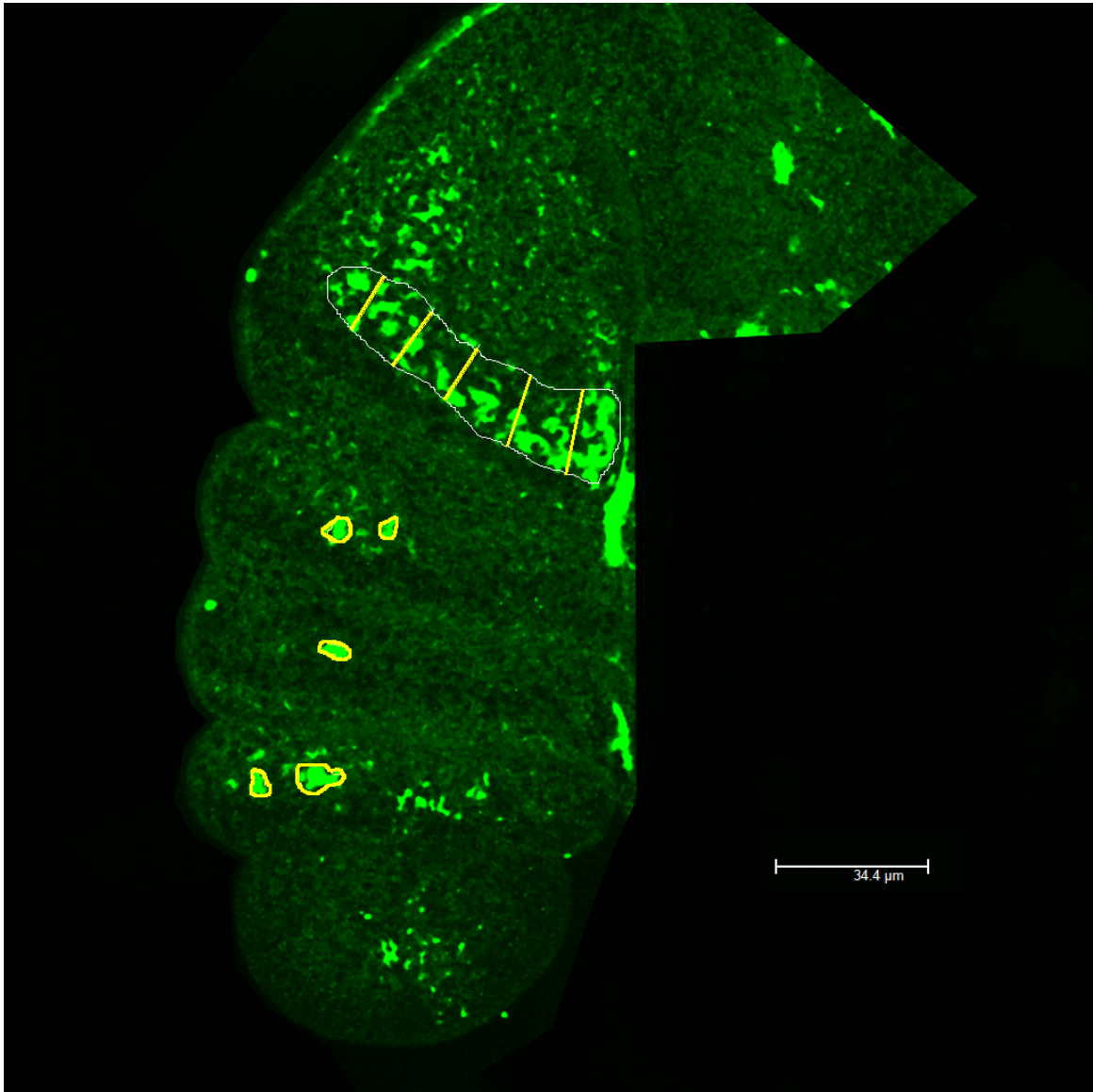


Figure S33. DSX^M expression on foreleg of Lowline

The white perimeter depicts the DSXM expression pattern in tarsus 1. The five yellow line segments in tarsus represent the width of the expression pattern at five different places. The DSX^M expression area in tarsus 2-4 is depicted by yellow perimeter. The scale bar is provided.

Image Number	line 1 width	line 2 width	line 3 width	line 4 width	line 5 width	Average	Cell cluster area	Genotype
Fig S1	106.58	137.40	120.34	78.65	95.66	107.726	15344.64	H
Fig S2	84.30	111.20	116.85	109.29	103.74	105.076	4663.30	H
Fig S3	84.90	94.43	77.51	110.96	119.87	97.534	12570.63	H
Fig S4	87.05	85.59	89.01	91.50	124.02	95.434	14635.00	H
Fig S5	92.93	79.36	88.21	77.94	75.57	82.802	7225.34	H
Fig S6	81.12	107.50	88.32	92.97	90.95	92.172	3723.26	H
Fig S7	55.69	80.45	67.77	73.45	74.74	70.420	11040.77	H
Fig S8	90.51	71.50	97.18	96.93	82.46	87.716	6460.42	H
Fig S9	80.74	98.39	89.02	89.22	102.73	92.020	6294.53	H
Fig S10	130.52	81.72	81.43	86.09	79.41	91.834	7391.23	H
Fig S11	51.92	70.12	67.08	79.06	114.67	76.570	5621.76	H
Fig S12	79.50	90.64	78.08	80.07	82.23	82.104	5861.38	H
Fig S13	83.51	69.26	72.91	90.06	93.28	81.804	9612.29	H
Fig S14	82.76	70.78	48.71	75.92	78.81	71.396	2027.52	H
Fig S15	65.00	72.50	83.88	90.55	89.87	80.36	2838.53	H
Fig S16	61.54	62.33	78.18	82.03	76.49	72.114	1916.93	W
Fig S17	80.50	69.00	80.50	72.5	73	75.100	6147.07	W
Fig S18	48.28	60.11	58.22	89.02	122.07	75.540	11575.30	W
Fig S19	55.61	73.75	56.75	53.6	81.74	64.290	10349.57	W
Fig S20	91.23	79.62	83.88	78.1	89.17	84.400	14782.46	W
Fig S21	50.28	63.55	59.72	58.01	56.8	57.672	5584.90	W
Fig S22	60.11	57.14	52.50	51.71	48.68	54.028	4478.98	W
Fig S23	84.22	74.94	87.65	68.41	57.24	74.492	8616.96	W
Fig S24	81.52	91.61	85.97	95.66	99.3	90.812	2294.78	W
Fig S25	92.35	63.96	52.40	57.12	58.41	64.848	119.81	L
Fig S26	90.85	83.60	80.80	77.1	77.95	82.060	2340.86	L
Fig S27	52.20	48.17	48.51	27.58	82.53	51.798	2488.32	L
Fig S28	49.42	65.97	53.04	55.08	54.61	55.624	2340.86	L
Fig S29	48.50	67.31	67.54	62.02	56.31	60.336	331.78	L
Fig S30	46.46	57.56	57.31	57.56	46.46	53.070	3566.59	L
Fig S31	51.86	70.92	77.99	63.29	64.01	65.614	2045.95	L
Fig S32	43.57	68.01	79.56	67.72	46.02	60.976	903.17	L
Fig S33	57.88	62.80	54.08	67.36	78.54	64.132	1963.01	L

Table S1. Raw data of the DSX^M expression area pattern width at 5 different places in tarsus 1 and the area of DSX^M expression pattern (cell cluster area) in tarsus 2-4. The unit of the data is pixel. H is highline, W is Wildtype and L is lowline.